AD-A055 430 NAVAL POSTGRADUATE SCHOOL MONTEREY CALIF F/G 13/1
AN EXPERIMENTAL INVESTIGATION OF ENHANCED HEAT TRANSFER ON HORI--ETC(U)
MAR 78 D J REILLY
UNCLASSIFIED NPS69-78-011 NL

1 OF 3
ADA
055430

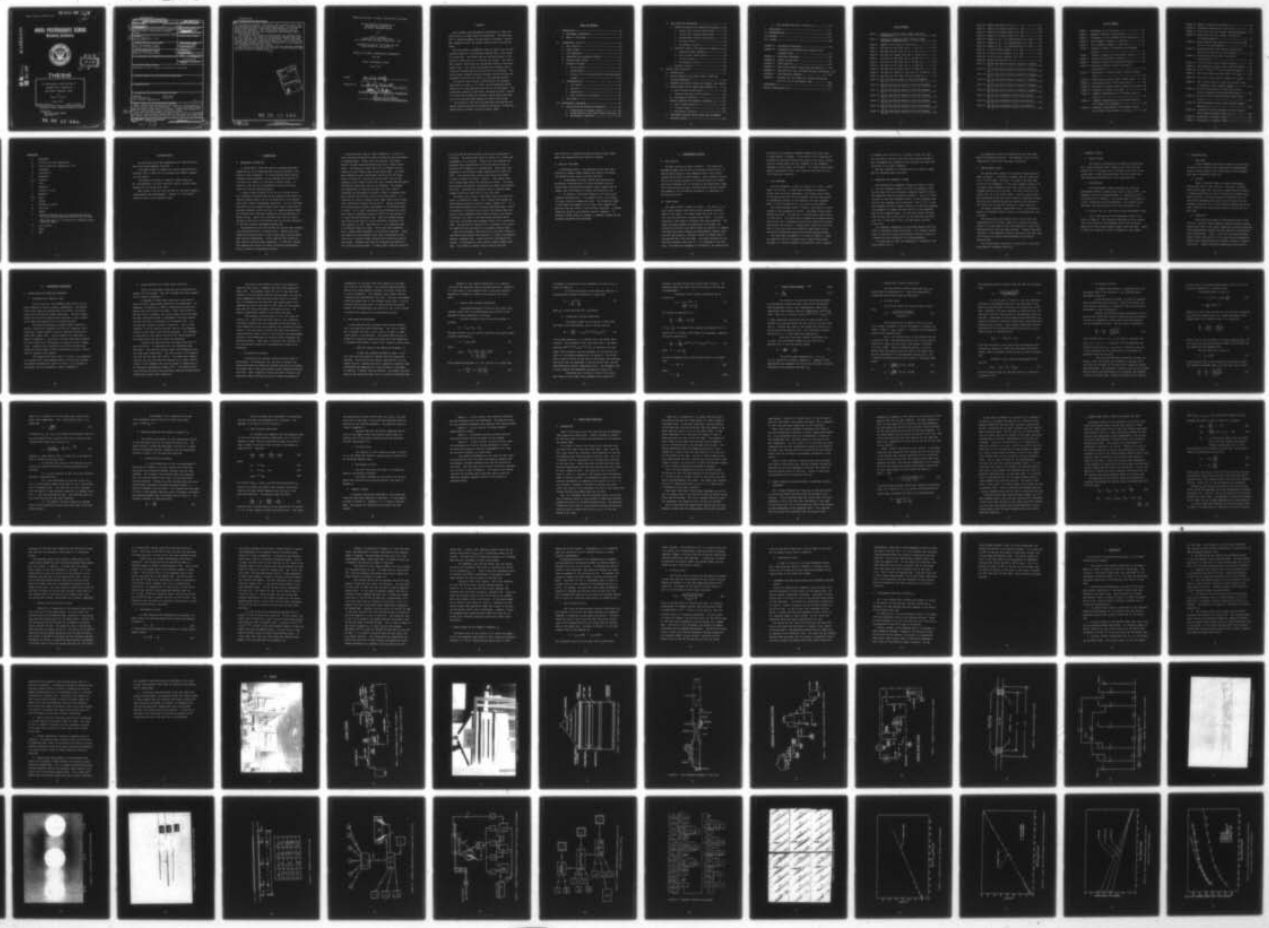

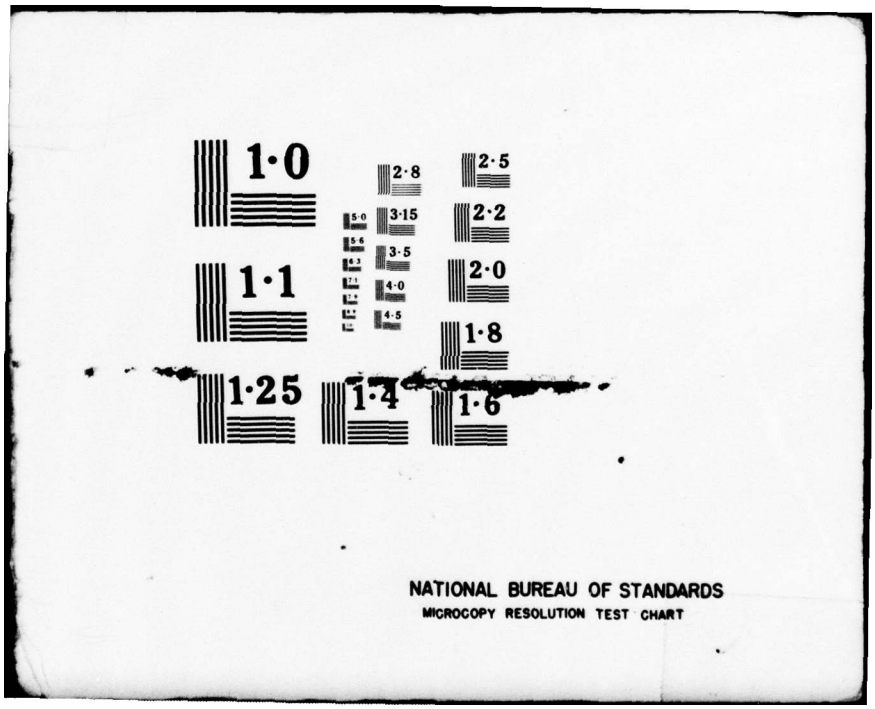
1·0
1·1
1·25
1·4
1·6
1·8
2·0
2·2
2·5
2·8
3·15
3·5
4·0
4·5
5·0
5·6
NATIONAL BUREAU OF STANDARDS
MICROCOPY RESOLUTION TEST CHART

Report Number--NPS69-78-011

NAVAL POSTGRADUATE SCHOOL
Monterey, California

THESIS

AN EXPERIMENTAL INVESTIGATION OF
ENHANCED HEAT TRANSFER ON
HORIZONTAL CONDENSER TUBES

by

David J. Reilly

March 1978

Thesis Advisor: Paul J. Marto

Prepared for:
Naval Sea Systems Command
Washington, D.C.

UNCLASSIFIED

SECURITY CLASSIFICATION OF THIS PAGE (When Data Entered)

REPORT DOCUMENTATION PAGE

READ INSTRUCTIONS BEFORE COMPLETING FORM

1. REPORT NUMBER: NPS69-78-011	2. GOVT ACCESSION NO.
3. RECIPIENT'S CATALOG NUMBER	
4. TITLE (and Subtitle): An Experimental Investigation of Enhanced Heat Transfer on Horizontal Condenser Tubes.	5. TYPE OF REPORT & PERIOD COVERED: Master's Thesis; [redacted] 1978
	6. PERFORMING ORG. REPORT NUMBER
7. AUTHOR(s): David J. Reilly, LT, USN	8. CONTRACT OR GRANT NUMBER(s)
9. PERFORMING ORGANIZATION NAME AND ADDRESS: Naval Postgraduate School, Monterey, California 93940	10. PROGRAM ELEMENT, PROJECT, TASK AREA & WORK UNIT NUMBERS: ~~N0002477-WR74134~~
11. CONTROLLING OFFICE NAME AND ADDRESS: Naval Postgraduate School, Monterey, California 93940	12. REPORT DATE: March [redacted]78 13. NUMBER OF PAGES: 214 (12 222 P.)
14. MONITORING AGENCY NAME & ADDRESS (if different from Controlling Office)	15. SECURITY CLASS. (of this report): Unclassified 15a. DECLASSIFICATION/DOWNGRADING SCHEDULE

16. DISTRIBUTION STATEMENT (of this Report)

Approved for public release; distribution unlimited.

17. DISTRIBUTION STATEMENT (of the abstract entered in Block 20, if different from Report)

18. SUPPLEMENTARY NOTES

19. KEY WORDS (Continue on reverse side if necessary and identify by block number)

Condenser
Film Condensation
Heat Transfer Augmentation
Swirl Flow
Convection

5/8-in.

20. ABSTRACT (Continue on reverse side if necessary and identify by block number)

Heat transfer and hydrodynamic performance of three different spirally fluted tubes was determined. The tubes were 5/8" in nominal diameter and were made of aluminum. Results were compared to 5/8" OD, smooth copper-nickel and aluminum tubes.

Data was taken by condensing steam at about 3 psia on the outside surface of a horizontally mounted tube in the center of a tube bank. The center tube was cooled by water on the inside at velocities of

5/8-in.

DD FORM 1 JAN 73 1473 (Page 1) EDITION OF 1 NOV 65 IS OBSOLETE S/N 0102-014-6601

UNCLASSIFIED

SECURITY CLASSIFICATION OF THIS PAGE (When Data Entered)

251 450 1

ACH

3 to 25 feet per second. The overall heat transfer coefficient was determined directly from experimental data. The inside and outside heat transfer coefficients were determined using the Wilson plot technique. The cooling water pressure drop was measured inside the tube and converted to the friction factor in the enhanced section.

The overall heat transfer coefficients of the enhanced tubes were as large as 1.75 times the corresponding smooth tube value for the same mass flow rate of cooling water. The inside heat transfer coefficients increased by about a factor of 3 while the outside heat transfer coefficients decreased by 10 to 20 percent when compared to smooth tube values.

The results of this work indicate that the required condenser surface area can be reduced by 50 percent if these enhanced tubes are used in place of smooth tubes.

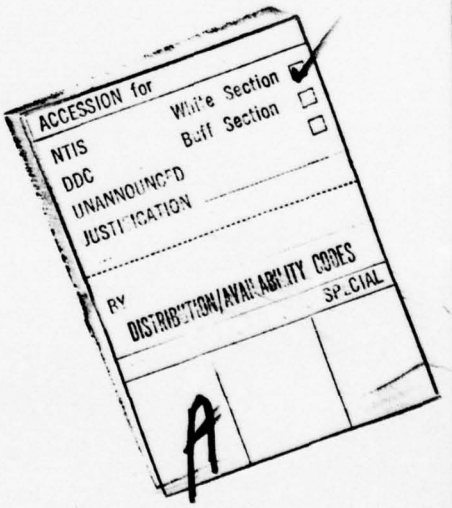

Approved for public release; distribution unlimited.

An Experimental Investigation of Enhanced Heat Transfer on Horizontal Condenser Tubes

by

David J. Reilly
Lieutenant, United States Navy
B.S., North Carolina State University, 1972

Submitted in partial fulfillment of the requirements for the degree of

MASTER OF SCIENCE IN MECHANICAL ENGINEERING

from the

NAVAL POSTGRADUATE SCHOOL

March 1978

Author: David J. Reilly

Approved by: Paul J. Marto
Thesis Advisor

Allen E Fuhs
Chairman, Department of Mechanical Engineering

George J. Haltiner
Dean of Science and Engineering

ABSTRACT

Heat transfer and hydrodynamic performance of three different spirally fluted tubes was determined. The tubes were 5/8" in nominal diameter and were made of aluminum. Results were compared to 5/8" OD, smooth copper-nickel and aluminum tubes.

Data was taken by condensing steam at about 3 psia on the outside surface of a horizontally mounted tube in the center of a tube bank. The center tube was cooled by water on the inside at velocities of 3 to 25 feet per second. The overall heat transfer coefficient was determined directly from experimental data. The inside and outside heat transfer coefficients were determined using the Wilson plot technique. The cooling water pressure drop was measured inside the tube and converted to the friction factor in the enhanced section.

The overall heat transfer coefficientsof the enhanced tubes were as large as 1.75 times the corresponding smooth tube value for the same mass flow rate of cooling water. The inside heat transfer coefficients increased by about a factor of 3 while the outside heat transfer coefficients decreased by 10 to 20 percent when compared to smooth tube values.

The results of this work indicate that the required condenser surface area can be reduced by 50 percent if these enhanced tubes are used in place of smooth tubes.

TABLE OF CONTENTS

LIST OF TABLES

LIST OF FIGURES

NOMENCLATURE

A	Area (ft^2)
Ac	Cross sectional area of test section (ft^2)
c_p	Specific heat (BTU/lbm)
D	Diameter (ft)
f	Friction factor
Fc	Flow calibration factor
G	Flow rate per unit area ($lbm/hr \cdot ft^2$)
g_c	Gravitational constant ($lbm \cdot ft/lbf \cdot sec^2$)
h	Heat transfer coefficient ($BTU/hr \cdot ft^2\ ^oF$)
HA	Helix Angle
hfg	Latent heat of vaporization hfg (BTU/lbm)
ID	Inside Diameter
J	J factor in Colburn Analogy ($StPr^{2/3}$)
k	Thermal conductivity ($BTU/hr \cdot ft \cdot ^oF$)
K	Abrupt entrance and exit coefficient
LMTD	Log mean temperature coefficient (^oF)
$\dot{m}$	Mass flow rate of water (lbm/hr)
M	Slope of Wilson Plot output from linear regression program.
Nu	Nusselt Number = hD/k

p	Pumping power ($ft \cdot lb_f/sec$)
P	Pressure (psi)
P_{bar}	Average of Pw_i and Pw_o (in)
Pw	Wetted perimeter (in)
Q	Heat flow rate
$\dot{Q}$	Volumetric flow rate (GPM)
R	Thermal resistance ($hr \cdot ft^2\ ^oF/BTU$)
Re	Reynolds number = DG/μ
St	Stanton number = Nu/RePr
t	Thickness (in)
T	Temperature (^oF, ^oR)
Tc	Temperature of cooling water (^oF)
TPF	Tube performance factor = 2J/f
U	Overall heat transfer coefficient ($BTU/hr \cdot ft^2\ ^oF$)
v	Water velocity (fph, fpm)
V	Volume (ft^3)
X	x axis input to linear regression program
Y	y axis input to linear regression program

GREEK SYMBOLS

Δ	Differential
μ	Dynamic viscosity ($lbm/ft \cdot hr$)
ρ	Fluid density (lbm/ft^3)
σ	Area ratio: $\frac{4Ac}{\pi D_i^2}$

Subscripts

a	Augmented
b	Fluid at the bulk temperature
br	Fluid at the bulk temperature in ^{o}R
c	Corrected
cn	Contraction
e	Expansion
ext	External
f	Film
h	Hydraulic
i	Inside, or inlet
m	Measured
met	Metal
n	Nominal
o	Outside, or outlet
pe	Plain end
s	Smooth
s'	Smooth end between tap 2 and the enhanced section or tap 6 and the enhanced section on the PT tubes
T	Length from tap 3 or 5 to the end of enhanced section on the PT tubes
TS	Test section
v	Vapor
w	Wall

ACKNOWLEDGEMENT

The work herein has been supported by Mr. Charles Miller, Naval Sea System Command, Code 0331.

The author wishes to express his sincere appreciation to Professor Paul J. Marto for his guidance and support throughout the project.

The author also wishes to thank Mr. James Selby and Mr. Ken Mothersell for their technical advice, and Mrs. Marty Delgado for her journalistic help.

Many thanks to my wife and children for the moral support, understanding and encouragement. Without it, this project certainly would not be complete today.

I. INTRODUCTION

A. BACKGROUND INFORMATION

In recent years, there has been an increased awareness regarding the use of enhanced heat transfer surfaces in the design of heat exchangers. By using enhanced heat transfer surfaces, heat exchangers can be designed to be smaller in size which can result in a savings in capital costs. In addition, they can also be designed to be more efficient which will save on operating costs.

A recent study by Search [1] of an air aircraft carrier main condenser concluded that marine condenser heat loads, at constant pumping power, can be increased by up to 50 percent using heat transfer enhancement techniques. He also concluded that the use of corrugated copper-nickel tubes can be used to decrease condenser weight and cost for constant pumping power and constant heat load when compared to the conventional condenser design. Search also concluded that size and weight savings on the order of 40 percent could be realized depending on the heat transfer enhancement method used.

The possibilities of such savings has spurred much research and many design efforts in recent years. Bergles [2,3] has summarized extensive works in both single phase and two phase heat transfer enhancement. He has compiled and listed the many efforts that have been undertaken. In addition, Bergles has compared the results of several different experimenters using a variety of performance criteria.

In the particular case of steam condensers, a variety of tests have been conducted to study the behavior and performance of enhanced tubes. Palen, Chan, and Taborek [4] tested several Turbotec tubes manufactured by Spiral Tubing Corporation. The purpose of these tests were to compare the performance of the Turbotec tube to the smooth tube. The tests were conducted using a tube bundle consisting of 196 tubes. Steam at 55 psig or 105 psig was on the shell side of the condenser, while water at mass flow rates between 380,000 lbm/hr and 800,000 lbm/hr were used on the tubeside. The average bulk temperature of the cooling water was 245 to 320 ^{o}F. Eissenberg [5] performed an extensive study of condenser tube heat transfer coefficients using a multi-tube bundle. He conducted his tests on copper-nickel roped tubes using a steam vapor temperature between 160 and 300 ^{o}F. Newson and Hodgson [6] conducted heat transfer experiments on 32 different types of tubes. All of their experiments were conducted with saturated steam at atmospheric pressure (212^{o}F) on the outside of a single vertically mounted tube. Water was pumped through the inside of the tube at a rate sufficient to maintain the LMTD constant at 11^{o}F. Watkinson et al. [7] conducted tests on 18 Noranda Forge Fin tubes. Their tests were conducted with a single tube orientated in a horizontal position. Steam was supplied to the outside of the tube at atmospheric pressure or at a slightly higher pressure while water was used on the inside. Catchpole and Drew [8] conducted experiments on five radially grooved tubes. In these tests steam was supplied

at 2 psia and the cooling water velocity was maintained at 10 ft/sec. The tubes could either be tested in a single tube arrangement or as a bundle. Young et al. [9] compared the Korodense tube, manufactured by the Wolverine Division of Universal Oil Products, to a smooth tube. These tests were conducted at two different steam temperatures of 100°F and 212°F. The cooling water velocity was varied from about 3 ft/sec to about 6.5 ft/sec. Rothfus [10] tested internally finned tubes made from aluminum and copper. The tubes were mounted horizontally and measured for water side performance only. The water was heated by means of heating tapes wrapped around the outer walls of the test tube.

The tubes used in each of the above tests are widely different in geometrical shape. Still another tube design has been proposed recently by General Atomic Company [11]. It is fabricated differently than the above mentioned tubes, resulting perhaps in different heat transfer performance when compared to other enhanced surface tubes already on the market. In addition, for each of the experiments mentioned above, there was a different test procedure and/or set of conditions used. The need exists therefore for a systematic and consistent method to test and analyze all enhanced surface tubes.

Beck [12] designed a test facility at the Naval Postgraduate School that permits the testing of a single, horizontally mounted, condenser tube. Pence [13] built and tested this system. He conducted his tests using a smooth copper-nickel tube. The results of Pence's tests indicate that the

test facility is technically sound and that further experiments with enhanced-surface tubes are possible.

B. GOALS OF THIS WORK

As mentioned earlier, the enhanced-surface tube manufactured by General Atomic Company was ready to be tested. The purpose of this thesis was then two-fold:

1. to determine the heat transfer and pressure drop performance characteristics of three different spirally fluted tubes manufactured by General Atomic Company and to compare their performance to smooth tube operation, and

2. to develop a consistent method for arriving at performance characteristics. To accomplish this, two alternative data reduction schemes were used. One scheme was based on the smooth end geometry of the tube, which seemed to be what was used most often in the existing literature. A second method was based on the enhanced section's geometry. To accomplish these reduction schemes, a computer program and the necessary equations were developed.

II. EXPERIMENTAL FACILITY

A. TEST FACILITY

The test facility is seen in Figure 1. The layout was designed by Beck [12] and built and tested by Pence [13]. A detailed description of the components used in the various systems may be found in these reports. Only a general description of the various systems will be found within this report. Particular attention will be focused on the experimental tubes, their construction and their location within the test section. See Appendix A for calibration procedures of components requiring calibration.

B. STEAM SYSTEM

The steam system is shown in Figure 2. The boiler is an electrically heated Fulton Boiler which produces saturated steam at 100 lbm/hr. The steam leaves the boiler via a 3/4 inch line and the boiler-isolation valve (MS-1). The water contained in the steam is removed by the steam separator. The steam continues through the system past a flow meter and through the throttle valve (MS-3) where the pressure is reduced. The steam next passes through the desuperheater wherein water from the feed system is injected in order to remove some of the sensible heat from the steam. The steam continues on into the test condenser where part of it is condensed on the test tube. The steam not condensed is collected in the vapor outlet

and sent to the secondary condenser wherein the latent heat of vaporization is removed. If the boiler fails, steam may be provided via the house-steam-cross-connect valve (MS-2). Steam could be routed around the test condenser to the secondary condenser via the bypass valve (MS-4). All steam lines (except section downstream of MS-3, see [13]) were insulated with one inch fiberglass insulation.

C. TEST CONDENSER

The test condenser is shown in Figures 3, 4, and 5. Steam enters via the top. It then passes through the expansion section over the baffle separators, and through three layers of 150 mesh screen and flow straightener into the tube bundle. The condensate collects at the bottom of the test condenser where it flows through two 1/2 inch lines to the hotwell.

The viewing window, shown in Figure 3 and Figure 4, allows viewing of the condensation process. Two types of pyrex glass windows were used. One type was a standard pyrex glass plate, 1/2 inch thick. The second type of window was an Owens-Corning pyrex glass with a transparent electrically conducting coating applied over the surface. A Lambda power supply set at 20 VDC and 1.5 A was used with this window to supply power to the electrically conducting surface to minimize fogging effects.

The tube sheet arrangement is as seen in Figure 5. There are eight 5/8 inch OD, 18 gauge, 90-10 copper-nickel tubes arranged in a typical condenser configuration, with a spacing

to diameter ratio (S/D) of 1.5, around a single test tube. The test tube is the only tube with water passing through it. This arrangement was selected to best simulate the steam flow conditions in an actual condenser.

The test condenser is insulated with two inches of Johns-Manville Aerotube sheet insulation.

D. CONDENSATE AND FEEDWATER SYSTEMS

The condensate and feedwater systems are shown in Figure 6. The test condenser hotwell collects the condensate from the test tube, while the secondary condenser hotwell collects the condensate from the secondary condenser. Valve C-1 allows isolation of the test condenser hotwell so the condensate mass from the test condenser may be measured. Valve C-4 is a vent valve between the test condenser hotwell and the test condenser. The condensate is pumped from the hotwells to the feedwater tank by the condensate pump. The feed pump routes the water from the feed tank to the boiler via the solenoid-controlled valve FW-3, a hot-water filter, and the boiler-isolation valve, FW-4.

The feedwater temperature is maintained between 130^{o}F and 140^{o}F by thermostat controlled heaters. This reduces fluctuations in the boiler output and provides a source of water at a temperature near saturation for the desuperheater.

If house steam is used, the condensate is returned to the house system via C-3.

The condensate lines are insulated with 3/4 inch Johns-Manville Aerotube insulation. The feedwater lines are insulated with 1/2 inch thick fiberglass insulation.

E. COOLING WATER SYSTEM

The cooling water system is a partially-closed system as shown in Figure 7. The water is pumped from the supply tank via a 7-1/2 HP pump. The water is routed to the test tube via one of two rotameters. A low flow rotameter allows up to 1.48 gpm to flow through the test tube, while a high flow rotameter permits up to 18.8 gpm. The water returns to the supply tank via a dry cooling tower. The dry cooling tower was constructed using four large radiators connected in series. The water was directed through the radiators and outside air was forced over the cooling surface by a centrifugal fan.

The bypass-rotameter, downstream of CW-3, is provided to permit an increased volume of water to flow through the cooling tower.

The system piping was reduced from 1 inch to 5/8 inch (approximate OD of all test tubes) at a distance of approximately 2-1/2 feet ahead of the test condenser to insure fully developed flow at the test-tube entrance. Pressure taps were installed in the permanent piping at the ends of the test tube (see Figure 8) to permit the measurement of the overall pressure drop.

The cooling water lines were insulated with 1 inch thick Johns-Manville Areotube insulation.

F. SECONDARY SYSTEMS

1. Vacuum System

The vacuum is maintained by a mechanical-vacuum pump and a vacuum regulator which induces an air leak into the vacuum line. A nitrogen trap is provided at the inlet to the vacuum pump to remove entrained water from the vacuum line thus preventing contamination of the vacuum pump oil.

2. Desuperheater

The desuperheater removes sensible heat from the superheated steam by injecting feed water at about 150^{o}F. The feedwater flow into the desuperheater is controlled by DS-1 and measured by a rotameter. The excess water is collected in a tank, located below the desuperheater, and returned to the feed-water tank periodically during the experimental runs.

3. Pressure Tap (PT) Tube Pressure Drop Measurement System

The PT tube pressure drop measurement system is as shown in Figure 9. This system was designed to allow connecting of the PT-tube to the manometer and to facilitate the measuring of the various pressure drops across the tube. Figure 10 shows how a typical PT tube is connected in the system.

G. INSTRUMENTATION

1. Flow Rates

Fulton rotameters were used to measure the flow rate of water in the cooling water system and the desuperheater, while an Ellison Annubar and a differential water manometer were used to determine steam flow.

2. Pressure

Several different types of pressure measurement devices were used in this facility. They were: a Bourdon tube pressure gage which was used to measure boiler pressure, a compound gage which was used to measure the secondary condenser pressure, an absolute pressure transducer and a 30 inch mercury manometer which were used to measure the test condenser pressure, and a 12-foot mercury manometer which was used to measure the cooling water pressure drop across the test tube.

3. Temperature

There were three types of thermocouples used in this facility. Stainless steel sheathed, copper-constantan thermocouples were used as the primary temperature monitoring devices. Eleven temperatures required for data reduction were measured using these devices. Table 1 lists the locations monitored. Figure 2 shows the location of six vapor space thermocouples. Cooling water thermocouples were located as shown in Figure 7. Teflon coated copper-constantan thermocouples were used as

secondary measuring devices. Table 2 lists the locations monitored using these thermocouples and an iron-constantan thermocouple was used to measure the boiler temperature.

4. Data Collection and Display

An Autodata collection system was utilized to record and display the temperatures in degrees Celsius obtained from the primary thermocouples and to record and display the pressure in cm Hg inside the test condenser. See Table 1 for channel numbers of the temperature monitoring devices.

A 28 channel-digital pyrometer was utilized to display the temperatures obtained from the secondary thermocouples and a single channel pyrometer displayed the temperature from the iron-constantan thermocouple. See Table 2 for channel numbers.

H. TEST TUBES

The enhanced tubes tested during this study were manufactured by General Atomic Co. Three aluminum tubes were made. Each has an overall length of 48 inches and an enhanced section length of 36 inches. They have helical flutes on both the inside and outside surfaces, which are formed by running a flat strip through rollers which cause the flat surface to become wavy. The wavy strip is then spirally wound and seam welded to form a tube. Figure 11 shows a short section of spirally fluted tube rolled from strip and the start of a roll from strip. Figure 12 shows the three tubes and their

respective helix angles (HA) manufactured for this experiment. Figure 13 shows a cross section view of each of these tubes.

As seen in Figure 12, the helical portion of the test tube, henceforth referred to as the enhanced section, is welded to a smooth piece of aluminum tube, hereafter referred to as the smooth end. Each end of the tube has this smooth end to facilitate installation into the condenser tube sheet.

In addition to the above tubes, three special tubes were manufactured by General Atomic Co. to permit the measurement of the pressure drop throughout the test section. These tubes are shown in Figure 14. Three static pressure holes were drilled in each tube's enhanced section by the EDM process. The holes located at each end of the enhanced section were inspected with a boroscope by General Atomic Co. and found to be free of burrs. Figure 15 shows the relative location of these taps as well as the static pressure taps in the smooth ends.

III. EXPERIMENTAL PROCEDURES

A. INSTALLATION AND OPERATING PROCEDURES

1. Preparation of Condenser Tubes

Prior to any run, the condenser tubes had to be properly prepared to insure filmwise condensation. The preparation of the tubes was standardized in an effort to minimize errors due to different surface conditions. The wall thermocouple also had to be prepared and installed in such a manner as to reduce the possibility of introducing errors.

The tubes manufactured by General Atomic required a special installation procedure into the test condenser since they have a larger diameter along the enhanced section than along their smooth ends. These procedures are described in detail in Appendix B. Basically, the test tubes were prepared by first installing a thermocouple to measure the wall temperature. Secondly, their exterior and interior surfaces were cleaned to insure proper wetting characteristics and to insure that all deposits were removed.

The copper-nickel tube, tube 4 in Table 3, was prepared in accordance with the procedure given in Pence [13], whereas the smooth aluminum tube, tube 5 in Table 3, was prepared in accordance with the procedures listed in Appendix B.

2. System Operation and Steady State Conditions

Pence [13] developed a detailed set of operating procedures for this system. They are included, with minor changes, in this report as Appendix C.

In general it takes about three hours from initial light off until steady state conditions are established. The feedwater is heated up to 140^{o}F by energizing the feed tank heaters and recirculating the water. After installation of the test tube is complete, the vacuum system can be activated. The data collection system is programmed, including setting the date and time in accordance with reference [14]. The cooling water system is placed in operation. The 18.8 gpm rotameter is set at about 50 percent flow to allow adequate venting of both legs of the 12-foot manometer. The rotameter is then reset to the lowest flow point for system operation. The steam system can now be placed into operation.

Steady state conditions must be established prior to data collection. To determine this, two parameters were monitored. They were the cooling water inlet temperature and the steam vapor temperature. The cooling water inlet temperature did not rise more than 1^{o}F/hr. The steam vapor temperature did not vary more than 6^{o}F between the six vapor thermocouples in the condenser nor did the change in temperature at an individual thermocouple exceed 0.5^{o}F. The steaming conditions and cooling water flow conditions remained constant while establishing steady state conditions.

The time for the system to stabilize was generally about one hour which is somewhat less than that reported by Pence [13]. The probable reason for this is that with the addition of a much higher capacity cooling tower, the cooling water temperature stabilized much faster than in his tests. This is evidenced by the fact that the cooling water inlet temperatures were on the order of $10^{o}F$ lower for this experiment than for those experiments performed by Pence. The ambient temperatures, however, were nearly the same.

The procedure outlined above is for a full data collection run. There were two other types of runs conducted. Isothermal pressure runs were conducted on the test tubes to allow comparison of the non-isothermal and isothermal friction factors. Also the special pressure tap tubes were tested by connecting these tubes to the PT tube pressure drop measurement system to allow measurement of pressure drops throughout the enhanced sections. Both types of pressure runs required only the cooling water system and instrumentation systems to be energized.

3. Maintenance Procedures

Periodically the systems required various forms of maintenance. Following each run, the boiler received two bottom blow downs to remove any sediment that may have settled. The supply tank in the cooling water system required occasional refilling. Water treated by routing tap water through a commercially rented resin bed was used to reduce the amount of

contaminants in the water that could deposit on the tubes. The filter in the feedwater line required changing approximately every three months to prevent low boiler levels due to lack of feedwater. The condenser glass window required cleaning after approximately five runs. This was true whether using the heated glass or the standard pyrex glass. Prior to reinstalling the pyrex glass, a light coating of Glycerol Reagent ACS $HOCH_2CHOHCH_2OH$, was applied to the inside surface to enhance the viewing of the condensation process.

B. DATA REDUCTION PROCEDURES

In evaluating the data obtained from the heat transfer runs, two objectives were established. The first of these was to present the data in such a way as to make it immediately useful to the designer. The second objective was to establish a reduction scheme that would allow the comparison of enhanced tubes based on their actual internal surface areas.

1. Reduction Based on the Smooth End Diameter, D_i

To meet the condenser designer's needs, it was felt that the data should be reduced using the smooth end diameter. This would allow a direct substitution of an enhanced tube for a smooth tube and is especially important when considering the comparison of a wide variety of tube types. In addition, a nominal area was defined. The nominal area was based on the outside surface area of a 5/8-inch OD smooth tube.

Appendix D, the sample calculations, is a complete listing of the equations used to evaluate the data. Appendix E is a derivation of the probable error in the data reduction equations, followed by a sample error analysis for tube 2, 45^{o}HA.

a. Overall Heat Transfer Coefficient

The method employed to arrive at the overall heat transfer coefficient is straightforward and similar to that employed by many researchers in the past.

The heat transfer rate to the cooling water is given by

$$Q = \dot{m}\, c_p\, (Tc_o - Tc_i) \qquad (1)$$

The heat transfer rate can also be found from the overall heat transfer coefficient by

$$Q = U_n\, A_n\, LMTD \quad , \qquad (2)$$

where

$$LMTD = \frac{(T_v - Tc_i) - (T_v - Tc_o)}{\ln\left(\frac{T_v - Tc_i}{T_v - Tc_o}\right)} \quad . \qquad (3)$$

After combining equations (1), (2), and (3) it is found that

$$U_n = \frac{\dot{m}\, c_p}{A_n} \ln\left(\frac{T_v - Tc_i}{T_v - Tc_o}\right) \quad . \qquad (4)$$

A schematic illustration of the procedures to arrive at U_n is shown in Figure 16.

To remove the effect of the tube wall material, a corrected heat transfer coefficient is found from

$$U_c = \frac{1}{\frac{1}{U_n} - \frac{1}{R_w}} \quad , \tag{5}$$

where R_w is the calculated wall resistance.

b. Inside Heat Transfer Coefficient

The Nusselt number on the inside is found from the Sieder Tate relationship, found in Holman [15] as:

$$Nu = \frac{h_i D_i}{k_b} = c_i \, Re^{0.8} \, Pr^{1/3} (\mu/\mu_w)^{0.14}. \tag{6}$$

In the above equation, c_i is referred to as the Sieder Tate constant. The remainder of the right hand side of the above equation ($Re^{0.8} \, Pr^{1/3} (\mu/\mu_w)^{0.14}$) will be referred to as the Sieder Tate parameter, and the procedure for arriving at this value is illustrated schematically in Figure 17. The Wilson plot is used to arrive at the value of the Sieder Tate constant. The Wilson plot was developed in 1915 by Wilson [16], and has been modified by several researchers since. The procedure used in this research was developed by Briggs and Young [17].

The Wilson plot is merely a plot of $1/U_n$ versus the inverse of the Sieder Tate parameter which should be a

straight line when varying the cooling water velocity. The reasoning behind the Wilson plot can be seen in the following development.

The overall heat transfer coefficient can be written as:

$$U_n = \frac{1}{\frac{D_o}{D_i h_i} + R_w + \frac{1}{h_o}} \quad . \tag{7}$$

The inverse of equation (7) is:

$$\frac{1}{U_n} = \frac{D_o}{D_i h_i} + R_w + \frac{1}{h_o} \quad . \tag{8}$$

If $(R_w + \frac{1}{h_o})$ is assumed to be constant and equation (6) is solved for h_i in terms of the Sieder Tate parameter, equation (8) can be rewritten as:

$$\frac{1}{U_n} = \frac{D_o}{c_i k_b} Re^{-0.8} Pr^{-1/3} (\mu/\mu_w)^{-0.14} + B \quad , \tag{9}$$

where $B = R_w + \frac{1}{h_o}$.

The form of equation (9) is then exactly that of a straight line,

$$Y = MX + B \quad , \tag{10}$$

where:

$$Y = \frac{1}{U_n} \quad , \tag{10a}$$

$$X = \frac{1}{\text{Sieder Tate parameter}} \quad , \text{ and} \tag{10b}$$

$$M = \frac{D_o}{c_i k_b} \quad . \tag{10c}$$

The values of $1/U_n$ and the Sieder Tate parameter are obtained by varying the water velocity and holding the other parameters, such as water temperatures, steam vapor temperatures and condenser tube wall temperature, nearly constant. When $1/U_n$ is plotted versus $Re^{-0.8} Pr^{-1/3} (\mu/\mu_w)^{-0.14}$, a linear regression subroutine [18] fits these points to a straight line and then solves for the slope, M, and the intercept, B. Knowing the slope, M, the Sieder Tate constant, c_i, can be found from equation (10c). The inside heat transfer coefficient, h_i, is then found from equation (6).

Once the inside heat transfer coefficient, h_i, is known, then the Nusselt number can be solved for in equation (6), to find the Stanton number,

$$St = \frac{Nu}{RePr} = \frac{h}{c_p G} \quad . \tag{11}$$

The cooling water properties (ρ, μ, k, c_p, Pr) are solved for as shown in Appendix D. Appendix D also demonstrates the procedure for arriving at the water viscosity evaluated at the condenser tube wall, μ_w.

c. Outside Heat Transfer Coefficient

The outside heat transfer coefficient, h_o, can now be found from equation (7). Figure 18 schematically illustrates the various steps outlined above.

d. Friction Factor

The friction factor for the test tube is found from:

$$f_{TS} = \frac{(\rho_b)(\Delta P_{TS})(144)(2g_c)}{4(L_{TS}/D_i)\ G^2} \quad . \qquad (12)$$

The variables used in equation (12) are solved for as shown in Appendix D, while the geometric constants are found in Table 3. ΔP_{TS}, however, is reduced from the measured pressure drop outlined below.

ΔP_{TS} is the pressure drop in the enhanced section of the test tube. The measured pressure drop, ΔP_m as seen in Figure 8, is taken over the entire tube length, a distance of 51-1/8 inches. Since the enhanced section is only 36 inches long, the pressure drop over each of the smooth ends must be subtracted off of the measured pressure drop. This is done by calculating the friction factor in the smooth ends using:

$$f_s = \frac{0.079}{Re^{0.25}} \text{ for } Re < 30{,}000 \quad , \qquad (13)$$

or

$$f_s = \frac{0.046}{Re^{0.2}} \text{ for } Re > 30{,}000 \quad . \qquad (14)$$

The smooth-end-section pressure drops can then be calcualted from,

$$P_s = \frac{(f_s)(4)(L_{TS}/D_i)(G^2)}{(\rho_b)(144)(2g_c)} \quad . \qquad (15)$$

As can be seen in Figure 13, the cross sectional flow area of the enhanced section of the test tube is less than the cross sectional flow area of the smooth end of the tube. Therefore, the water undergoes an expansion and a contraction at the exit and entrance to the enhanced section of the tube. Associated with the expansion and contraction processes are certain irreversible losses which cause additional pressure drops to occur. These pressure drops must also be subtracted off of the measured pressure drop and are calculated as shown in reference [19]:

$$\Delta P_{e/cn} = \rho v_{TS}^2 (K_e + K_{cn}) \quad . \qquad (16)$$

Since the variations in the contraction and expansion coefficients K_{cn} and K_e are slight over the range of Reynolds numbers used, an average of these values was used in equation (16).

Therefore, ΔP_{TS} is found using equations (15) and (16):

$$\Delta P_{TS} = \Delta P_m - \Delta P_s - \Delta P_{e/cn} \quad , \qquad (17)$$

and the friction factor for the test section is solved for in equation (12).

e. Performance Criteria

To compare the enhanced, or augmented tubes with the smooth tube, it was necessary to use some meaningful performance criteria.

Using the Colburn Analogy, as found in reference [20], provided one such criterion. Using this analogy, the heat transfer performance is compared to the friction-factor performance as seen in Appendix D.

Bergles [3] outlines several performance criteria based on the inside heat transfer coefficients by solving for the ratio of augmented to smooth tube areas while holding various parameters constant. One such ratio is defined by

$$\frac{A_a}{A_s} = \frac{h_s}{h_a} = \frac{Nu_s/Pr^{0.4}}{Nu_a/Pr^{0.4}} \quad , \tag{18}$$

which assumes that Q, $\dot{m}$, D_i, T_b and LMTD are constant, and $R_{ext} = R_w + 1/h_o = 0$. In equation (18) the augmented heat transfer coefficient h_a is the value h_i referred to earlier. In this situation the flow velocities for the smooth and augmented tubes are the same.

The area ratio defined by equation (18) does not, however, take into account the increases in pressure drop and hence the increases in friction factor caused by enhancement techniques. The increase in pressure drop can be included when evaluating the performance of an enhanced tube compared to that of a smooth tube. Bergles [3] shows this by defining

an area ratio for constant pumping power as well as for conditions as defined for in equation (18).

The pumping power is given by:

$$P = (\rho v \frac{\pi}{4} D^2) 4 f (\frac{L}{D}) (\frac{v^2}{2g_c}) \qquad (19)$$

$$= (\frac{\rho}{2g_c}) (\pi DL) f v^3 \quad ,$$

where πDL is the inside surface area for the tube in question. By setting the pumping power of a smooth tube equal to the pumping power of an enhanced tube, it is found that:

$$\frac{A_a}{A_s} = \frac{v_s^3 f_s}{v_a^3 f_a} = \frac{Re_s^3 f_s}{Re_a^3 f_a} \quad . \qquad (20)$$

Notice, that in this situation of constant pumping power, the flow velocities and hence Reynolds numbers are different for the smooth and the augmented tube.

The heat flow rate is given by:

$$Q = h_i A_i LMTD_i \quad . \qquad (21)$$

Since the heat flow is also assumed to be constant in both the enhanced and smooth tubes, the area ratio can be found

$$\frac{A_a}{A_s} = \frac{h_s}{h_a} = \frac{Nu_s/Pr^{0.4}}{Nu_a/Pr^{0.4}} \quad . \qquad (22)$$

Equation (20) can now be set equal to equation (22) to show:

$$\frac{A_a}{A_a} = \frac{Nu_s/Pr^{0.4}}{Nu_a/Pr^{0.4}} = \frac{Re_s^3 f_s}{Re_a^3 f_a} \quad . \tag{23}$$

If Nu_s is replaced in the above equation by the Dittus Boelter relationship as found in [15]:

$$Nu_s = 0.023 Re_s^{0.8} Pr^{0.4} \quad , \tag{24}$$

and f_s is replaced by equation (14):

$$f_s = \frac{.046}{Re_s^{0.2}} \quad , \tag{14}$$

equation (23) can be solved for the smooth tube Reynolds number in terms of the augmented conditions:

$$Re_s = \sqrt{\frac{Re_a^3 f_a}{2Nu_a/Pr^{0.4}}} \quad . \tag{25}$$

In these expressions,

$$Re_s = \frac{\rho D_i v_s}{\mu} \quad . \tag{26}$$

Knowing Re_s, equation (23) can be solved for the resulting area ratio.

Since a sizeable portion of the overall resistance in a naval condenser could be caused by the wall resistance and the outside thermal resistance, the area ratios as defined

by Bergles [3] should be expanded to include these external resistances. If the heat flow is written by equation (2):

$$Q = U_n A_n \text{ LMTD} \quad , \tag{2}$$

and a thin wall thickness is assumed, then the external resistance effects on the area ratio can be included in the analysis. The wall thickness must be assumed to be small since the nominal area is based on an outside diameter of 5/8-inch.

Invoking all of the assumptions made earlier, then the results of the constant pumping power case are again:

$$\frac{A_a}{A_s} = \frac{v_s^3 f_s}{v_a^3 f_a} \quad . \tag{20}$$

In addition, constant heat flow results in:

$$\frac{A_a}{A_s} = \frac{U_s}{U_a} \quad . \tag{27}$$

As before, these two area ratios can be set equal, and it is found that:

$$\frac{A_a}{A_s} = \frac{U_s}{U_a} = \frac{v_s^3 f_s}{v_a^3 f_a} \quad . \tag{28}$$

As mentioned by Search [1], for smooth tubes, it is found in general that:

$$U_s = C \sqrt{v_s} \quad , \tag{29}$$

where C is a constant for a given tube size, material and water inlet temperature. Also, from equation (14), it is known that

$$f_s = \frac{.046}{Re_s^{0.2}} \quad . \tag{14}$$

By choosing v_a, U_a, and f_a and substituting equation (26) for Re_s into equation (14), equation (28) can be solved for the corresponding smooth tube velocity, as:

$$v_s = \left[\frac{f_a\, v_a^3\, C}{(U_a)(.046)} \left(\frac{\rho D_i}{\mu}\right)^{1/5}\right]^{\frac{1}{2.3}} \quad . \tag{30}$$

Knowing v_s, then equation (29) is solved for U_s and equation (28) is solved for the area ratio.

In selecting the values of the constants to substitute into equation (30), the following procedures were utilized:

(1) U_a was corrected to 70°F using the procedure defined in reference [21],

(2) C was determined by using the values of U_n and v for the smooth copper-nickel tube in run 4, and solving for C in equation (29). The value for C is not a constant over the range of flows observed, therefore, an average value of C = 251, was obtained and used. The resulting error in U_s at any velocity was less than 7 percent.

(3) The dynamic viscosity used was an average value of the viscosities at each flow point used in the area ratio analysis.

See Appendix F for a summary of the area ratio procedures and the results for both cases where $R_{ext} = 0$ and $R_{ext} \neq 0$.

2. Reduction Based on the Hydraulic Diameter, D_h

The reduction procedures for this method were similar to the procedures used for the reduction based on D_i. The major obstacle in obtaining meaningful results was in determining the enhanced section's geometry, and once determined, how best to apply it to the available equations.

a. Enhanced Section Geometry

It is well-known how critical the measurement of the hydraulic diameter is to heat transfer and fluid flow. There were two alternative methods available and both were examined. The volumes of the enhanced tubes were measured and, by using the length of the tube, the cross-sectional area was obtained. Knowing the cross-sectional area and using the perimeter information provided by General Atomic, a hydraulic diameter could be found. This diameter was discarded in favor of the diameter found by using a planimeter to measure the wetted perimeter from an enlarged view of Figure 13. The hydraulic diameter is then found from:

$$D_h = \frac{4A_c}{Pw} \quad . \tag{31}$$

Similar problems were encountered in determining the wall thickness and subsequent wall resistance. See Appendix G for details of this procedure.

b. Heat Transfer Coefficients

To introduce this geometry into the equations used to solve for the heat transfer coefficients, it is first necessary to recall that the resistance to heat flow across a tube is equal to the sum of the individual resistances as shown earlier. Therefore,

$$\frac{1}{A_o U_o} = \frac{1}{A_o h_o} + \frac{R_w}{A_{met}} + \frac{1}{A_i h_i} \quad , \tag{32}$$

where:

$$A_o = 2\pi \, Pw_o \, , \tag{33}$$

$$A_i = 2\pi \, Pw_i \, , \text{ and} \tag{34}$$

$$A_{met} = 2\pi \, P_{bar} \, . \tag{35}$$

By setting $1/A_o U_o = 1/A_n U_n$, and multiplying through by A_o allows us to obtain the overall heat transfer coefficient based on the same nominal geometry that was used in the plain-end reduction. The equation takes the form:

$$\frac{A_o}{A_n U_n} = \frac{1}{h_o} + \frac{A_o R_w}{A_{met}} + \frac{A_o}{A_i h_i} \quad . \tag{36}$$

Equation (36) is solved exactly as was equation (8) in section B. 1.a. of this chapter to obtain the Wilson plot. The inside

and outside heat transfer coefficients (h_i and h_o) are then solved for as they were in the plain-end reduction except as modified by the different geometry. The equations used are listed in Appendix D.

Equation (36) was verified by comparing the results of the copper-nickel and aluminum smooth tubes for equation (36) to the results obtained using the equations derived from equation (8).

c. Friction Factor

The analysis for this reduction scheme is identical to the smooth end reduction scheme except as modified by the different geometry used.

d. Performance Criteria

The area ratios were not used in the reduction based on the hydraulic diameter.

The Colburn Analogy was used exactly as for the smooth end reduction case described earlier, and shown in Appendix D.

3. Computer Program

A computer program was developed to facilitate both rapid and consistent reduction of the data. A flow diagram is shown in Figure 19. Appendix H is a listing of the program. The program can essentially be divided into four regions.

Region 1. In this section, the transport properties and flow characteristics are determined. The equations used for the transport properties were obtained from reference [22].

Region 2. In this section, the heat transfer coefficients are found.

Region 3. The enhanced section pressure drop and resulting friction factor are found in this section.

Region 4. In this section, the ratio of heat transfer performance to friction factor performance is found. The area-ratio equations were not programmed at this time, but could be included at a future date.

The program development was such that the data would be evaluated for both the smooth end diameter geometry and the hydraulic diameter geometry each time the program was activated. This was done using a simple interation technique and a series of logic statements. The copper-nickel smooth tube and the aluminum smooth tube were used to proof the hydraulic diameter geometry section of the program as mentioned above.

IV. RESULTS AND DISCUSSION

A. INTRODUCTION

Table 3 lists the various runs made and the corresponding tubes used during these tests. Tables 4 through 12 contain all the data used to evaluate the performance of the enhanced and smooth tubes.

It is seen in Table 3 that several more runs were made for tube 1 and tube 4 than the other tubes. Tube 1 was the first tube tested and, therefore, the procedures for testing the enhanced tubes were evaluated using this tube. Run 3 on 11 October 1977 was conducted with a twisted tape installed at the tube inlet. These tapes were provided with each tube and were manufactured such that they had the same helix angle as their respective tube. The results of this run can be found in Table 13. Basically, the pressure drop increased by about 15 percent without a corresponding increase in the heat transfer performance as compared to the results of run 2. It was originally intended to include the twisted tape tests within the scope of this experiment, but due to time constraints further testing using these tapes was not done.

Run 7 on 7 November 1977 was conducted solely for the purpost of making a movie of the alternate flooding and draining between the flutes of the 45^{o} HA enhanced tube. The movie was filmed such that views of the alternate flooding and draining would be seen as viewed from the top as well as from the bottom of the tube.

Figure 20 is a sequence of six frames from this movie. The arrow on the top left frame points to a short length of reflected light. In the next frame down, the arrow points to the same spot, but the reflected light now appears to be about twice as long as it was in the first frame. In the third frame down, it is seen that the length of light is about the same as it was in the top frame. The sequence of three frames to the right show the same type of behavior, but in a different spot on the periphery of the tube. This figure demonstrates how the condensate builds up in the troughs to a certain level and then drains off as drops fall off the bottom of the tube. The set of three frames on the right demonstrates how this flooding and draining shifts from trough to trough. As the movie is viewed, the periodic nature of this alternate flooding and draining is evident.

Run 11 was the repeatability run for the 45^{o} HA tube. The results of this run were compared to the results of run 2. As can be seen in Tables 14 and 15, the results are well within the experimental error band. The Sieder Tate constant for run 2 is about 0.081 while in run 11 it is about 0.078, a difference of less than 4 percent.

Both tube 2 and tube 3 results were repeatable as can be seen in Tables 16 and 17 for the 30^{o} HA tube and Tables 18 and 19 for the 60^{o} HA tube. Run 10 on 5 January 1978 was a poor run; therefore, the results of this run are not included.

Run 4, taken with the copper-nickel smooth tube, was conducted to insure that this experimenter could duplicate other

experimenters' results for a smooth tube. As can be seen in Table 20, the Sieder Tate constant was about .025 as compared to .027, the value most often found in the literature.

Runs 5 and 6 were conducted to determine the effect of the wall thermocouple location on the wall temperature recorded. It was determined that the circumferential location of the thermocouple had a profound impact on the value of the wall temperature. For this reason, all of the data runs were conducted with the wall thermocouple located on the bottom of the tube, thus insuring that the location of the wall thermocouple would not introduce unaccountable differences in the results.

Since a linear regression subroutine was used to obtain the slope for the Wilson plot, the heat transfer information obtained was very much dependent on how well the linear regression program could fit the data. Figure 21 shows that the generated curve fit the data very well.

B. RESULTS BASED ON FLOW RATES USING 1.48 GPM AND 18.8 GPM ROTAMETERS

The 1.48 gpm rotameter was installed so that more points at low cooling water velocities could be included in the analysis. It was installed after the initial data runs were completed, since it was felt that information in the range of velocities from 1 to 4 ft/sec would be useful when evaluating the performance of the augmented tubes. This required that the results for velocities over the range of both

rotameters be compared to the results for velocities over the range of just the 18.8 gpm rotameter. The heat transfer results for the range of flow velocities for both rotameters did not compare well with the heat transfer results obtained for the flow velocities for just the 18.8 gpm rotameter. It was found however that by basing the results of the later runs on the flow velocities over the range of the 18.8 gpm rotameter only, repeatability of the results for the initial data run was possible.

After a careful examination of the results, it was determined that the reason for this anomaly was due to variations in the outside heat transfer coefficient at low velocities. Since at low flow velocities the average cooling water temperature increases, the tube wall temperature also increases which in turn causes the outside heat transfer coefficient to vary significantly as can be seen from Nusselt's equation [15]:

$$h_o = c_o \left[\frac{\rho(\rho-\rho_v)\, g\, h_{fg} k_f^3}{\mu_f\, D\, (T_v - T_w)}\right]^{1/4} . \qquad (37)$$

The overall heat transfer coefficient, based on the outside area, is a function of h_i, h_o, and R_w as discussed earlier and as seen in equation (7) which is re-written below:

$$U_n = \frac{1}{\frac{D_o}{D_i h_i} + R_w + \frac{1}{h_o}} . \qquad (7)$$

As was shown in Chapter III, equation (7) is reduced to the form of a straight line where h_i is a function of the Reynolds number and thus the water velocity, assuming both the wall resistance and h_o remain constant over the range of water velocities used. The fact that h_o, as shown by equation (37) above, may not be constant at low water velocities violates one of the basic requirements of the Wilson Plot technique. Since, at low velocities, it is impossible to keep the variation in h_o small, the Wilson Plot for the flow velocities of the 1.48 gpm and 18.8 gpm rotameters together will yield a significantly different value for the Sieder Tate constant than for the velocities over one rotameter's range. This is seen in Figure 22. By superimposing a straight line over the 1.48 gpm rotameter points, it is obvious that the slope of the straight line would be greater than that of the straight line obtained from the linear regression subroutine [18]. On the other hand, if a straight line is superimposed over the 18.8 gpm rotameter points, a slope somewhat less would be realized. The smaller slope would in turn result in a higher Sieder Tate constant as seen in equation (10c). This is precisely what happens when the 1.48 gpm rotameter points are not used in evaluating the data.

Since the initial data runs were taken without the 1.48 gpm rotameter points, and since the pressure drop information is felt to be more reliable at the higher velocities through the test tube, the results that follow therefore, are presented based on the 18.8 gpm rotameter points only unless specified otherwise.

C. PRESSURE DROP RESULTS USING THE PRESSURE TAP TUBES

The General Atomic Co. was successful in drilling three 0.024 inch diameter holes into the test section of three spirally fluted tubes similar to the heat transfer test tubes. (See Figures 14 and 15.) These tubes were connected to the pressure drop measurement system independently, and the pressure drops were measured at different water flow velocities through these tubes. The pressure drop measurements are summarized in Tables 21, 22, and 23. Figure 23 is a plot of the pressure drop for 60 percent flow through the 18.8 gpm rotameter for each of the three different General Atomic tubes. Note the linear variation of the pressure drop along the length of the tubes. Using this pressure drop information, it was possible to compute the friction factor inside the test section without having to apply any corrections. It was also possible to examine the actual expansion and contraction losses caused by the abrupt geometry change in the test tube.

The expansion and contraction losses were obtained by computing the appropriate pressure drops using equations (38) and (39) below:

$$\Delta P_{cn} = \Delta P_{5-6} - \Delta P_{Ac} - \Delta P_T - \frac{\Delta P_{s'}}{2} \qquad (38)$$

$$\Delta P_e = \Delta P_{2-6} - \Delta P_{5-6} - \Delta P_{5-3} - \Delta P_T + \Delta P_{Ac} - \frac{\Delta P_{s'}}{2} . \qquad (39)$$

where $\Delta P_{2-6,\ 5-6,\ 5-3,}$ are the pressure drops across the pressure tap tubes as seen in Figure 15, and where:

$$\Delta P_{Ac} = \frac{\rho_v 2}{2g_c} \left(1 - \sigma^2 \right) \tag{40}$$

$$\Delta P_T = \frac{\Delta P_{3-5}}{L_{3-5}} \left(36 - L_{3-5} \right) \text{ , and} \tag{41}$$

$\Delta P_{s'}$ = is the pressure drop across the smooth end of the tube between the hydraulic diameter section and tap 2 or tap 6.

Now the abrupt exit and entrance coefficient can be determined using equations (42) and (43):

$$K_{cn} = \Delta P_{cn} \frac{2g_c}{\rho v_{TS}^2} \text{ ,} \tag{42}$$

$$K_e = \Delta P_e \frac{2g_c}{\rho v_{TS}^2} \text{ .} \tag{43}$$

These values were found at specific flow velocities and then an average of these values was used in reducing the overall pressure drop to the pressure drop in the three foot enhanced section. Tables 24, 25, and 26 summarize this procedure.

Knowing K_{cn} and K_e and using equation (12) the friction factor inside the enhanced section was determined as outlined in Chapter III. Tables 27, 28, and 29 summarize the friction factors for the PT tubes. See Appendix H, sample calculations for PT tubes, for an in-depth demonstration of the procedure.

As can be seen when comparing the friction factors found in Table 14 to those found in Table 28, the friction factors

found by reducing the pressure drop using the values of K_{cn} and K_e as found in [20], are significantly different than the friction factors found by reducing the pressure drop using the values of K_{cn} and K_e found in this experiment.

The pressure drop across the PT tubes was significantly higher than the pressure drop across the corresponding tubes manufactured for the heat transfer measurements. The most obvious reason for this difference in pressure drop was due to the differences in the internal geometry of the pressure tap tubes as compared to the heat transfer tubes. The PT tubes were not from the same stock that the actual test tubes were from, but in fact they were tubes that had been manufactured earlier in order to test out the manufacturing technique. Since there is no convenient way of verifying the geometry of the PT tubes, the results presented hereafter are based upon the pressure drop measurements taken with the heat transfer tubes, using the data reduction scheme mentioned earlier. This procedure was used knowing that there is an error in the expansion and contraction loss factors.

D. RESULTS BASED ON THE SMOOTH END DIAMETER, D_i

In as much as the primary purpose of this experiment was to evaluate the performance of the augmented-condenser tubes manufactured by General Atomic, composite plots comparing the various performance parameters of these tubes and smooth tubes are provided. Although it would be highly desirable to compare these special tubes with other augmented tubes of

different geometries, comparison with existing results was avoided in most cases due to differences in experimental conditions. The reason for this is due to the uniqueness of this test facility as well as the fact that there are probable differences in the data reduction schemes.

1. Heat Transfer Coefficients

The first comparison is in Figure 24, which shows the corrected overall heat transfer coefficient versus mass flow rate. As expected, the enhanced tubes' overall heat transfer coefficients are superior to the overall heat transfer coefficients for the smooth tubes. At a cooling water mass flow rate of 1.3 lbm/sec, it is seen that the smooth tubes (both aluminum and copper-nickel) have a corrected overall heat transfer coefficient of approximately 1100 BTU/hr·ft^2 ^{o}F and that the 45^o HA enhanced tube has a coefficient of approximately 1689 BTU/hr·ft^2 ^{o}F. This is a 53 percent increase in corrected overall heat transfer coefficient for the General Atomic tube over the smooth tubes. If the overall heat transfer coefficients of the three augmented tubes are compared, it is seen that the 60^o HA tube (Table 3, Tube 3) outperforms the other two augmented tubes. The reason for this is clearly seen in Tables 14, 16, and 18. The outside heat transfer coefficient is higher for the 60^o tube, thus the outside thermal resistance is smaller. As can be seen in equation (7) this makes U larger. The probable cause of this is that the steeper helix angle allows for better condensate

drainage off this tube when compared to the 30^{o} and 45^{o} tubes. This fact will be discussed in more detail in a following section.

The corrected overall heat transfer coefficient of the copper-nickel smooth tube and the aluminum smooth tube compare well up to about 1.3 lbm/sec. At higher mass flow rates, there appears to be some divergence in the data. It is suspected that an oxide film builds up on the exterior of the aluminum tube more than on the copper-nickel tube. This in turn caused the outside thermal resistance of the aluminum tube to be higher than the corresponding resistance in the copper-nickel tube. This can be seen by referring to Table 20 and Table 30 where the outside heat transfer coefficient for the aluminum tube is less than for the copper-nickel tube. The inside heat transfer coefficients are, however, comparable.

2. Pressure Drop and Friction Factors

Figure 25 is a comparison of the pressure drops versus mass flow rate for the tubes tested. As can be seen, the pressure drops of the enhanced tubes increase at a much faster rate than the pressure drop for the smooth tubes. Neither the 30^{o} HA tube nor the 45^{o} HA tube has as dramatic a pressure drop as the 60^{o} HA tube. The reason for this is easily seen when referring to Figures 12 and 13. The flutes on the 30^{o} HA tube have the most gentle departure from the tube axis while the flutes on the 60^{o} HA tube have the most profound departure. Therefore, the flutes on the 60^{o} HA tube approach the geometry of straight radial fins which merely protrude into the inside

of a smooth tube, causing significant turbulent mixing to occur. The flutes on the 30^{o} HA tube are such that they tend to impart more swirl to the fluid, with less turbulent mixing.

These facts are further evidenced by referring to Figure 26. The friction factor for the 60^{o} HA tube at a Reynolds number of 40,000 is approximately 0.057. The friction factor for the smooth tube at this Reynolds number is about 0.0059. The friction factor of the augmented tube is then nearly ten times that of the smooth tube. The 45^{o} HA tube and the 30^{o} HA tube do not experience as great an increase in the friction factor, however, the rise is, nevertheless, significant. As expected the friction factor for the 30^{o} HA tube has the smallest value among the enhanced tubes for $Re > 10,000$. Below this Reynolds number, the friction factor for the 30^{o} HA tube is greater than for the 45^{o} HA tube. The reason for this was felt to be caused by inaccuracies in reading the pressure drop at low flows.

3. Performance Criteria

In 1883, Reynolds [23] mathematically expressed, for smooth tubes, the analogy between heat transfer and momentum transfer as:

$$St = \frac{f}{2} \quad . \tag{44}$$

In 1933 Colburn [24] extended this analogy to include Prandtl number effects:

$$St\ Pr^{2/3} = \frac{f}{2} \tag{45}$$

The Colburn Analogy then provides a useful method to compare the performance of the enhanced tube to the smooth tube. Figure 27 is such a comparison. It shows the tube performance factor, $2j/f$ as a function of Reynolds number. As can be seen, the ratio $2j/f$ is less than one for all three of the enhanced tubes, which indicates that the performance of these tubes is inferior to that of a smooth tube. But, as will be seen later, the tube performance factor is highly dependent on which tube diameter is used to evaluate the heat transfer and friction performance. The most important fact to glean from this figure, then, is the relative performance of the three enhanced tubes. The 30^{o} HA tube clearly outperforms the other two. The reason for this can be readily seen in Figures 28 and 26. Figure 28 shows that the inside heat transfer performance is very nearly constant for the three enhanced tubes while in Figure 26, the frictional resistance of the 30^{o} HA tube is seen to be much less than the other two tubes.

An area ratio such as defined by equation (22) in Chapter III can be found from Figure 28. In this figure, the Sieder Tate correlation is used in place of the Dittus Boelter correlation as used in equation (22). A value of $(Nu\ Pr^{-1/3}\ [\mu/\mu_w]^{-0.14})$ is found at the same Reynolds number for both the smooth tube and the enhanced tubes. The area ratio is then found by taking a ratio of these dimensionless groups. As can be seen, this area ratio would make the enhanced tubes appear to be very desirable for condenser use.

However, as explained in Chapter III, with this area ratio, the additional frictional resistance of the enhanced tubes is ignored. By evaluating the area ratio for a constant pumping power, these additional frictional effects are included in the results as shown in Figure 29.

The results in this figure, however, are for an external resistance equal to zero. As shown earlier, area ratios for a non-zero external resistance could also be found, and these results are plotted in Figure 30.

When Figures 29 and 30 are reviewed, the 30^{o} HA tube appears to have the best overall performance. The area ratio for this tube is under one over the entire range of Reynolds numbers used. In the range of Reynolds numbers that are of interest to the condenser designer (Re < 50,000) the highest area ratio is for the 45^{o} HA tube and is approximately 0.67. There are three facts of interest to note here. First, it appears that any of the three tubes tested would outperform the smooth tube. Secondly, the area ratio for the 60^{o} HA tube is less than the area ratio for the 45^{o} HA tube in Figure 30, while the opposite is true in Figure 29. The reason for this is felt to be caused by the higher external resistance in the 45^{o} HA tube than in the 60^{o} HA tube. This is seen in Table 14 and Table 18 wherein h_o is found to be on the average, 200 BTU/hr·ft^2 ^{o}F larger for the 60^{o} HA tube than for the 45^{o} HA tube. It is noted in Figure 29 that the area ratios are very nearly constant. This interesting fact apparently signifies that the ratio of heat transfer performance to hydrodynamic performance is constant, much the same as for the

smooth tube. Finally, when comparing Figures 29 and 30, the taking into account of R_{ext} has a significant effect on the results. The area ratio, as should be expected, will increase when the wall resistance is taken into account.

The uppermost curve and the lowest curve on Figures 29 and 30 are reproduced from Figure 9, Bergles [3], and are for an assummed $R_{ext} = 0$. These curves were reproduced herein to indicate the relative performance of the General Atomic tubes against the tubes included in reference [3].

Figures 31 and 32 are Figures 1 and 2 from reference [3] with the 30^{o} HA tube's results plotted thereon. In Figure 31, it is seen that the 30^{o} HA tube compares very favorably with the tubes included in reference [3]. Figure 32 shows the friction factor of the 30^{o} HA tube to be slightly above the average of the existing data. Of the tubes appearing on Figure 31 and Figure 32, tube 9, a repeated rib tube tested by Webb [25] apparently comes the closest to duplicating the General Atomic tube's performance. However, it must be remembered when comparing these tubes that they are all tested under different conditions which could affect their performance.

E. RESULTS BASED ON THE HYDRAULIC DIAMETER, D_h

The major thrust of this section is to permit the comparison of the augmented tubes based on their respective hydraulic diameters, in lieu of comparing them based solely on their

smooth end inside diameter. Consequently, it is recognized that this section will be of interest primarily to heat transfer experimenters.

As mentioned previously, the diameter used to compute such parameters as the Reynolds number and Nusselt number is extremely critical to the results. In reducing the data obtained in this experiment, the hydraulic diameter was found from the geometry of the enhanced section. As expected, the hydraulic diameter was much smaller than the plain end diameter. The effect of this is immediately seen in Table 31 through Table 36, the summaries of the enhanced section results. For example, for equal mass flow rates the Reynolds number will decrease and the mass flow rate per unit area will increase when compared to the smooth end diameter results. This in turn will cause the other results to change as well.

1. Heat Transfer Results

The inside and outside heat transfer coefficients are both smaller in value for the results based on the hydraulic diameter in comparison to the smooth end results. The major reason for this is due to the fact that the actual surface areas of the enhanced sections are larger than the surface area at the smooth ends. As shown in Chapter III, the heat transfer rate can be computed as:

$$Q = U_n A_n \text{ LMTD} = U_o A_o \text{ LMTD} \quad . \qquad (2)$$

For a measured value of Q and LMTD, the UA product must

remain constant. Using equation (32), it is easily seen that if A_i and A_o both increase when using the hydraulic diameter reduction scheme, it follows that the inside and outside heat transfer coefficients must decrease. In addition, as would be expected, the Nusselt number and Stanton number also decrease as seen in the tabular results.

2. Friction Factor

The friction factor found using the hydraulic diameter is much less than the corresponding friction factor using the smooth end diameter, as seen when comparing Figure 33 with Figure 26. The reason for the smaller friction factor is seen in the following friction factor equation:

$$f_{TS} = \frac{(\rho_b)(\Delta P_{TS})(144)(2g_c)}{4(L_{TS}/D)\ G^2} \quad . \qquad (46)$$

Since G, the mass rate of flow per unit area, is inversely proportional to diameter squared, then the friction factor is proportional to D^5. Since D_h is less than D_i, then the friction factor will decrease accordingly. As can be seen in Figure 33, however, the friction factor for the 30^o HA tube is less than the corresponding friction factor for a smooth tube. Since this is not reasonable, the hydraulic diameter used herein may be somewhat questionable. The 60^o HA friction factor is again very high and apparently becomes asymptotic at a Reynolds number of about 50,000. Both the friction factor curve for the 30^o HA tube and the friction factor

curve for the 45° HA tube have a similar shape to the curve for the smooth tube as seen in Figure 33.

3. Performance Criteria

As seen in Figure 34, the tube performance factor 2j/f, when using the hydraulic diameter, increases significantly for all three helix angle tubes when compared to the results based on the smooth end diameter.

F. ISOTHERMAL FRICTION FACTOR VERSUS NON-ISOTHERMAL FRICTION FACTOR

Pence [13] compared the isothermal friction factor with the non-isothermal friction factor for the smooth tube. His results showed a negligible difference. Isothermal friction factors were also found for each of the enhanced tubes tested in this experiment. The results are summarized in Tables 37, 38, and 39. Figure 35 compares the two friction factors for the 45° HA tube. As can be seen, the isothermal friction factor is higher than the non-isothermal friction factor up to a Reynolds number of about 40,000. At this value they apparently merge and remain approximately the same.

The reason for the lower friction factor with heat addition at the lower flow velocities is thought to be a result of the decrease in the measured pressure drop for these runs as compared to the isothermal runs. The reason for the reduced pressure drop must mean that less energy is expended to force the water through the enhanced tube under heated conditions.

Consequently, there must be some phenomenon occurring within the tube to aid the flow. It is felt perhaps that secondary flows generated within the flutes are enhanced by the heat addition. This fact was speculated by General Atomic and Figure 35 supports this. At the lower flow velocities, the heat input per lbm of water is greater than at the higher flow rates where the water residence time in the tube is less. Thus it would be expected that if the heat input did in fact enhance the secondary flow in the flutes, the difference in the isothermal and non-isothermal friction factors would be greatest at the lower velocities, as verified in Figure 35.

G. TUBE DRAINAGE AND HOW IT AFFECTS h_o

As is very evident when reviewing the summary of results in the tables, the outside heat transfer coefficient h_o decreases for the enhanced tube when compared to the results for the smooth Cu/Ni tube.

As noted earlier, one very important factor is the oxide film that apparently forms on the aluminum surfaces. Based on the differences in h_o for the results of run 4 and run 14, the degradation could be as high as 10 percent.

Perhaps, though, a more important factor to consider is tube condensate drainage. Because of the exterior flutes, and the high surface tension of the water, as condensation takes place, these grooves tend to flood with condensate, which drops off the tubes at regular intervals. As the

space between adjacent flutes fills with condensate, the thermal resistance on the outside increases. It is seen that the 60^{o} HA tube has the highest outside heat transfer coefficient among the enhanced tubes. The obvious reason for this is that the flutes are more conducive to condensate drainage than either the 45^{o} or 30^{o} HA tubes. This is so because the angle is 60^{o} to the tube axis which means that the effect of gravity on the water in the flutes is greater for this tube than for the others, thus providing for better drainage.

V. CONCLUSIONS

As a result of the above-mentioned tests, the following conclusions are reached.

1. The overall heat transfer coefficient of the General Atomic Co. tubes is superior to that of a smooth tube. The increase in the overall coefficient, when corrected for wall resistance, varied from about 1.5 to 1.75 times the corresponding smooth tube value at the same mass flow rate of cooling water.

2. Significant enhancement was realized for the inside heat transfer coefficient in the General Atomic tubes when compared to the smooth tube. Results based on the smooth end diameter, show an increase of about 3.5 times the smooth tube's value. Results based on hydraulic diameter show an increase of approximately 2.

3. The outside heat transfer coefficient of the augmented tubes was approximately 10 to 20 percent less than the corresponding outside heat transfer coefficient for the smooth tube.

4. Friction factors of the enhanced tubes were larger than the corresponding smooth tube values. At a Reynolds number of 50,000, based on D_i, the friction factor for the 60^o HA tube increased by a factor of 10 over the value for the smooth tube.

5. The heat transfer coefficients (h_i, h_o, U_c) are highest for the 60^o HA tube. The friction factor is also the highest

for this tube. The increase in friction factor dominates the increase in heat transfer coefficients as exhibited by low tube performance factors, 2j/f.

6. The 30^{o} HA has the highest tube performance factor of the three General Atomic enhanced tubes. The tube performance factor is about 0.67 for data reduced based on D_i and as high as 2.0 for data reduced based on the hydraulic diameter.

7. Condenser tube surface areas could be reduced by up to 50 percent using the 30^{o} HA tube. Significant material savings are also possible using the 45^{o} HA or 60^{o} HA tube.

8. Using the enhanced tubes, the non-isothermal friction factor is less than the isothermal friction factor at the lower water velocities. Perhaps secondary flows generated in the flutes are enhanced by heat addition.

9. The range of flow velocities over which the Wilson plot can be accurately used is limited because at low flow velocities, it becomes virtually impossible to maintain h_o constant. The Wilson plot assumes all variables are constant except for h_i.

10. The aluminum tubes have a higher outside thermal resistance due perhaps to an oxide film. The aluminum smooth tube's overall heat transfer coefficient compares favorably with the copper-nickel smooth tube up to about 60 percent flow in the system. At this point the two overall heat transfer coefficients diverge and the aluminum tube is about 10 percent less than the copper-nickel tube.

11. The hydraulic diameter used for the enhanced tubes may be in error since the 30^{o} HA tube's friction factors are less than the corresponding friction factor for a smooth tube.

VI. RECOMMENDATIONS

The results of this experiment have been encouraging and hopefully the greatest contribution to heat transfer will be to create a curiosity that will cause others to conduct experiments that will begin to answer so many of the unanswered questions and of course, to provide further experimental evidence to support the results herein. In an effort to offer some ideas for further experiments, the following recommendations are made.

1. To fully realize the potential of this condenser test system as presently configured, as many of the augmented tubes available commercially as well as newly conceived tubes should be tested and ranked with other tubes. This will present to the designer of Naval condensers, as well as other designers, a clear and non-proprietary reference by which to evaluate his possibilities. Figures 36 and 37 show tubes manufactured by Spiral Tubing Corp. and Wolverine Division of Universal Oil Products Co. respectively, which are examples of tubes that can be tested and ranked in the future.

2. The enhanced condenser tubes used in this study should be tested in a vertical orientation. As was discussed earlier, in a horizontal orientation, the condensate fills the area between the flutes which has a detrimental effect on the outside heat transfer coefficient. It is felt that a vertical orientation would provide a better outside heat transfer

coefficient since superior tube drainage would result in a vertical orientation. A preliminary design for modifying the existing system to allow a vertical orientation of the condenser tube was made by this experimenter and will allow modifications at a minimal cost. Included in this design are also various baffle designs to permit different angles for steam entry into the condensing section of the condenser. By directing the steam at different angles across the condensing surface, an optimum entry angle may be found which will give the highest outside heat transfer coefficient.

3. Tests of the most promising tubes should be expanded to include testing of horizontal banks of tubes. This type of test is needed to determine how the condensate drainage of the upper tubes affects the lower tubes' heat transfer coefficient.

4. Further hydrodynamic testing of augmented tubes is required. The pressure drops and hence the friction factors of augmented tubes cannot be accurately predicted by existing methods; therefore, tests which permit the exact measurements of pressure drops on tubes of known dimensions should be conducted.

5. Pressure drop measurements of the augmented tubes under various degrees of heat addition to the cooling water should be accomplished. This is needed to determine how much the heat addition affects the secondary flows induced in the flutes, and the resulting pressure drop. Also, tests which permit flow visualization under both heat transfer conditions

and isothermal conditions would be desirable as this type of test could possibly shed light on secondary flow enhancement in these tubes.

6. The fouling characteristics of any tube under test should be determined. As discussed within this report, there is some evidence that the aluminum tube forms an oxide film that increases the thermal resistance. By manufacturing and testing identically dimensioned tubes of different material, this effect could be determined. In addition to the outer film, the extent of the fouling problem on the cooling water side of the tube has to be determined.

VII. FIGURES

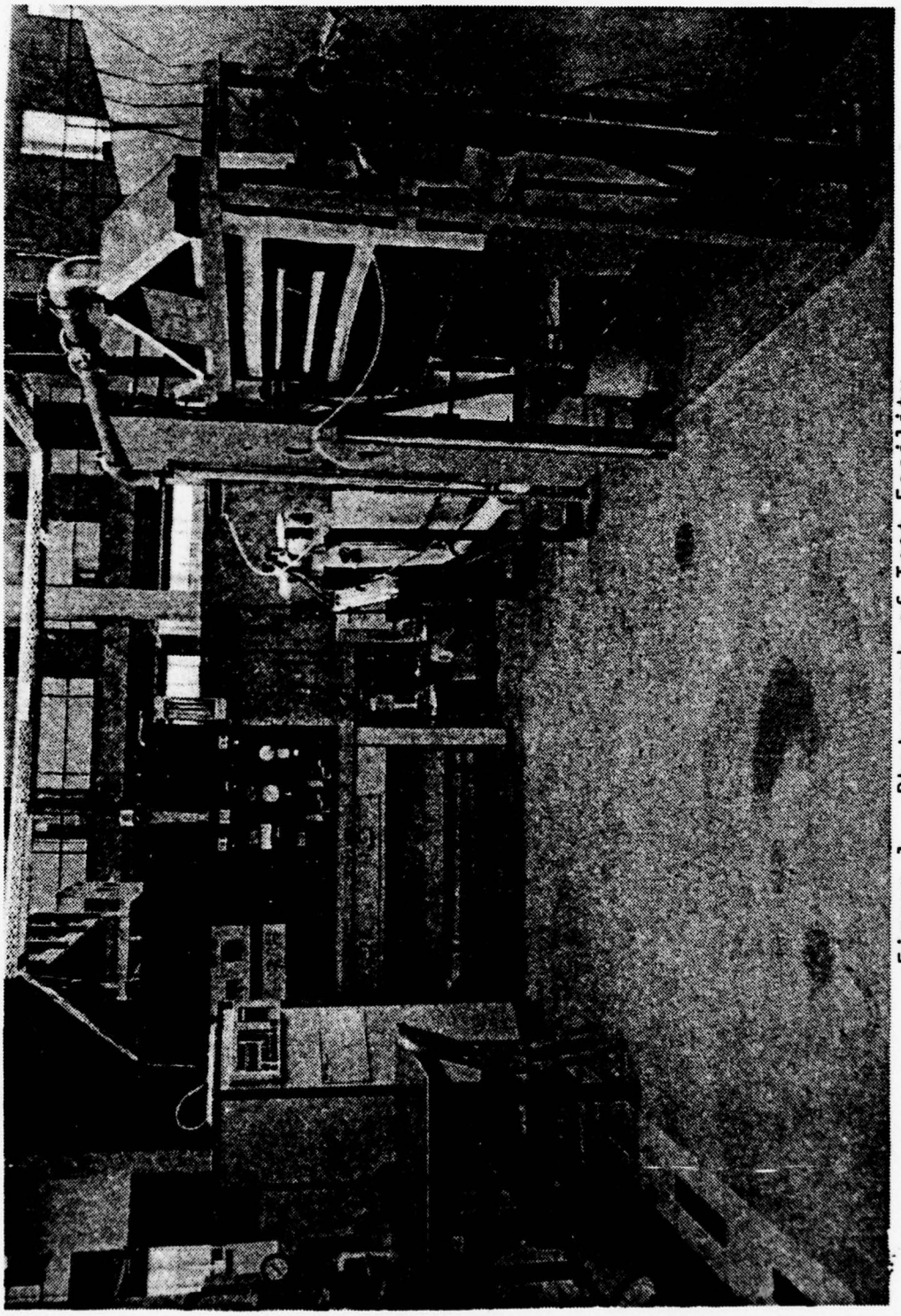

Figure 1. Photograph of Test Facility

STEAM SYSTEM

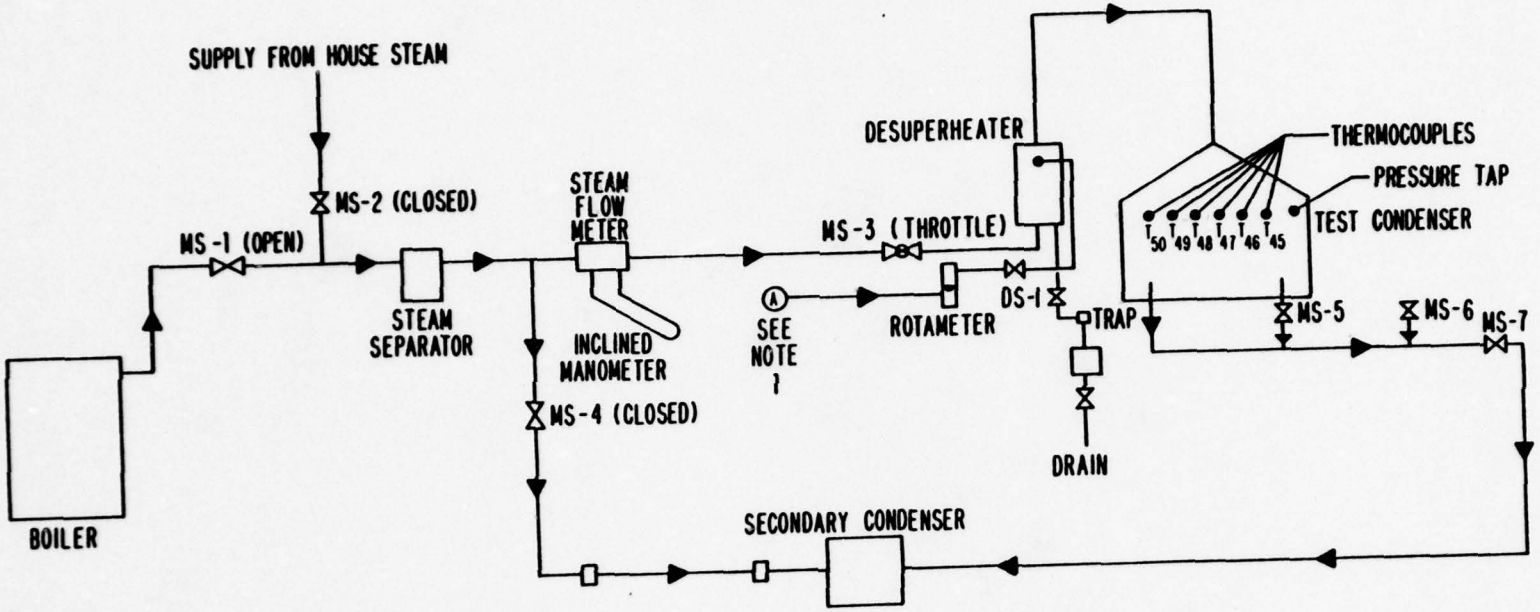

NOTE 1: FROM DISCHARGE OF FEED PUMP, SEE FIGURE 6.

Figure 2. Schematic Diagram of Steam System

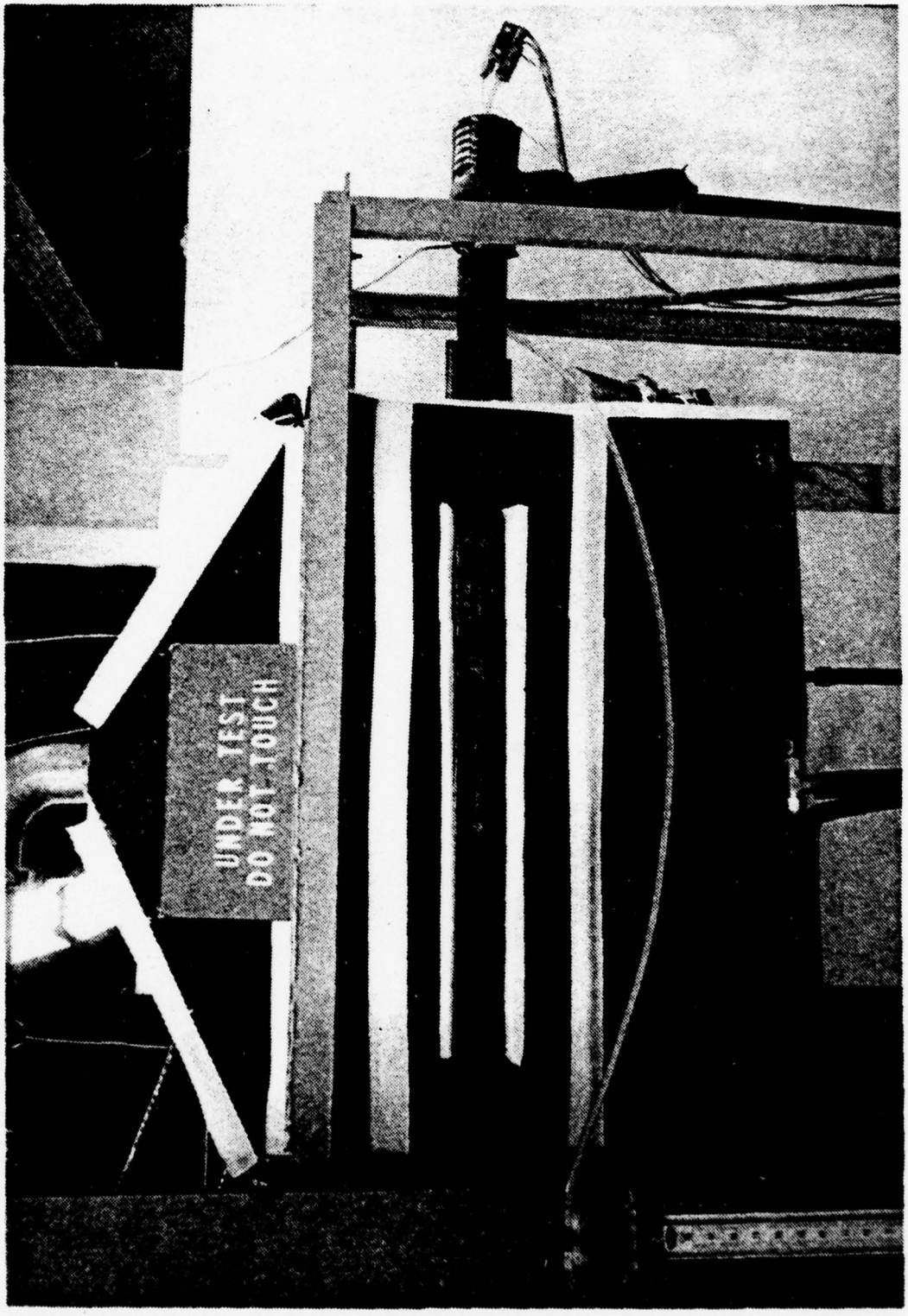

Figure 3. Photograph of Test Condenser with Insulation.

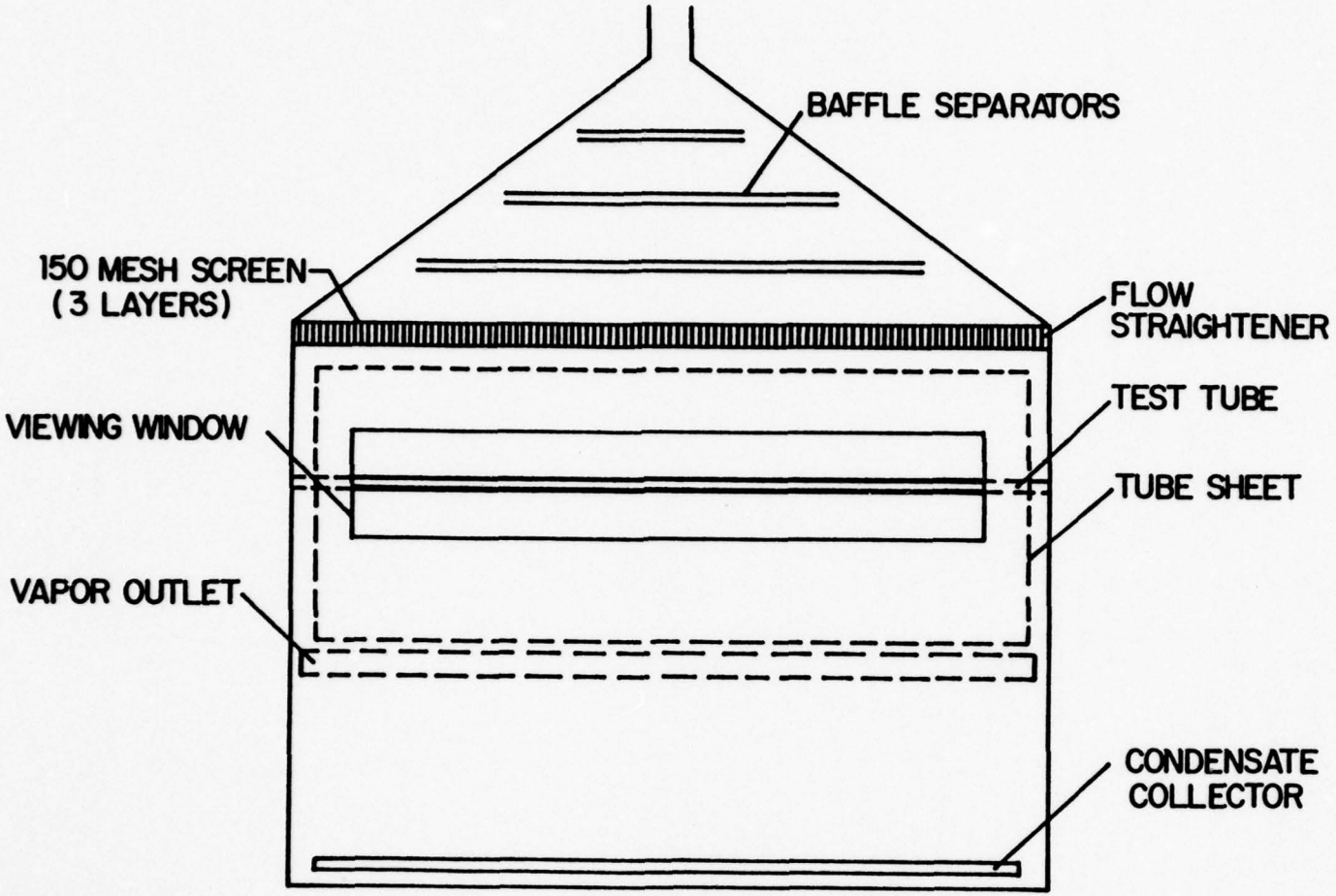

Figure 4. Test Condenser Schematic, Front View.

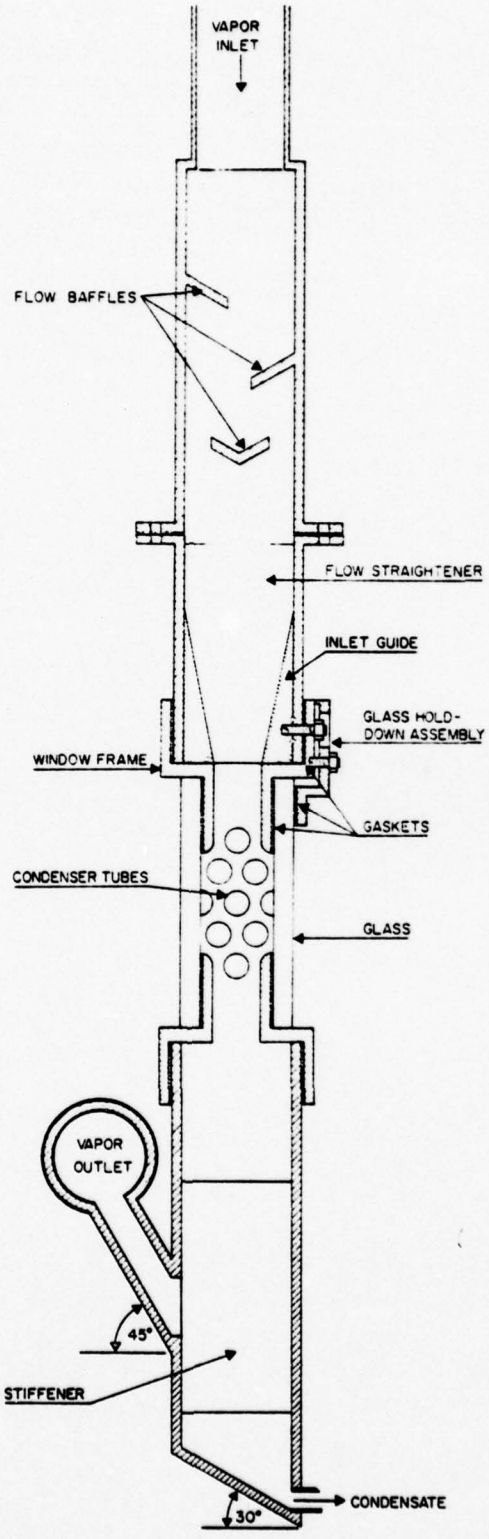

Figure 5. Test Condenser Schematic, Side View.

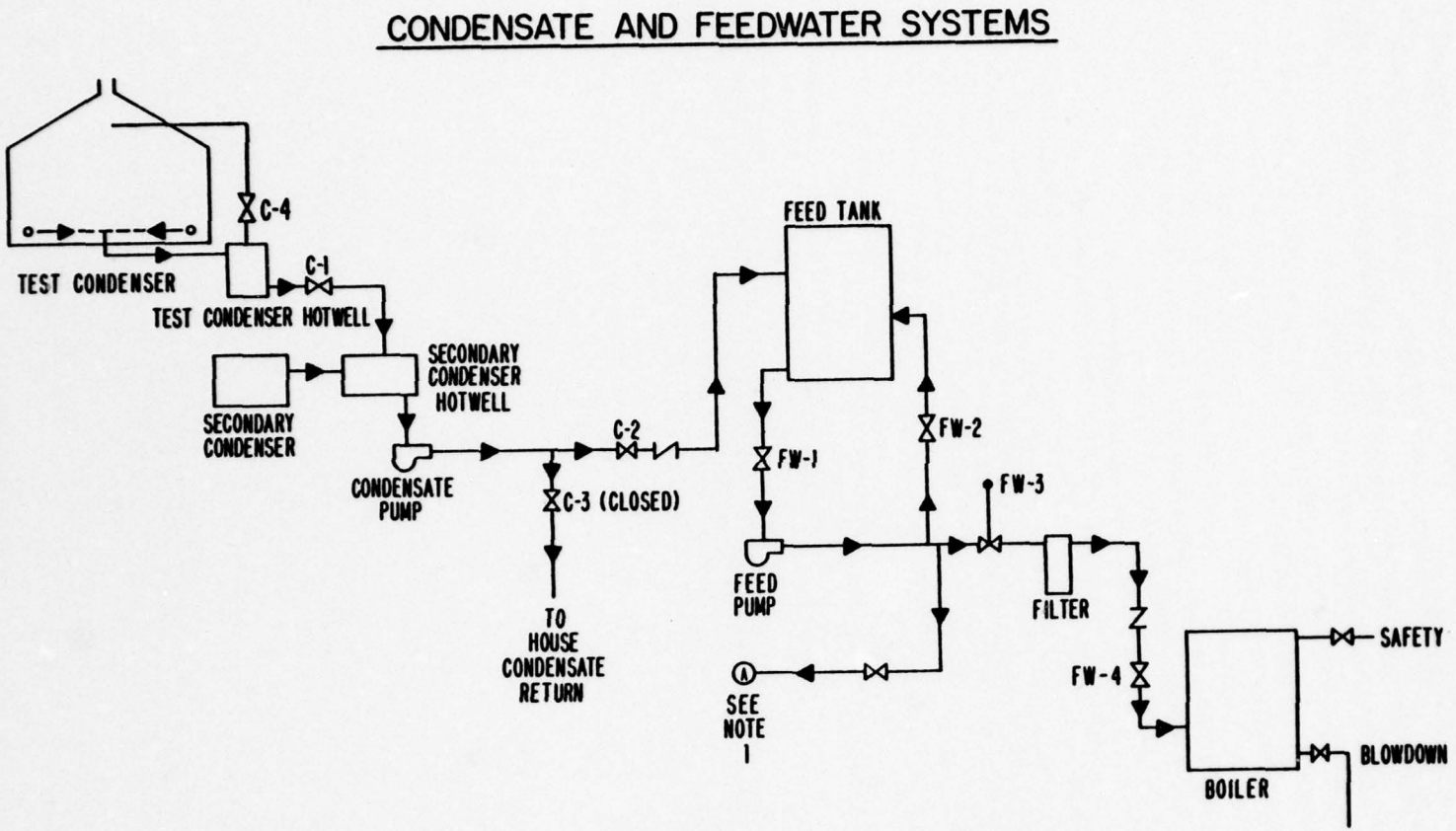

Figure 6. Schematic Diagram of Condensate and Feedwater System.

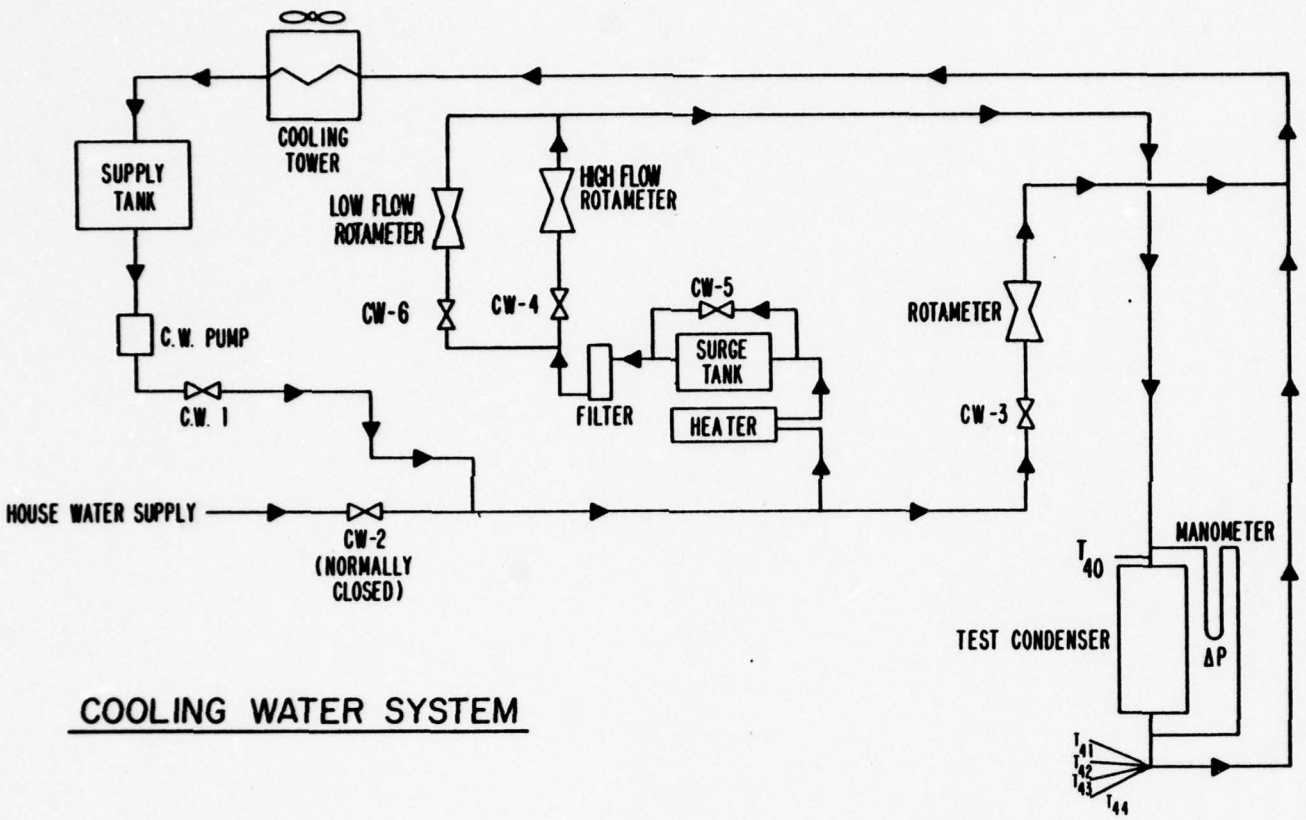

Figure 7. Schematic Diagram of Cooling Water System.

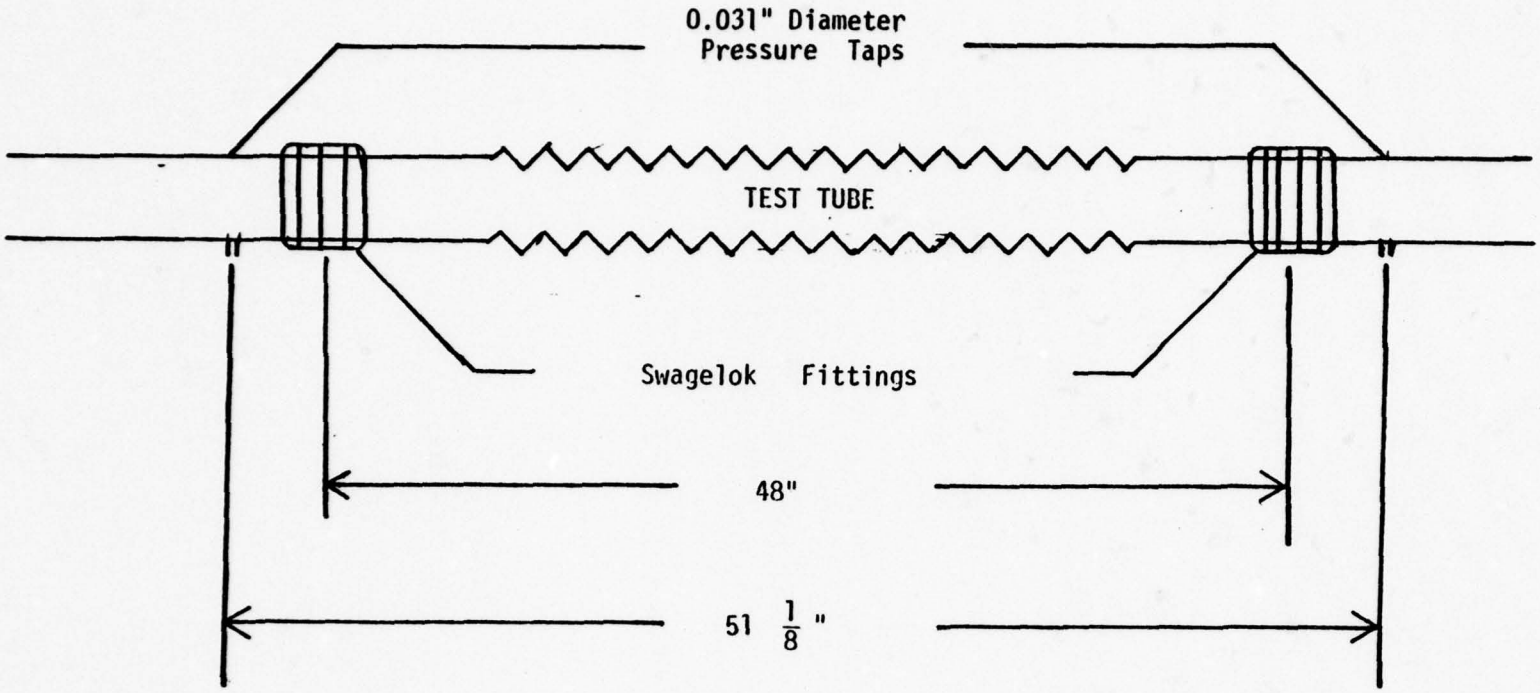

Figure 8. Enhanced Tube Schematic Drawing.

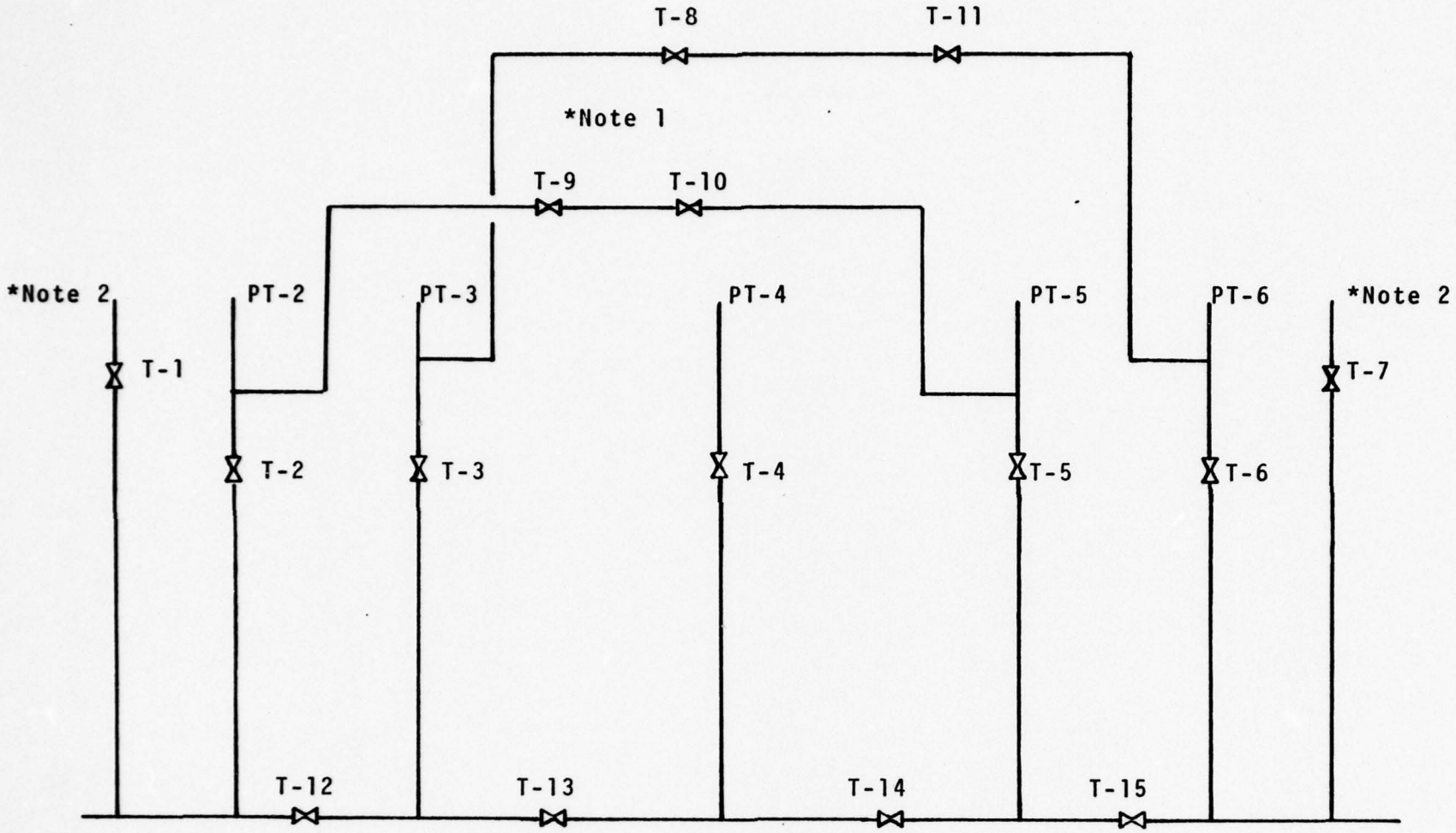

*Note 1 - Low Pressure Manometer Taps (Not Used).
*Note 2 - High Pressure Manometer Taps

Figure 9. Schematic Drawing of Pressure Tap System.

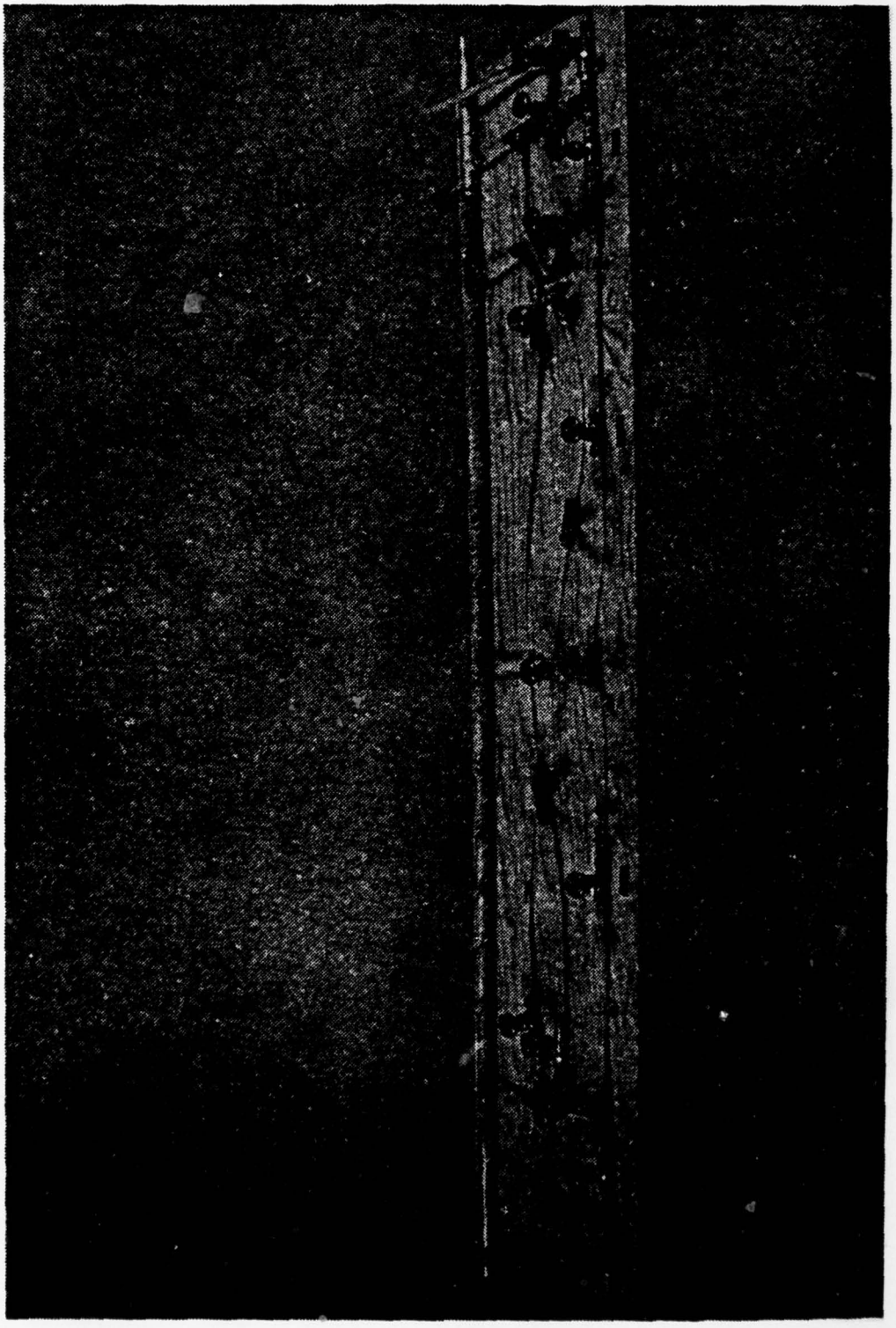

Figure 10. Photograph Showing Pressure Tap System Construction.

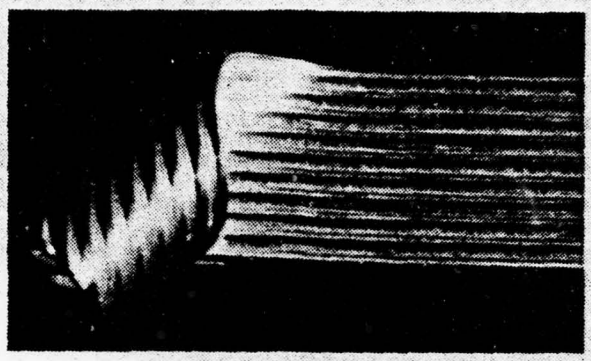

35-135-190-9

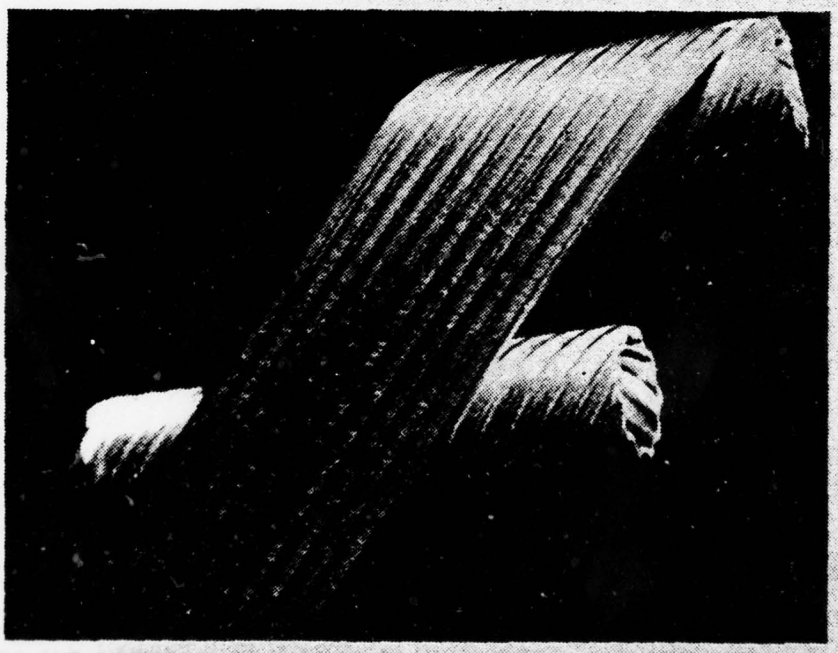

35-135-190-5

Figure 11. Photograph of Forming Process, Spirally Fluted Tubes.

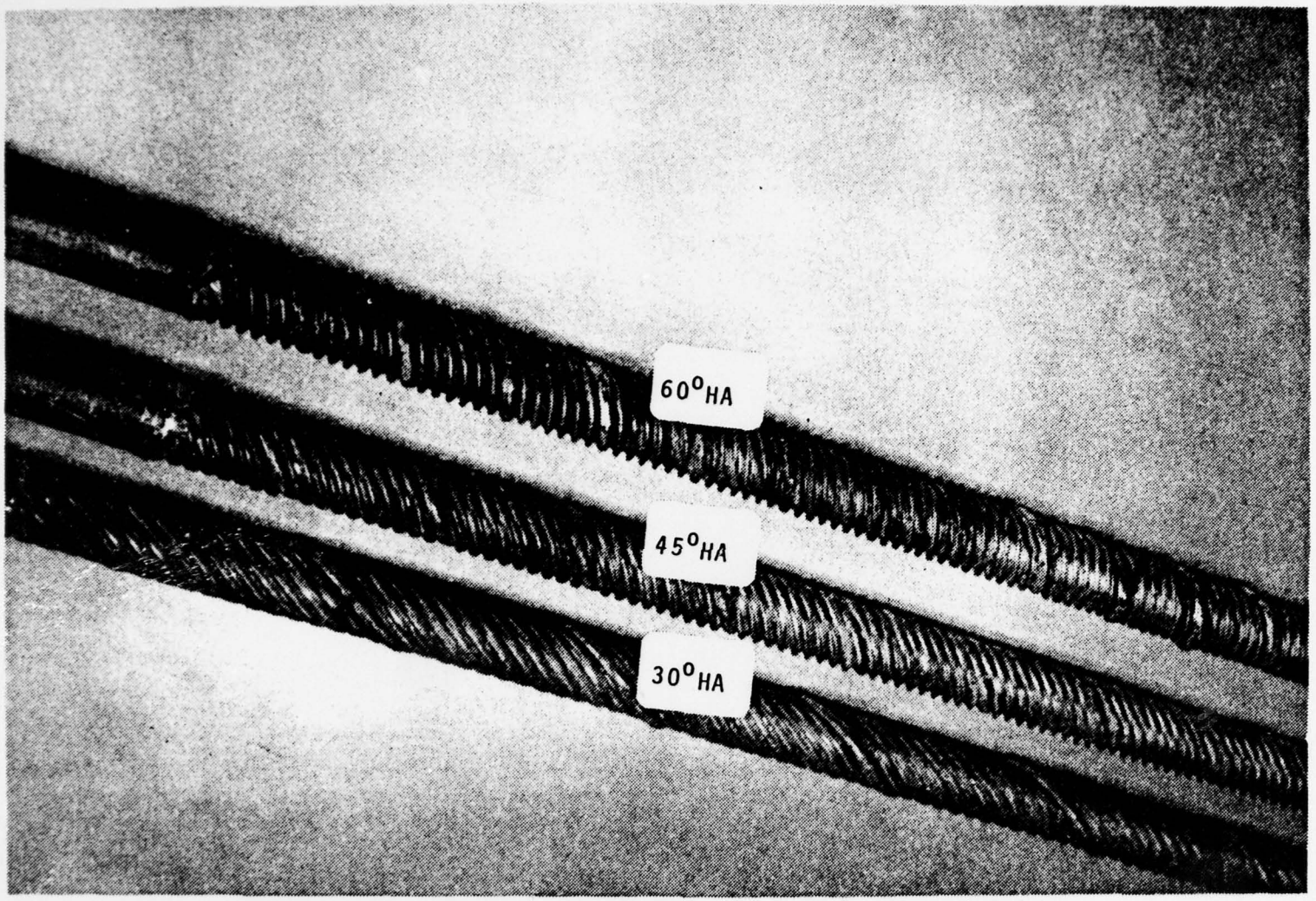

Figure 12. Photograph of General Atomic Fluted Tubes.

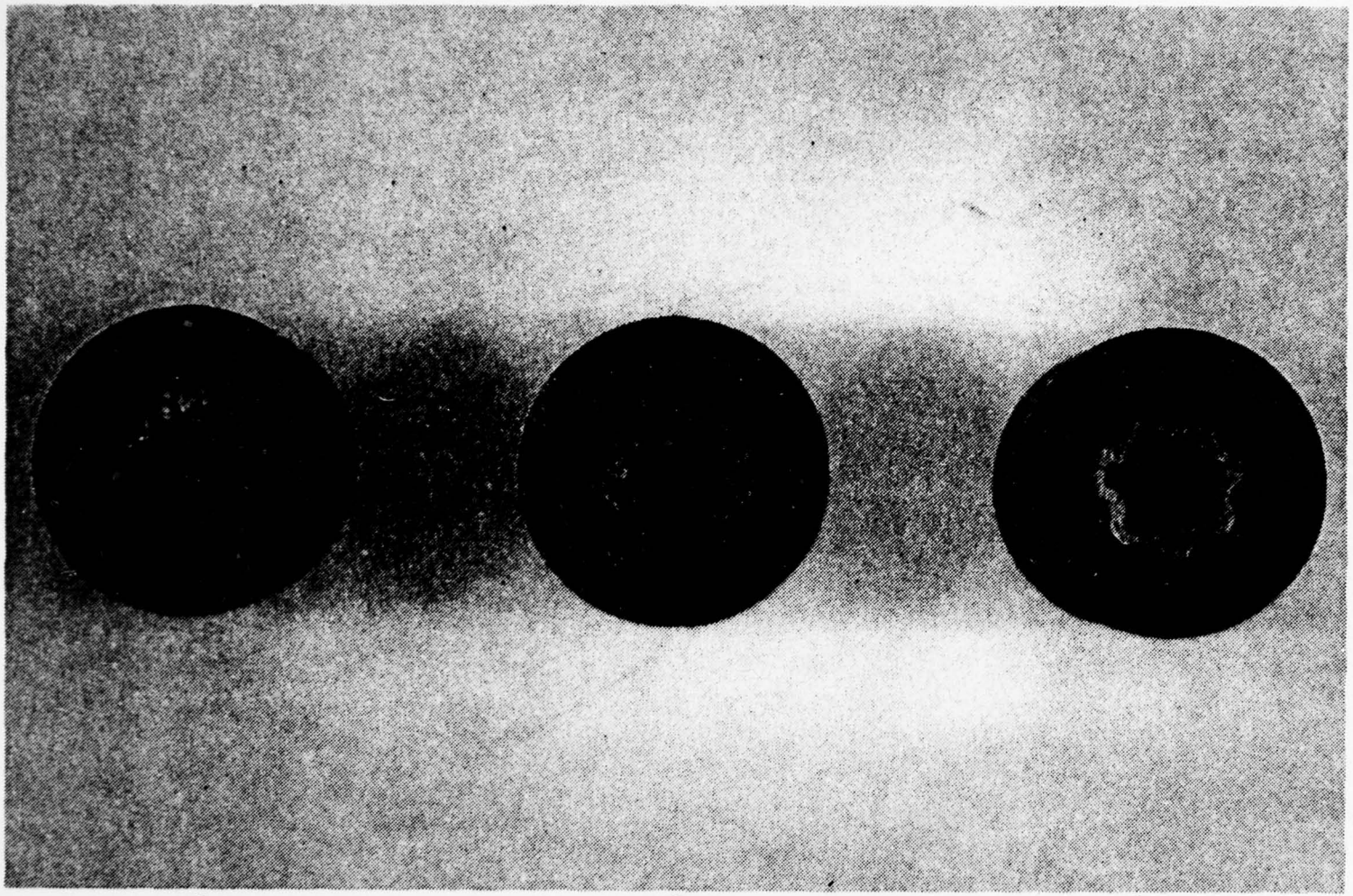

Figure 13. Crossectional View of GA Fluted Tubes.

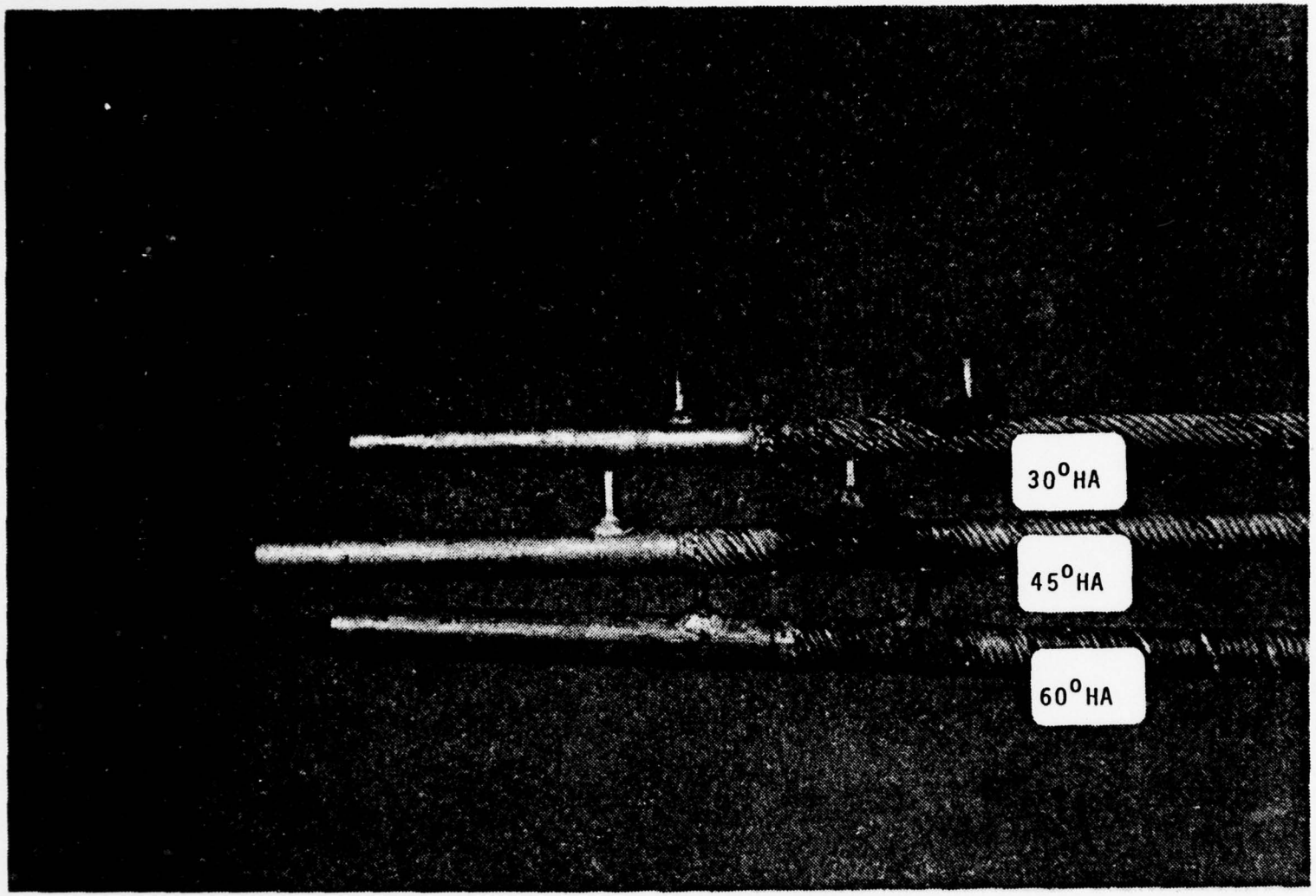

Figure 14. Photograph of General Atomic Pressure Tap Tubes.

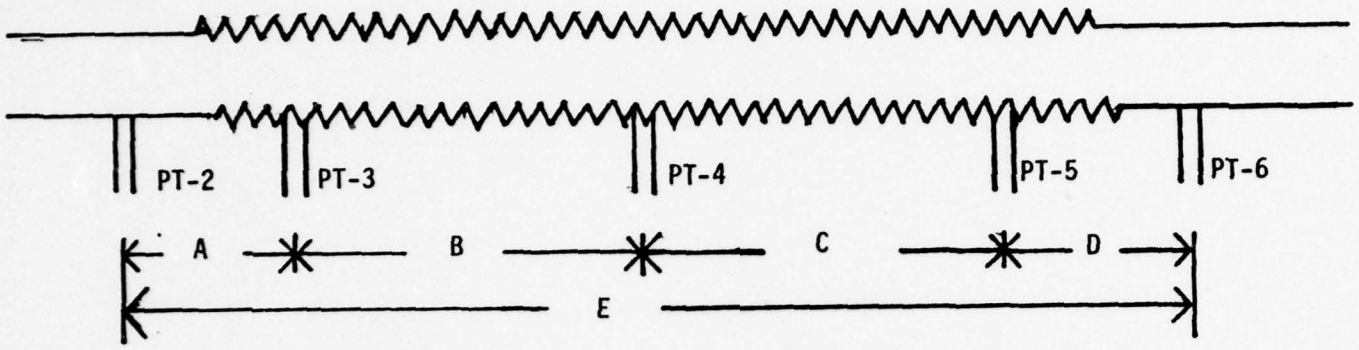

Tube	PT-1	PT-2	PT-3
A (in)	$4\frac{7}{16}$	$3\frac{3}{8}$	$2\frac{7}{8}$
B (in)	15	$15\frac{7}{8}$	$16\frac{7}{16}$
C (in)	$16\frac{1}{2}$	$15\frac{7}{8}$	$15\frac{19}{32}$
D (in)	3	$3\frac{1}{2}$	$3\frac{25}{32}$
E (in)	$38\frac{15}{16}$	$38\frac{5}{8}$	$38\frac{11}{16}$

Figure 15. Schematic of Pressure Tap Tube.

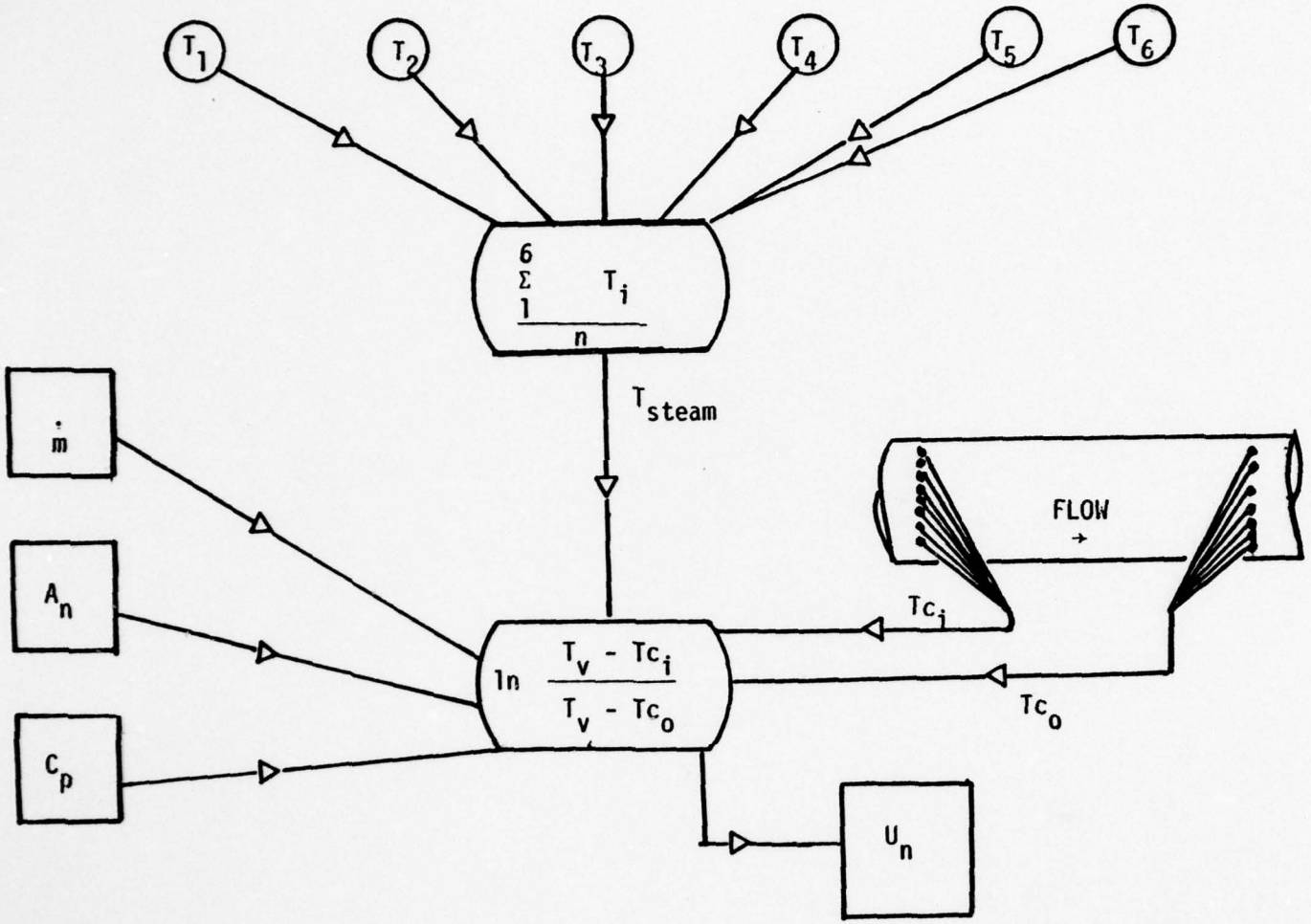

Figure 16. Schematic Representation of Procedure Used to Find U_n.

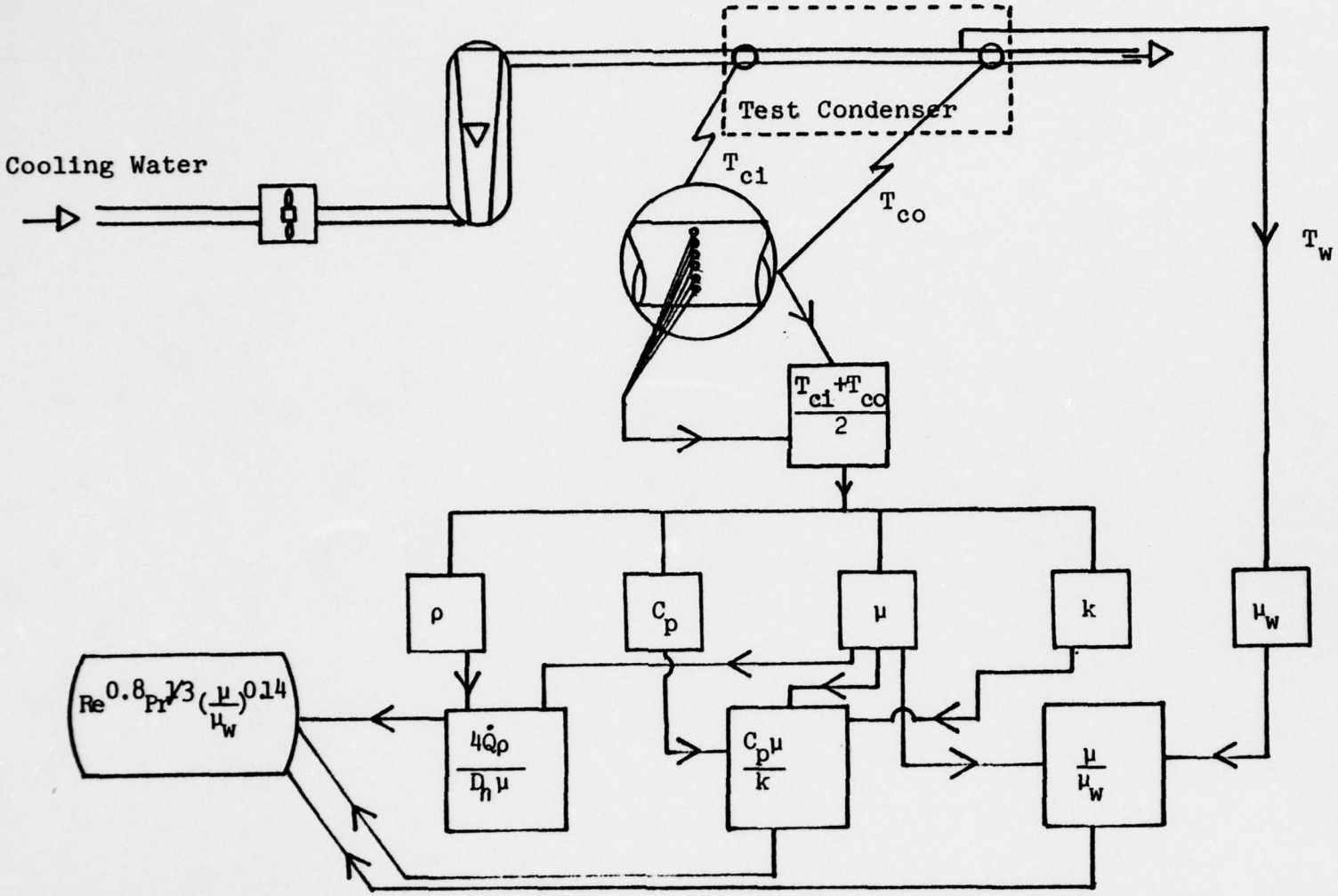

Figure 17. Schematic Representation of Procedure Used To Find Sieder Tate Parameter.

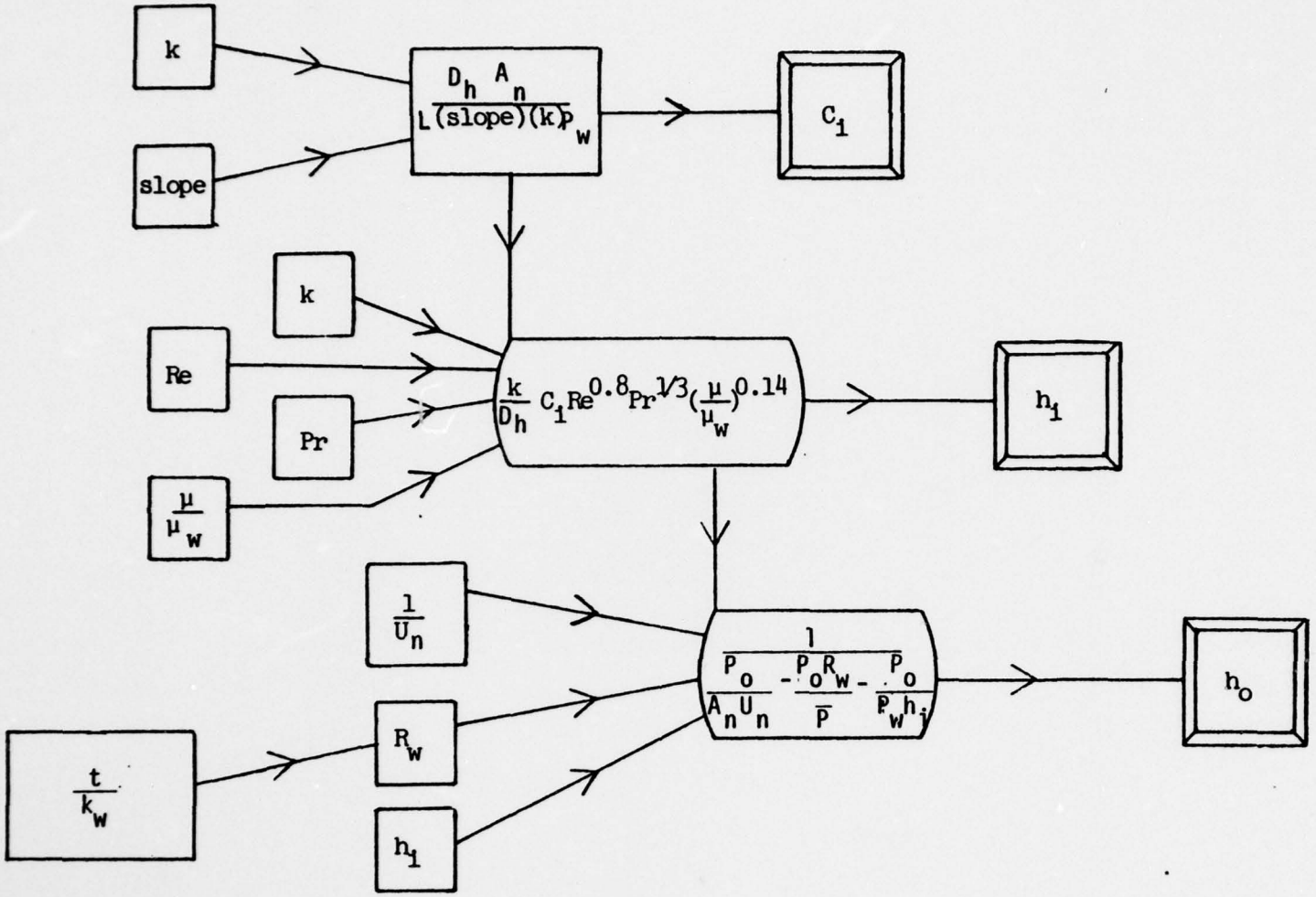

Figure 18. Schematic Representation of Procedure Used to Find Sieder Tate Constant, h_i and h_o.

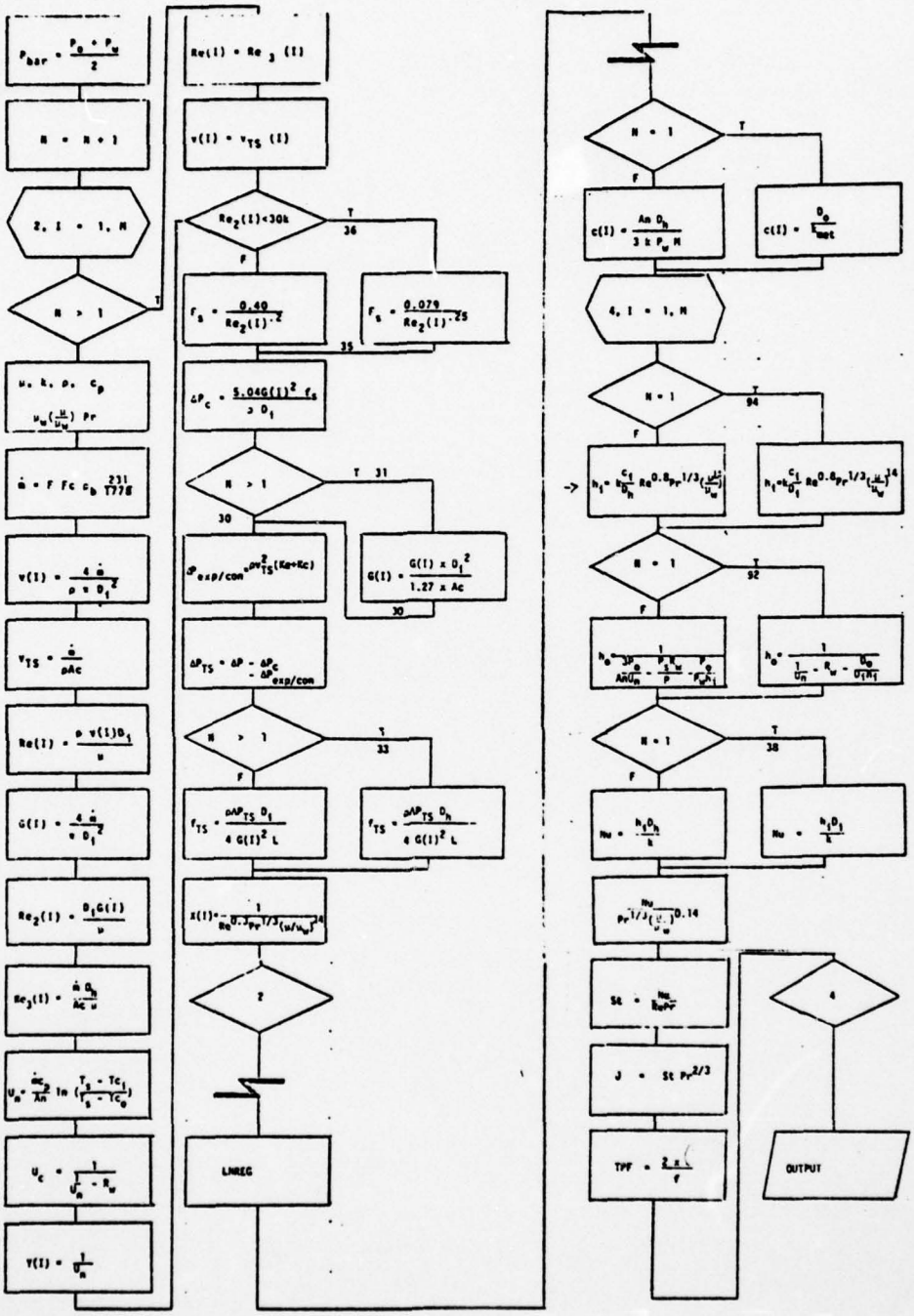

Figure 19. Computer Program Flow Diagram.

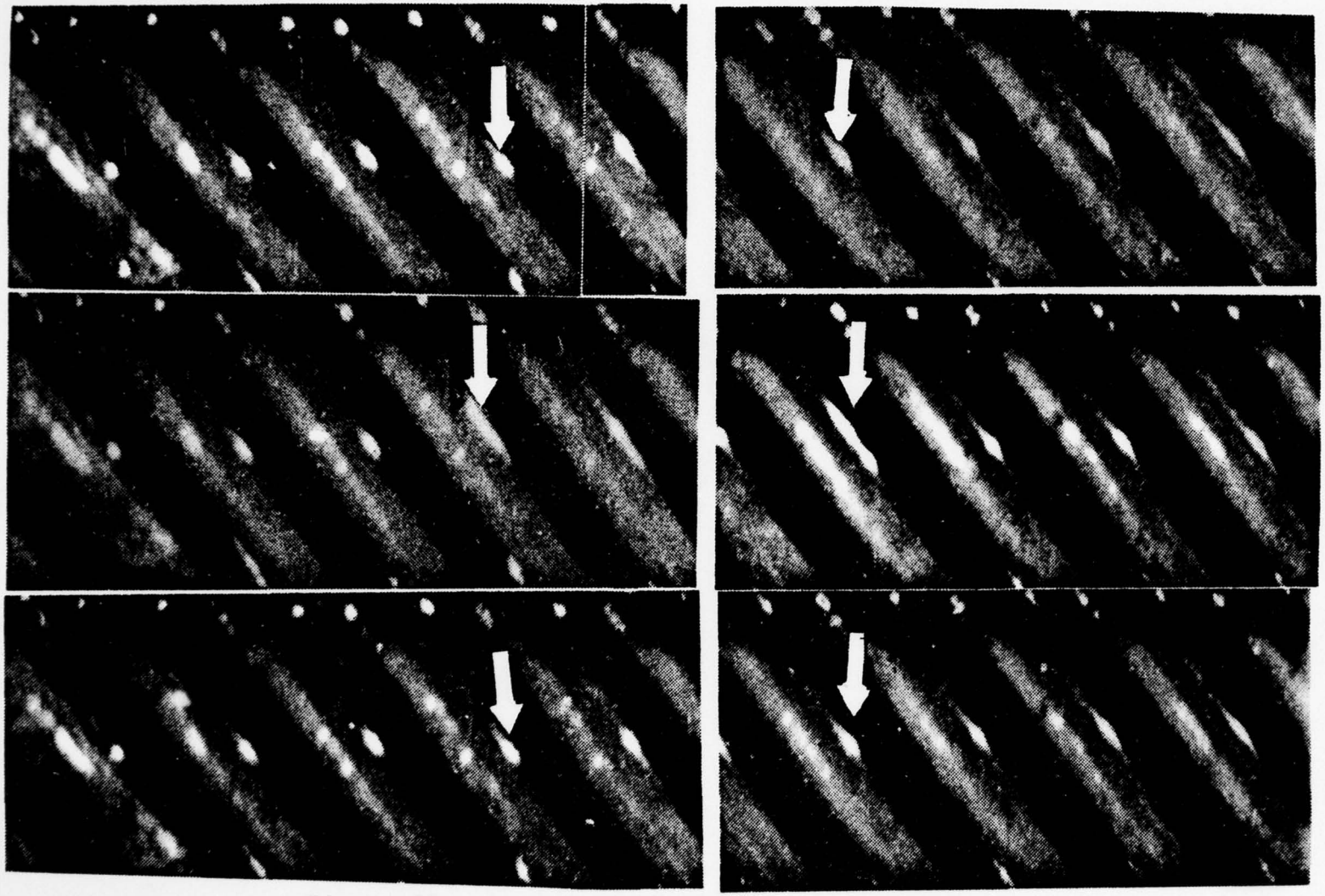

Figure 20. Condensate Drainage off Fluted Tube.

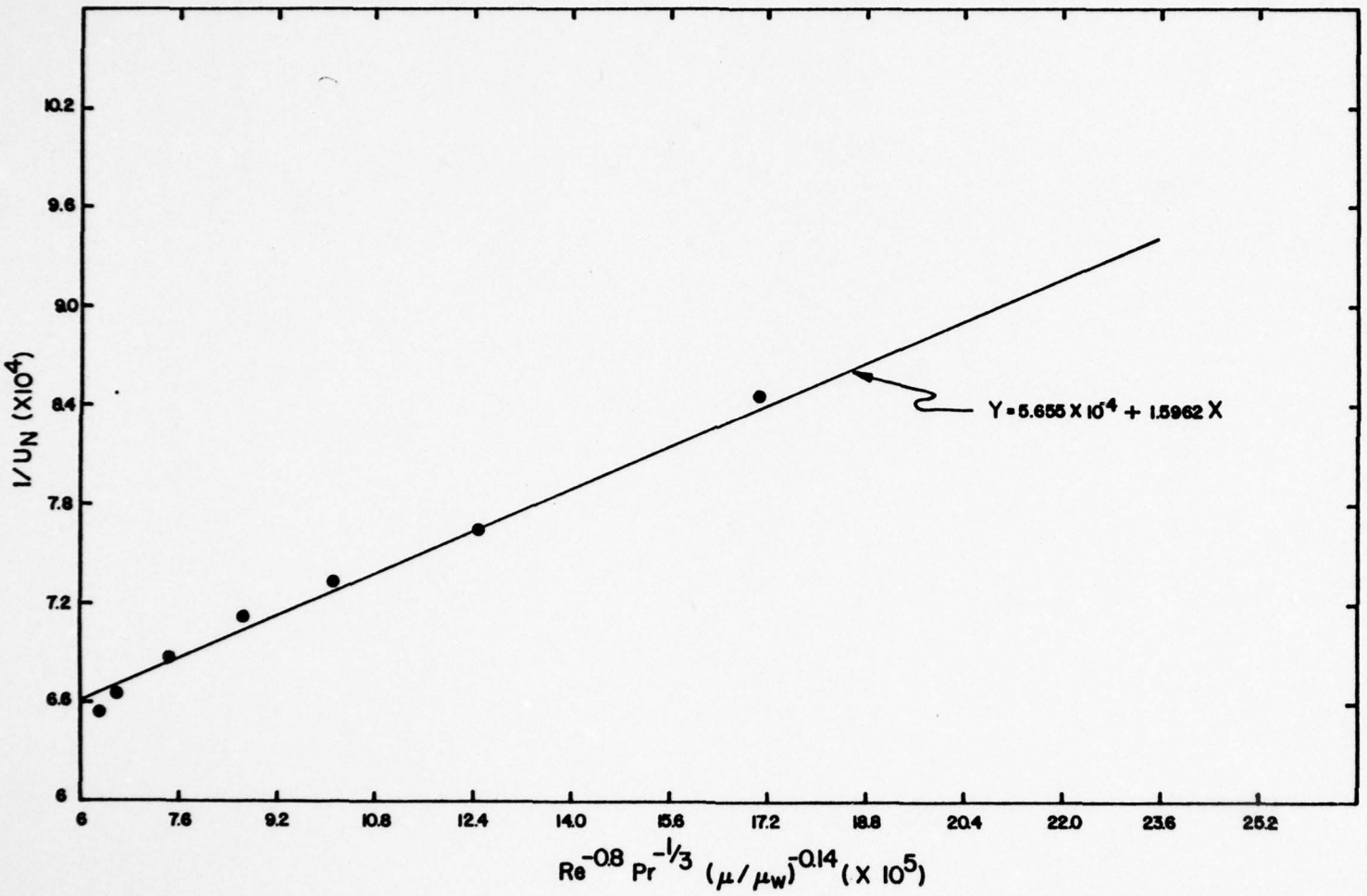

Figure 21. Wilson Plot for Flow Through 18.8 GPM Rotameter.

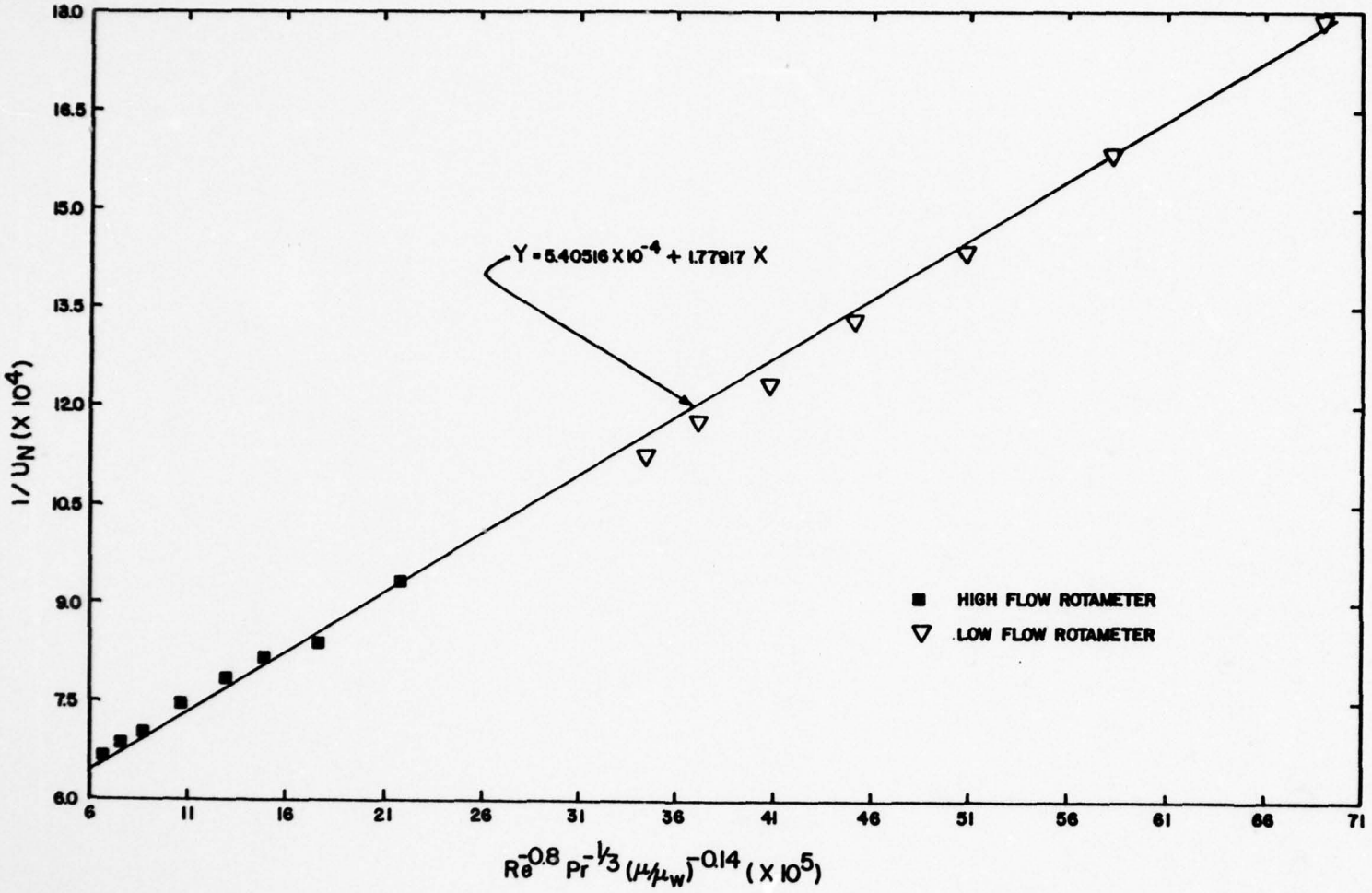

Figure 22. Wilson Plot For Flow Through 1.48 GPM and 18.8 GPM Rotameter.

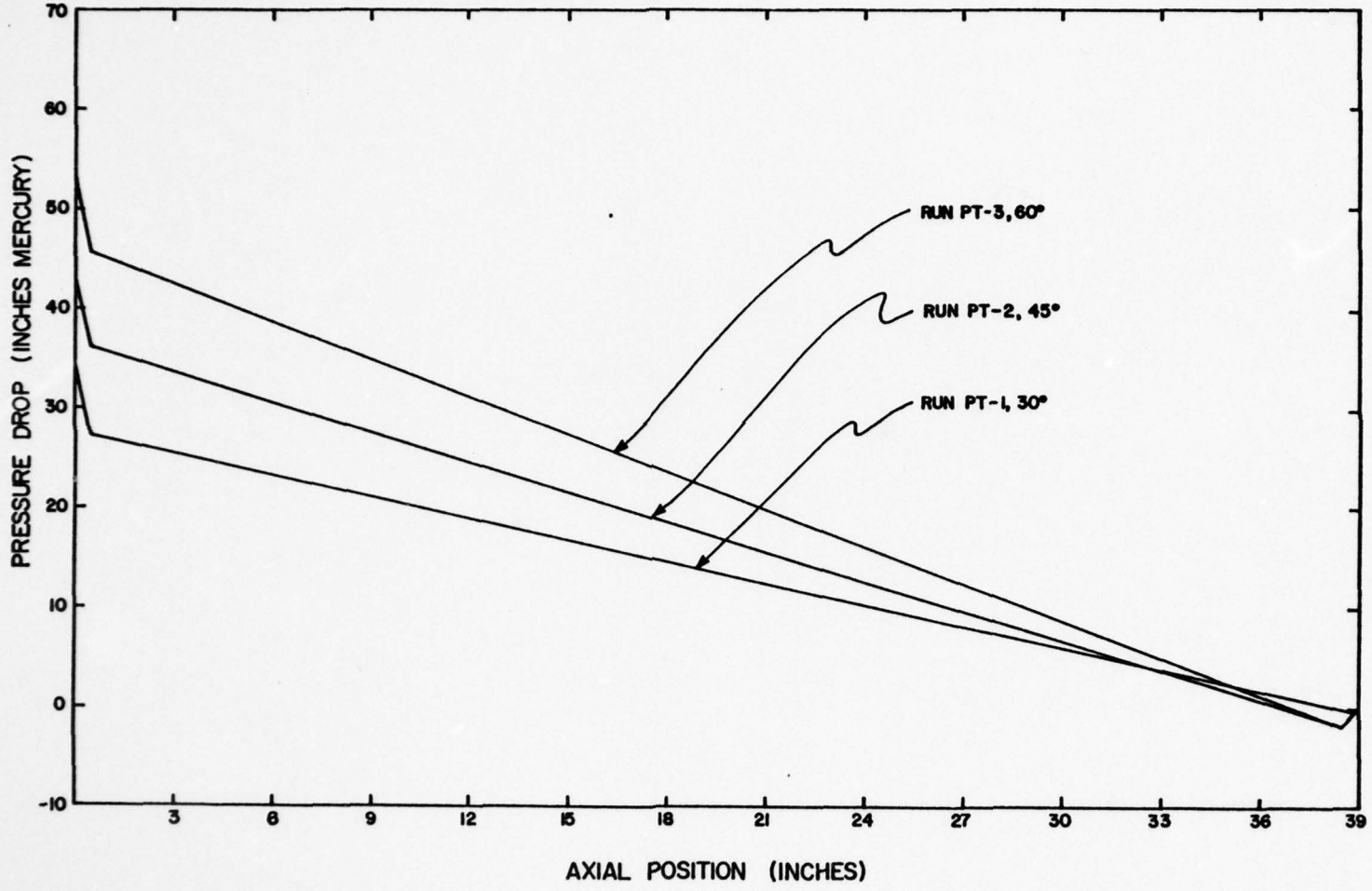

Figure 23. Water Pressure Drop Versus Axial Position at 60% Flow on 18.8 GPM Rotameter.

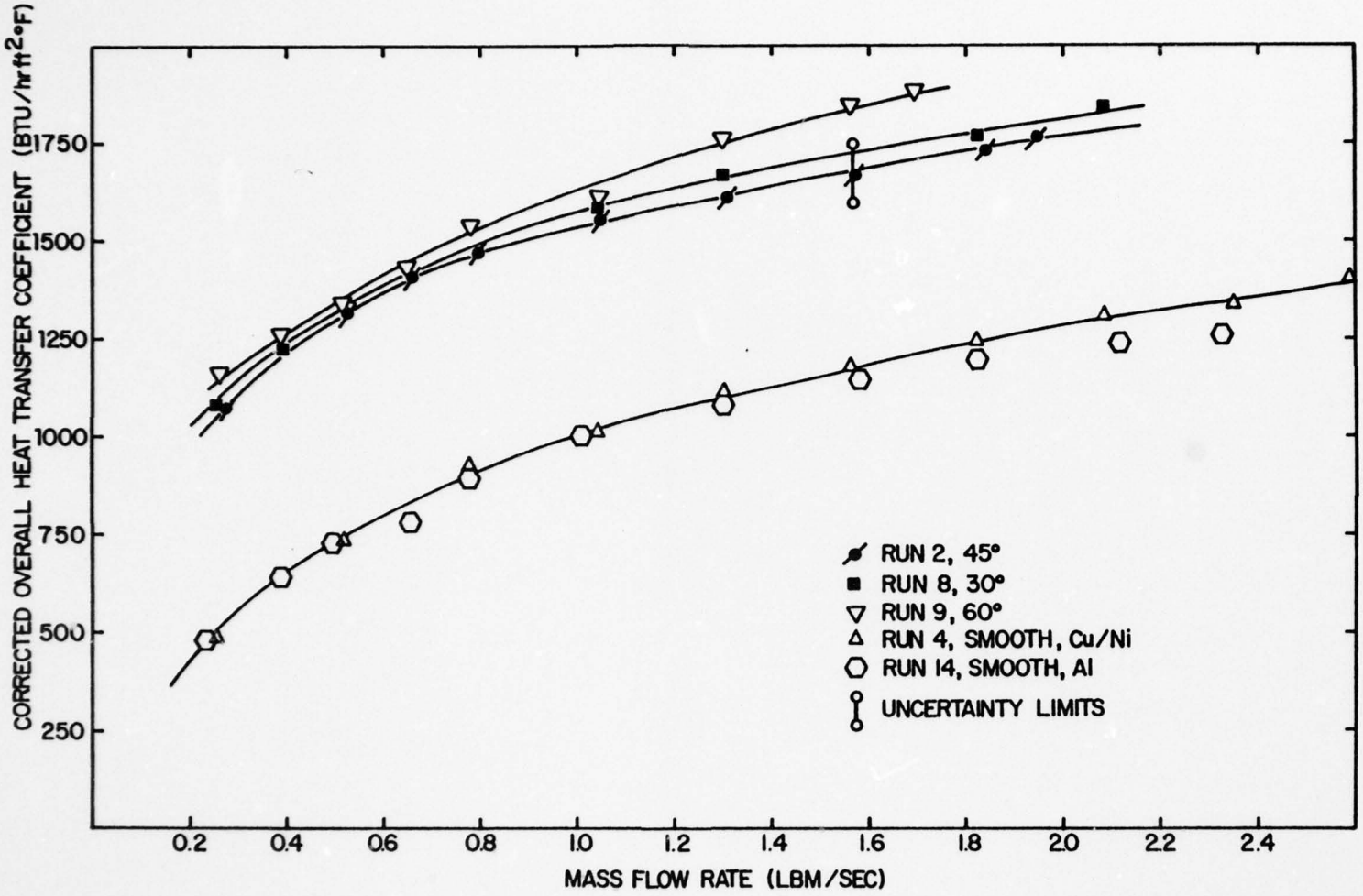

Figure 24. Corrected Overall Heat Transfer Coefficient versus Mass Flow Rate of Cooling Water.

AD-A055 430 NAVAL POSTGRADUATE SCHOOL MONTEREY CALIF F/G 13/1
AN EXPERIMENTAL INVESTIGATION OF ENHANCED HEAT TRANSFER ON HORI--ETC(U)
MAR 78 D J REILLY

UNCLASSIFIED NPS69-78-011 NL

2 OF 3
ADA
055430

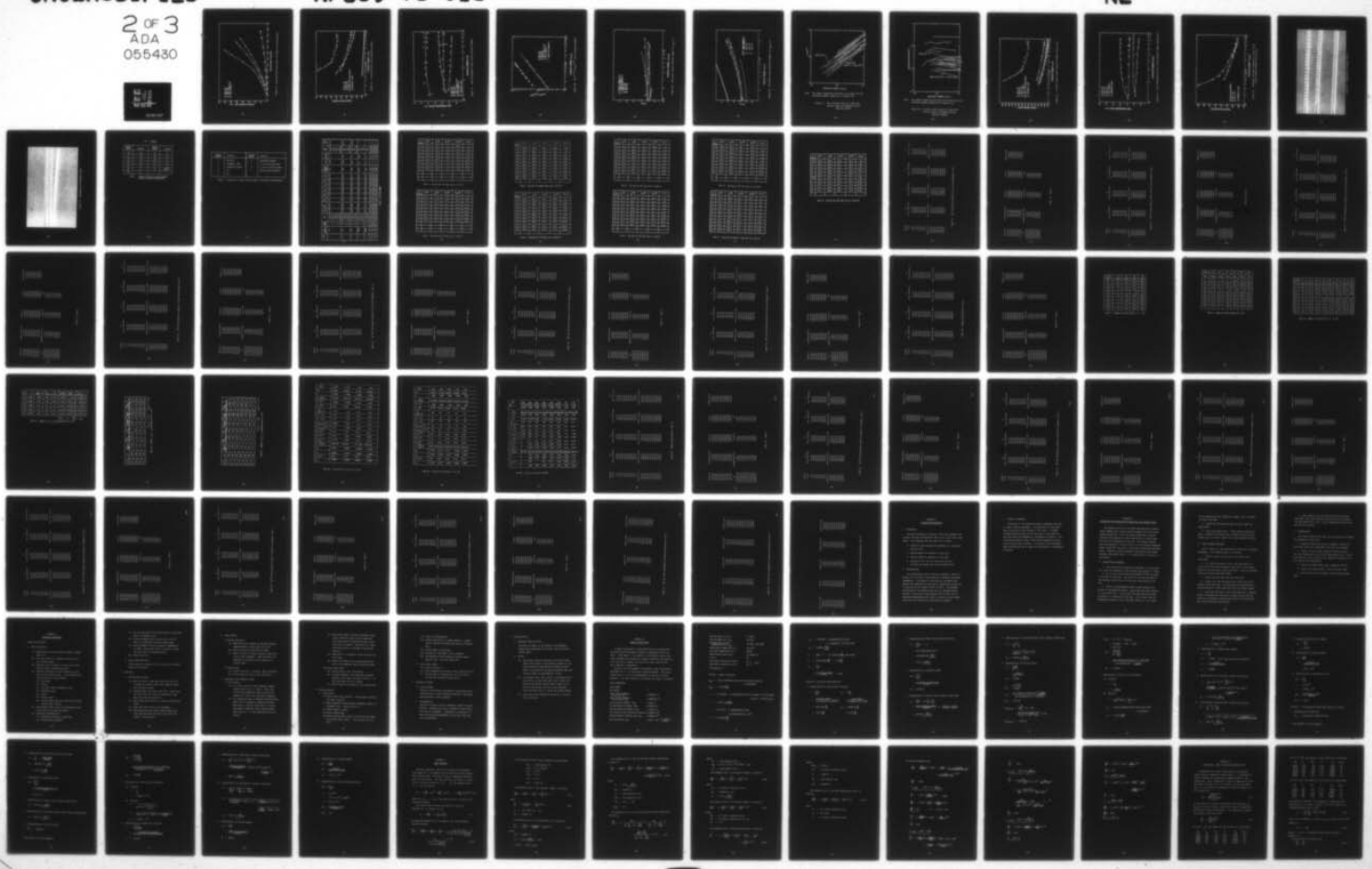

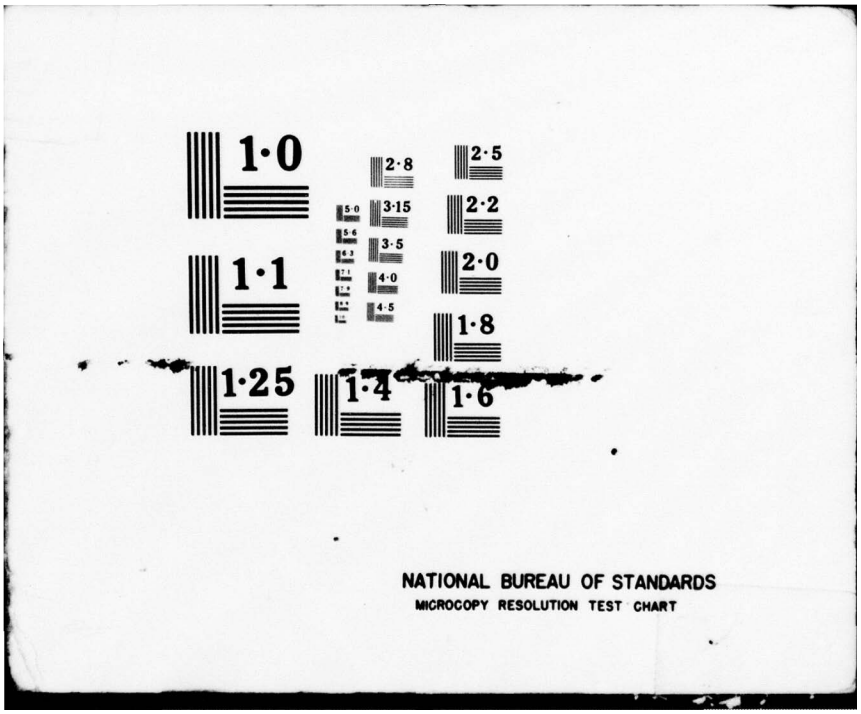
1·0
1·1
1·25
1·4
1·6
1·8
2·0
2·2
2·5
2·8
3·15
3·5
4·0
4·5
5·0
5·6
NATIONAL BUREAU OF STANDARDS
MICROCOPY RESOLUTION TEST CHART

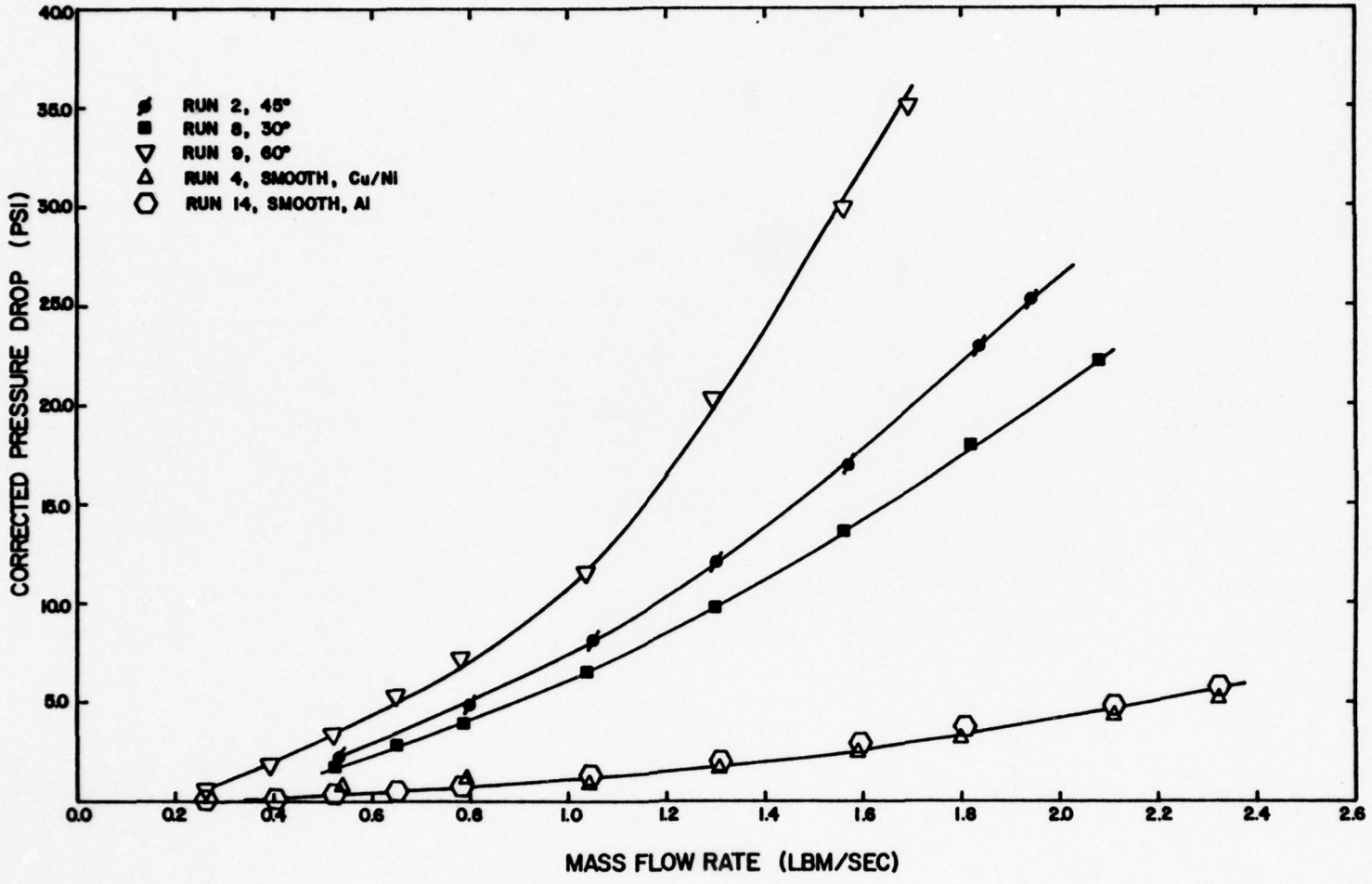

Figure 25. Pressure Drop Versus Mass Flow Rate of Cooling Water.

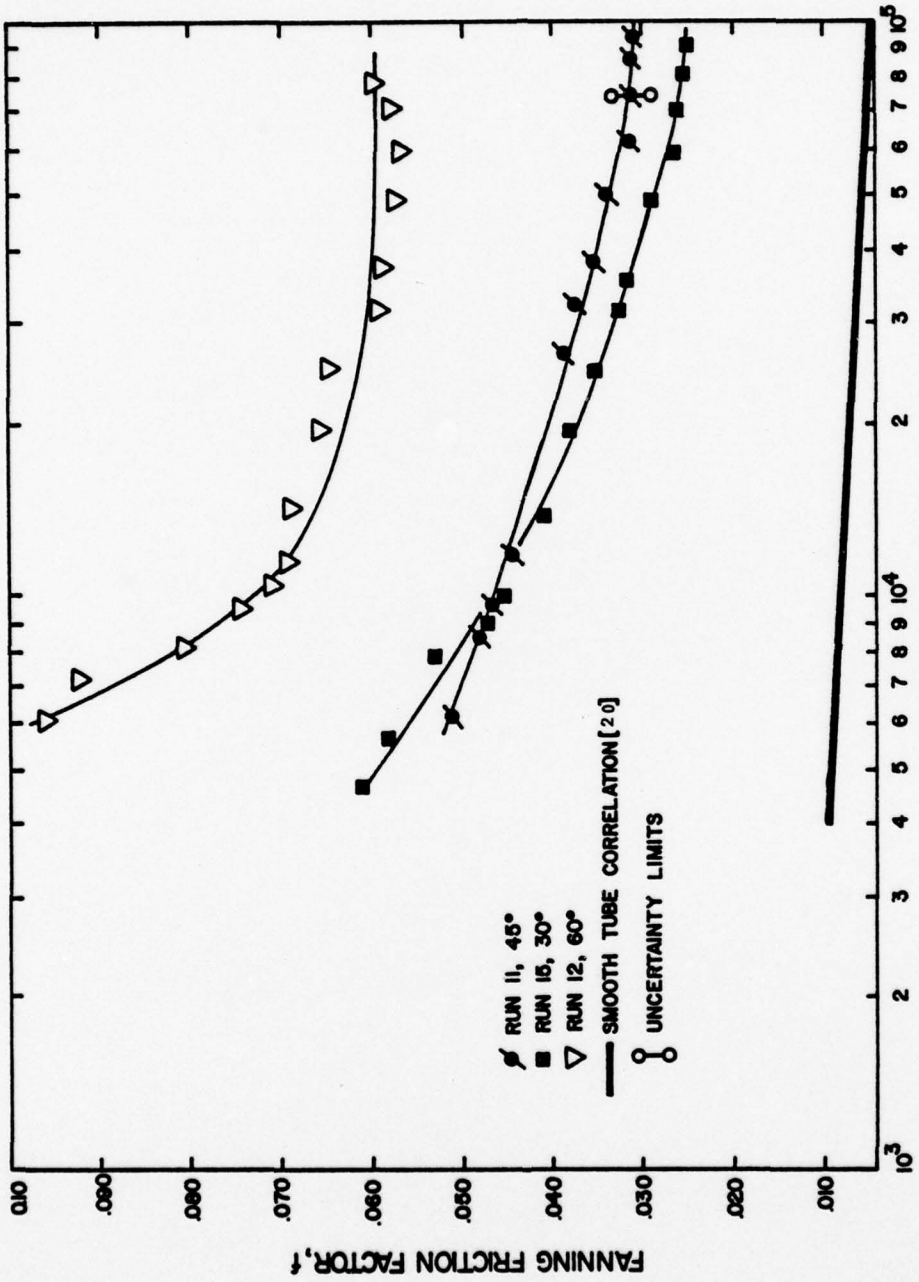

Figure 26. Friction Factor versus Reynolds Number.

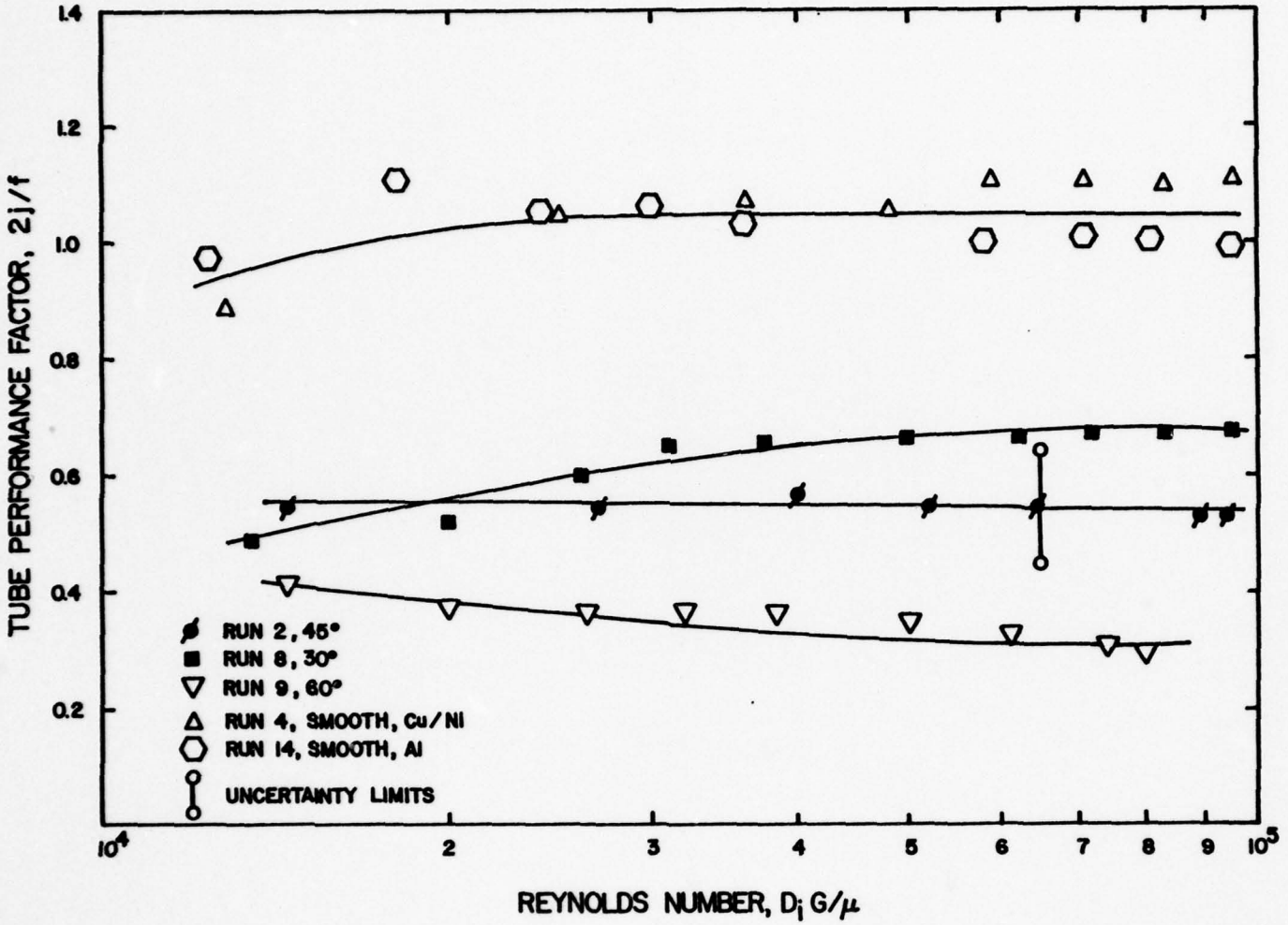

Figure 27. Tube Performance Factor versus Reynolds Number.

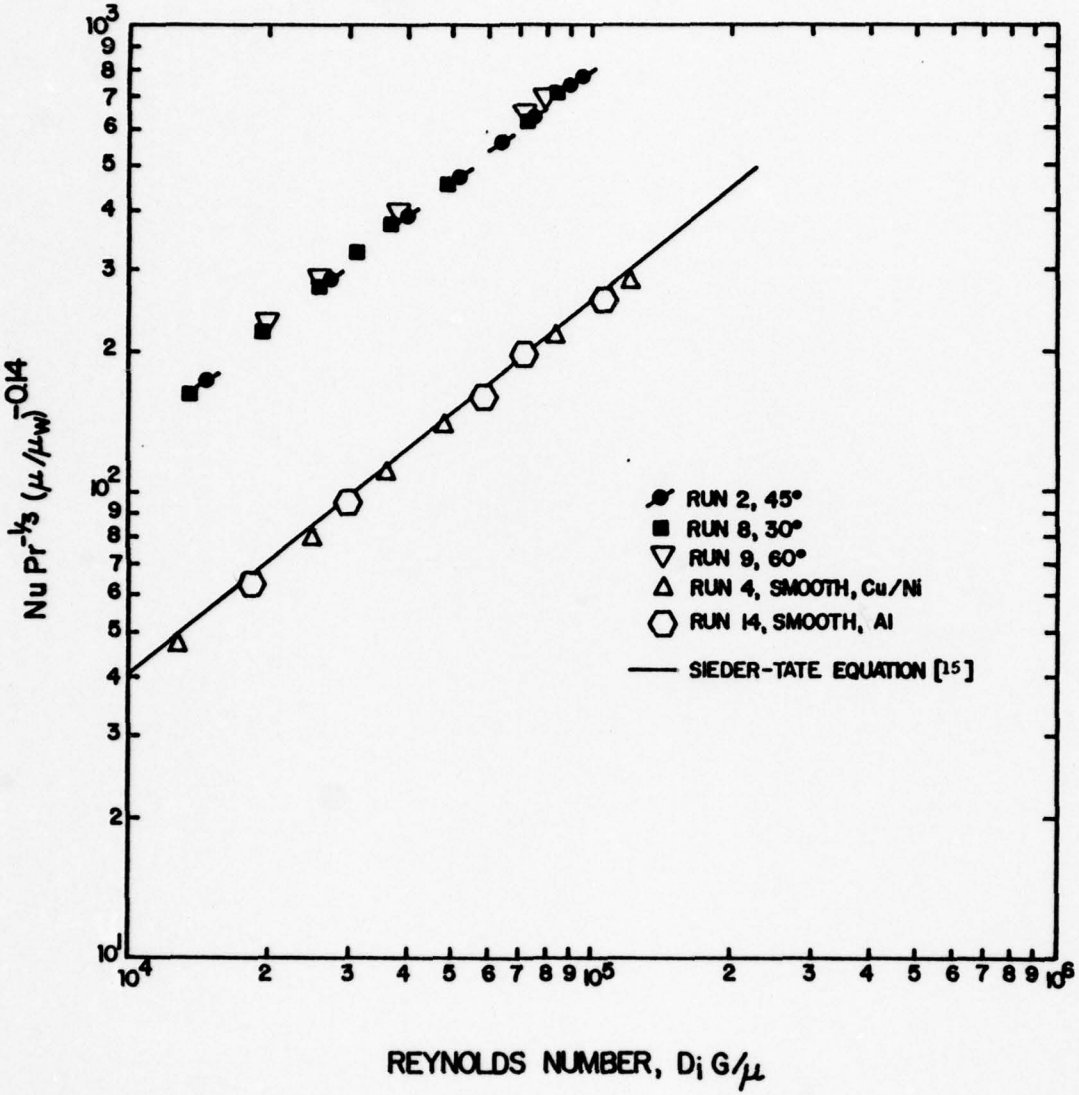

Figure 28. Nu $Pr^{-1/3}$ $(\mu/\mu_w)^{-0.4}$ versus Reynolds Number.

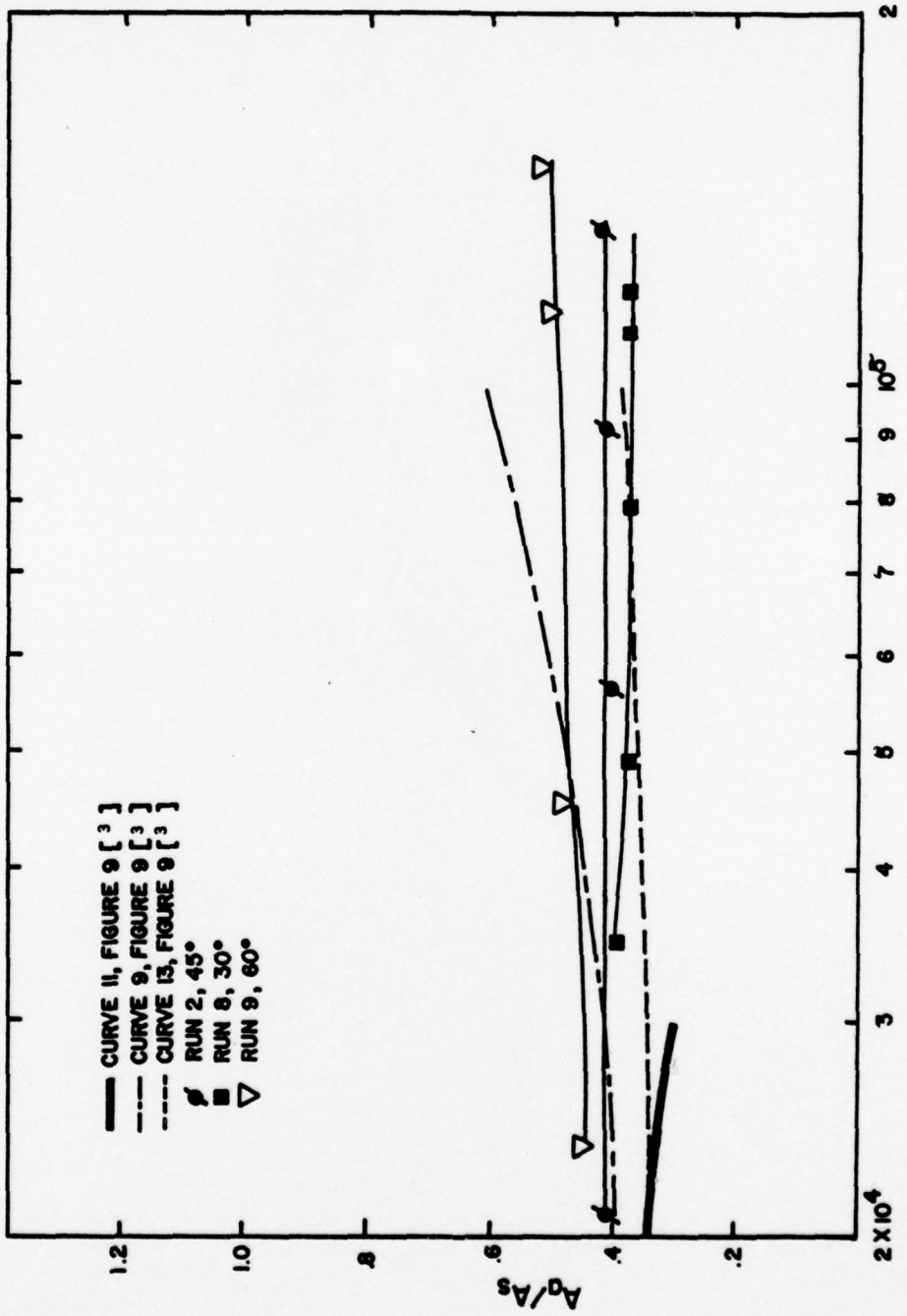

Figure 29. Area Ratio versus Reynolds Number for $R_{ext} = 0$.

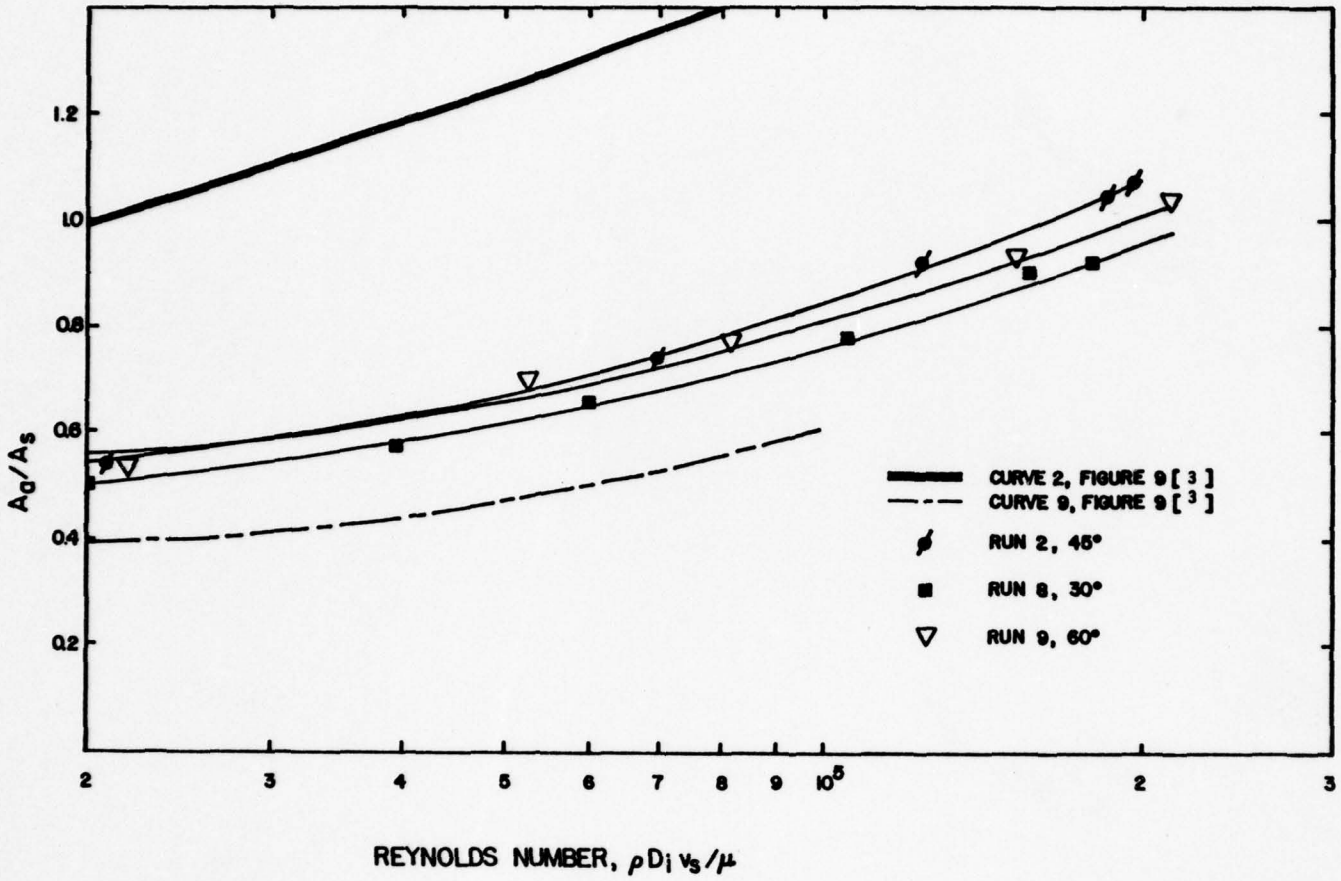

Figure 30. Area Ratio versus Reynolds Number for $R_{ext} \neq 0$.

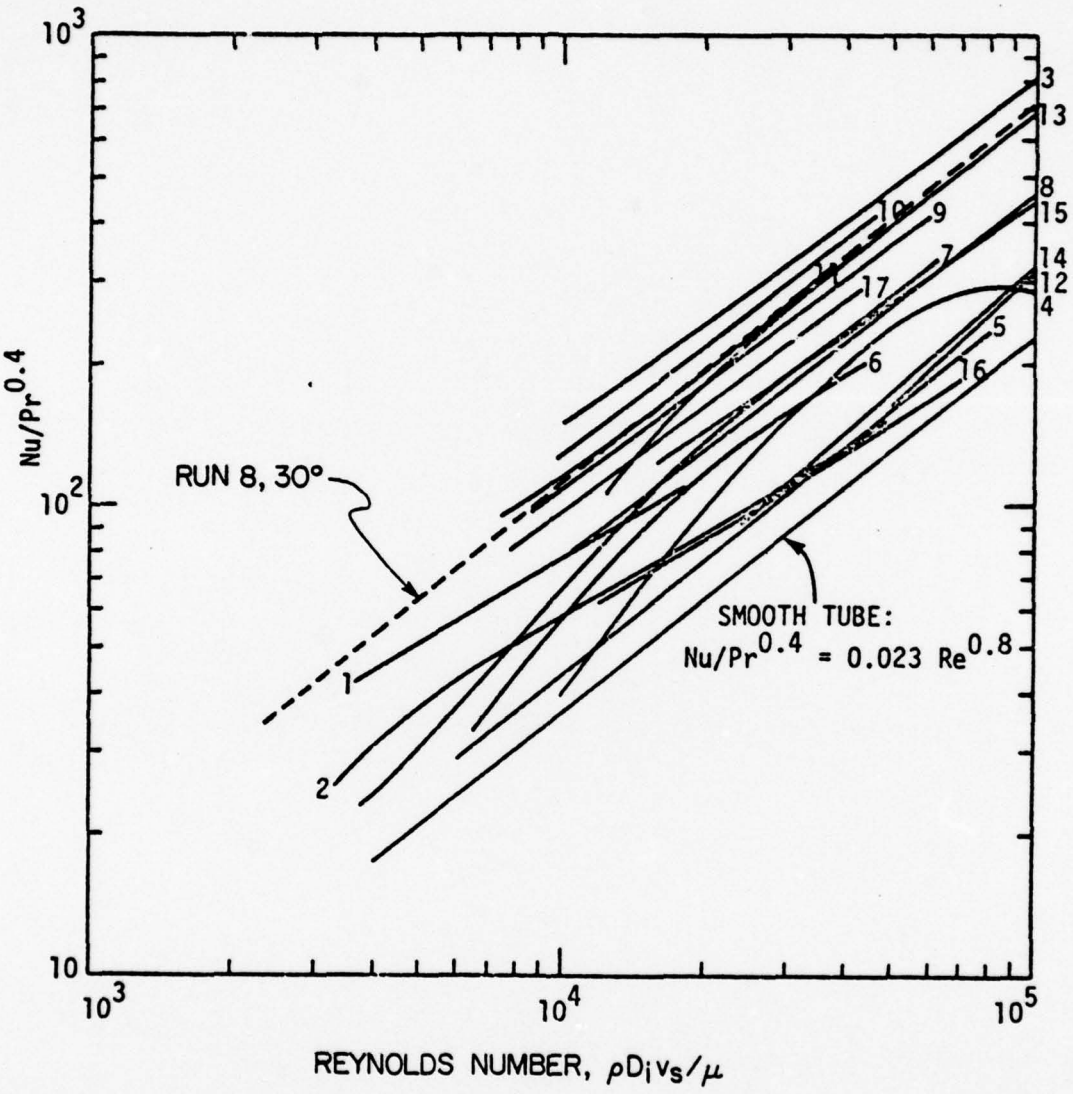

Note: The numbers appearing with each curve above are the reference numbers appearing in Bergles [3].

Figure 31. Heat Transfer Data For Tubes with Various Types of Roughness versus Reynolds Number.

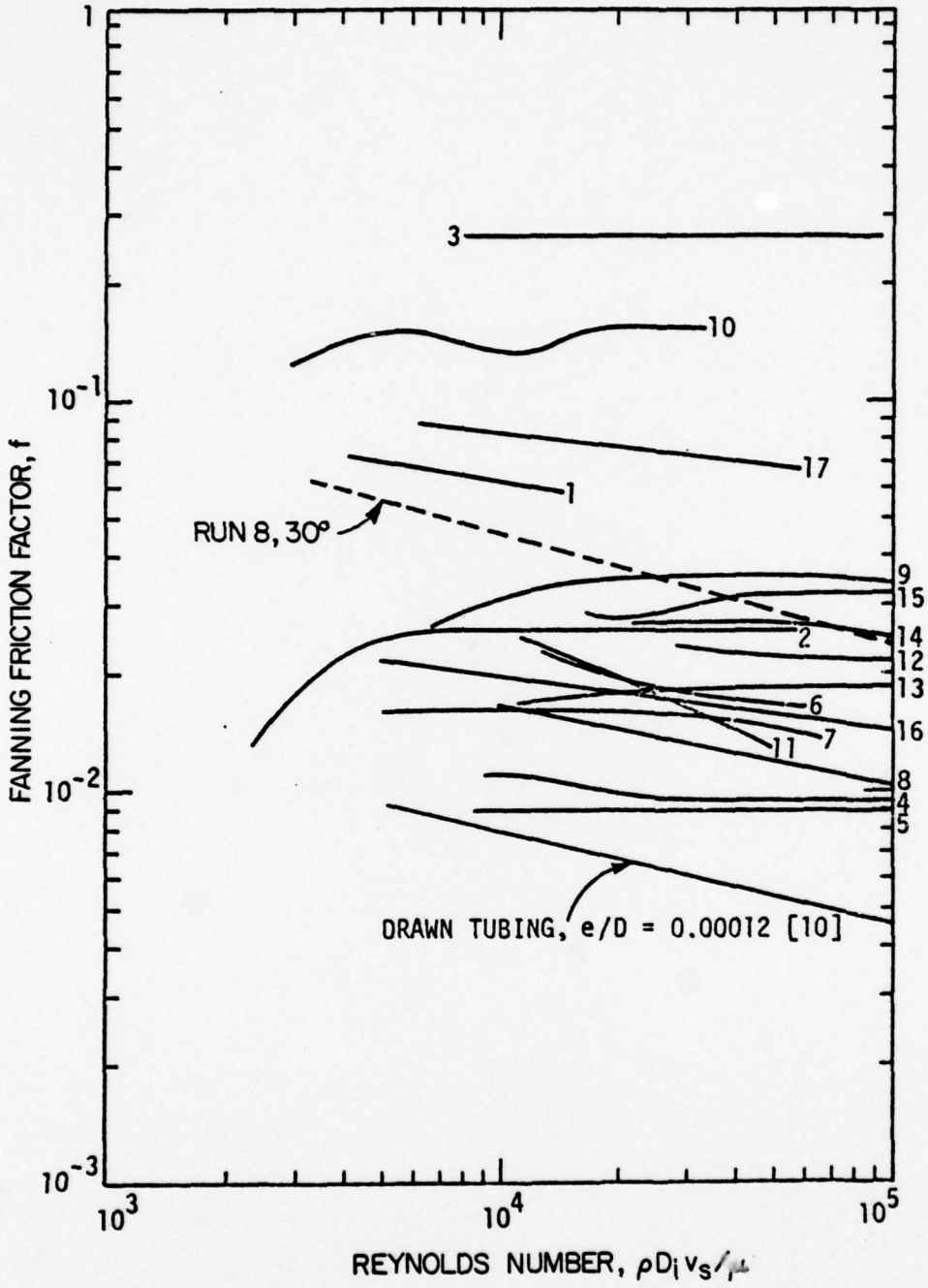

Note: The numbers appearing with each curve above are the reference numbers appearing in Bergles [3].

Figure 32. Friction Factor Data For Tubes With Various Types of Roughness Versus Reynolds Number.

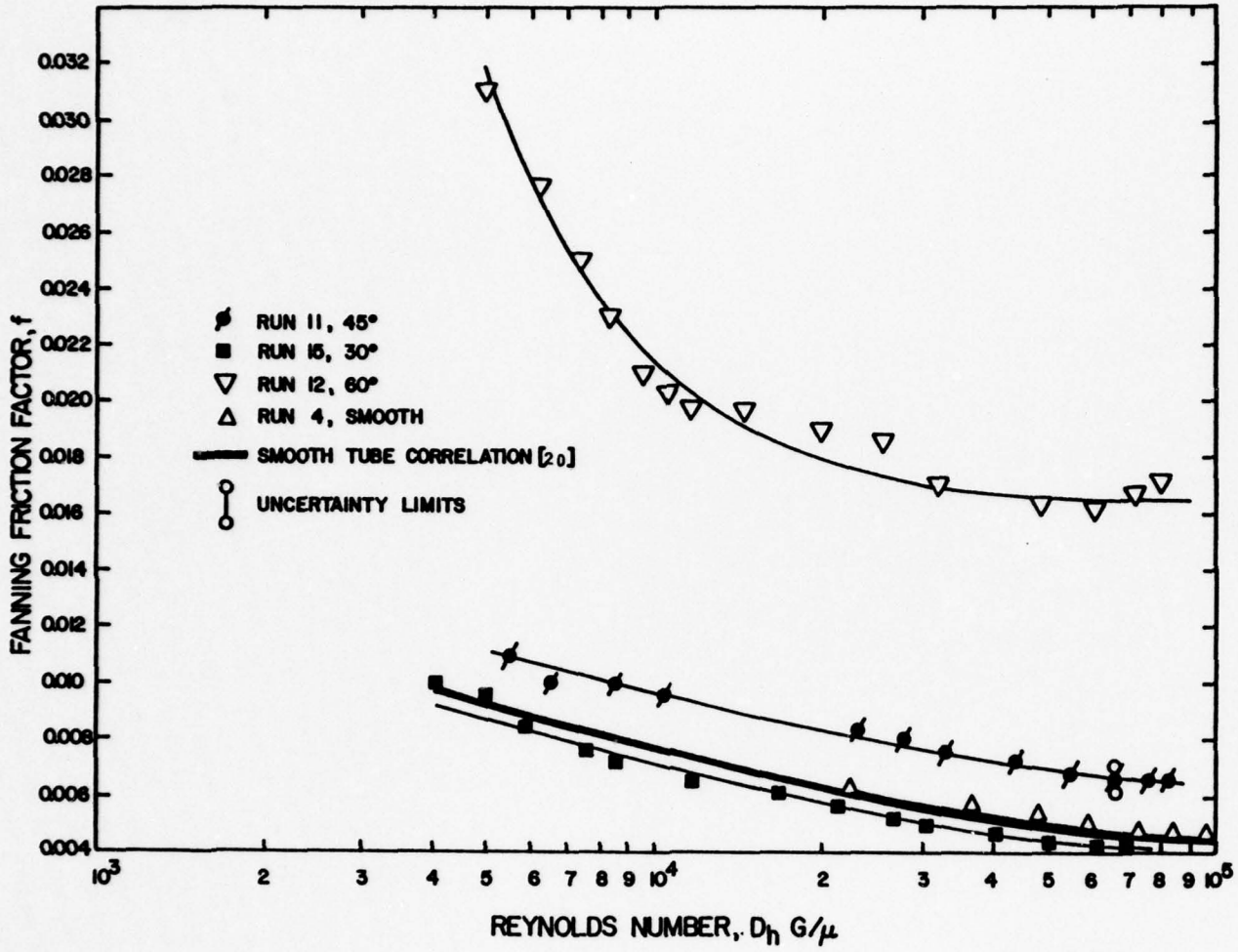

Figure 33. Friction Factor Versus Reynolds Number Based on D_h .

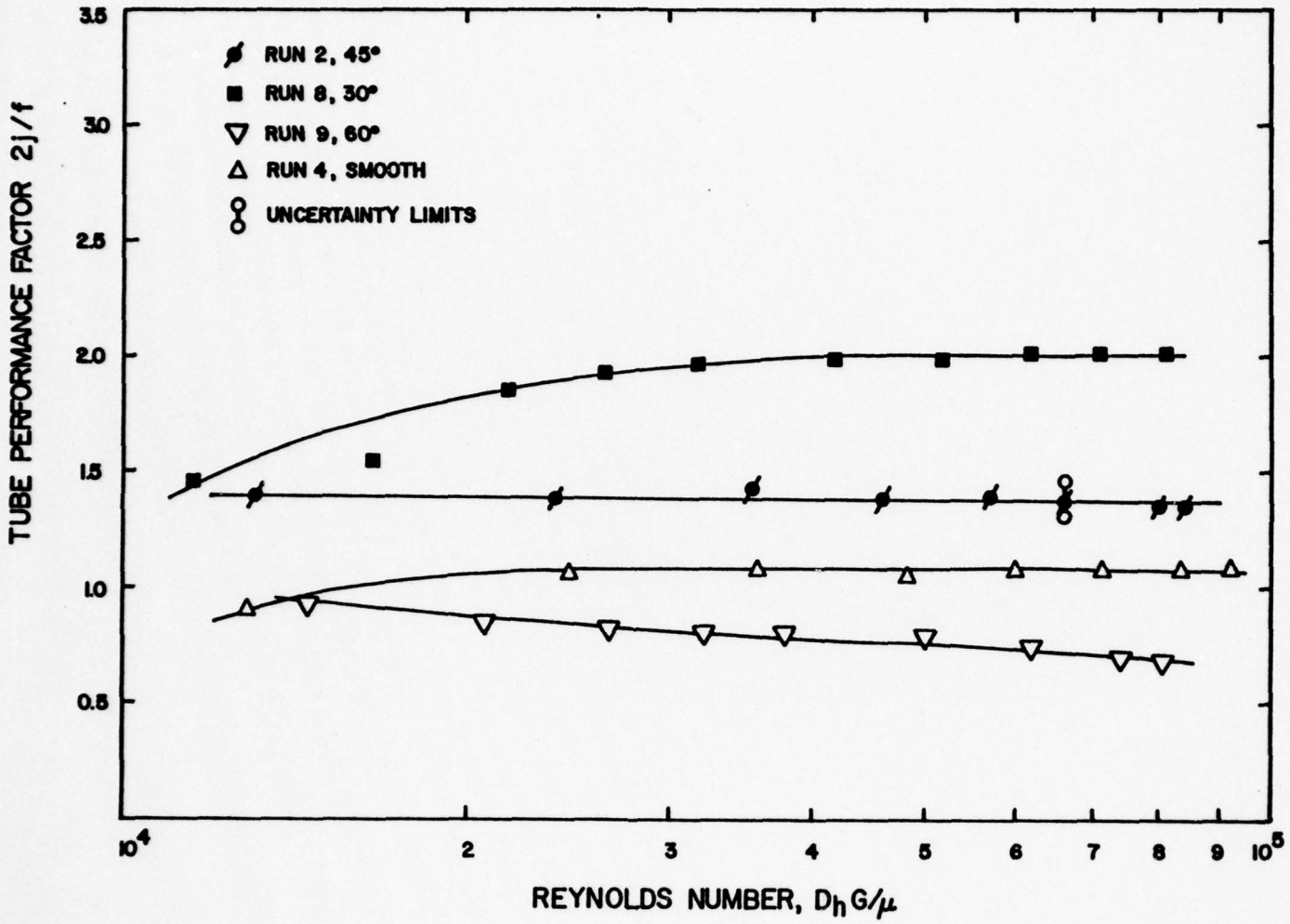

Figure 34. Tube Performance Factor Versus Reynolds Number Based on D_h.

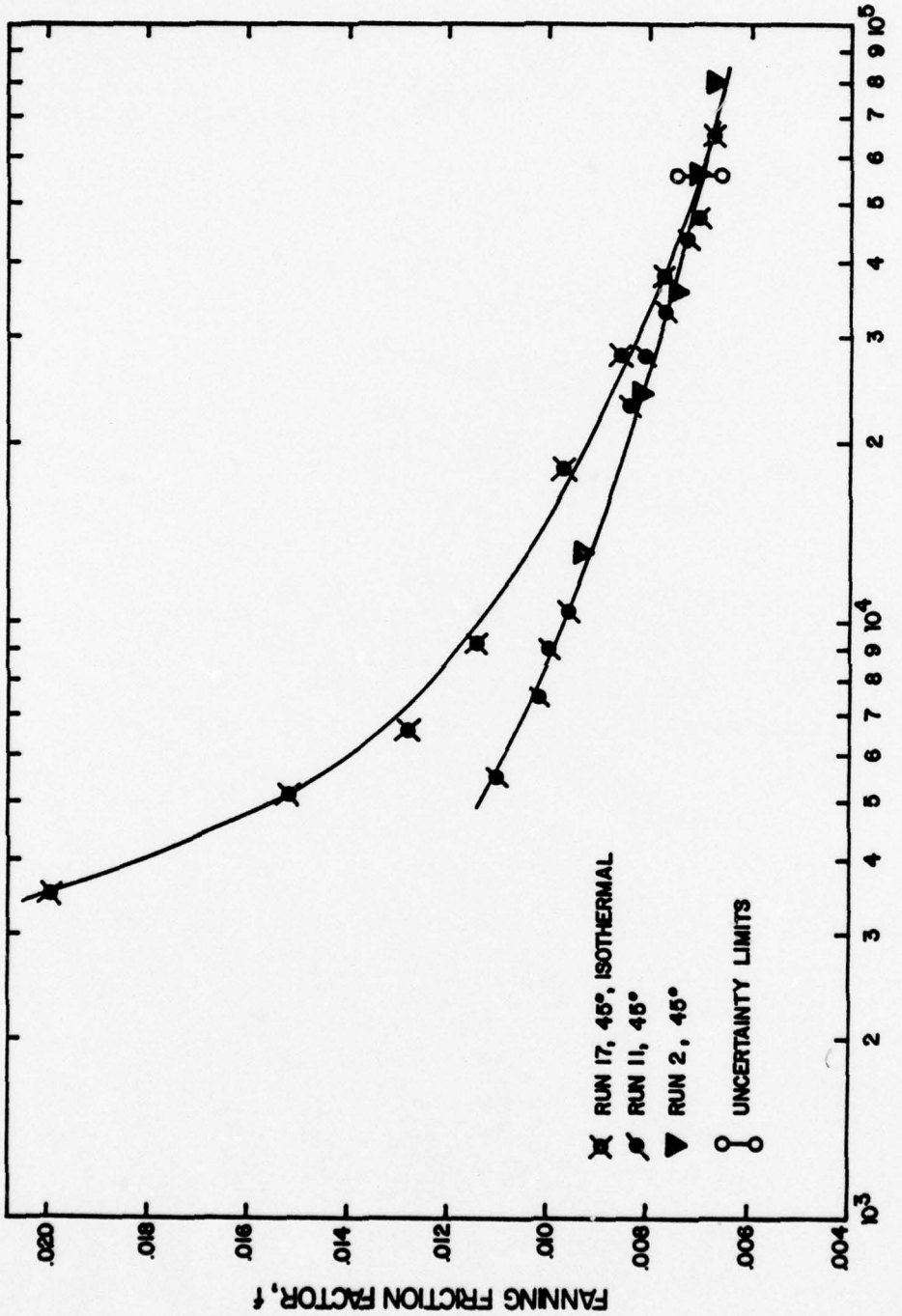

Figure 35. Isothermal and Non-isothermal Friction Factor Versus Reynolds Number Based on D_h.

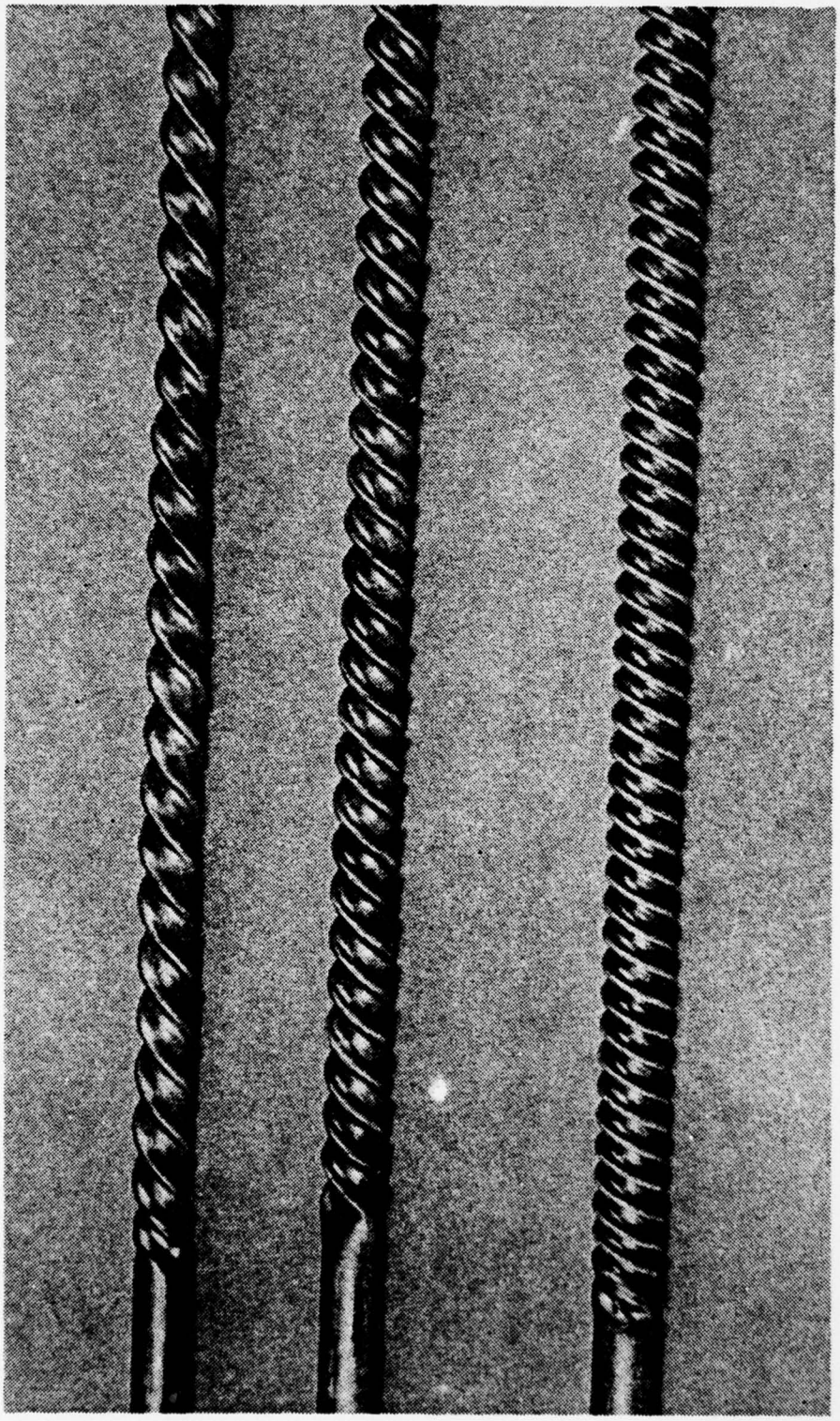

Figure 36. Photograph of Turbotec Tubes.

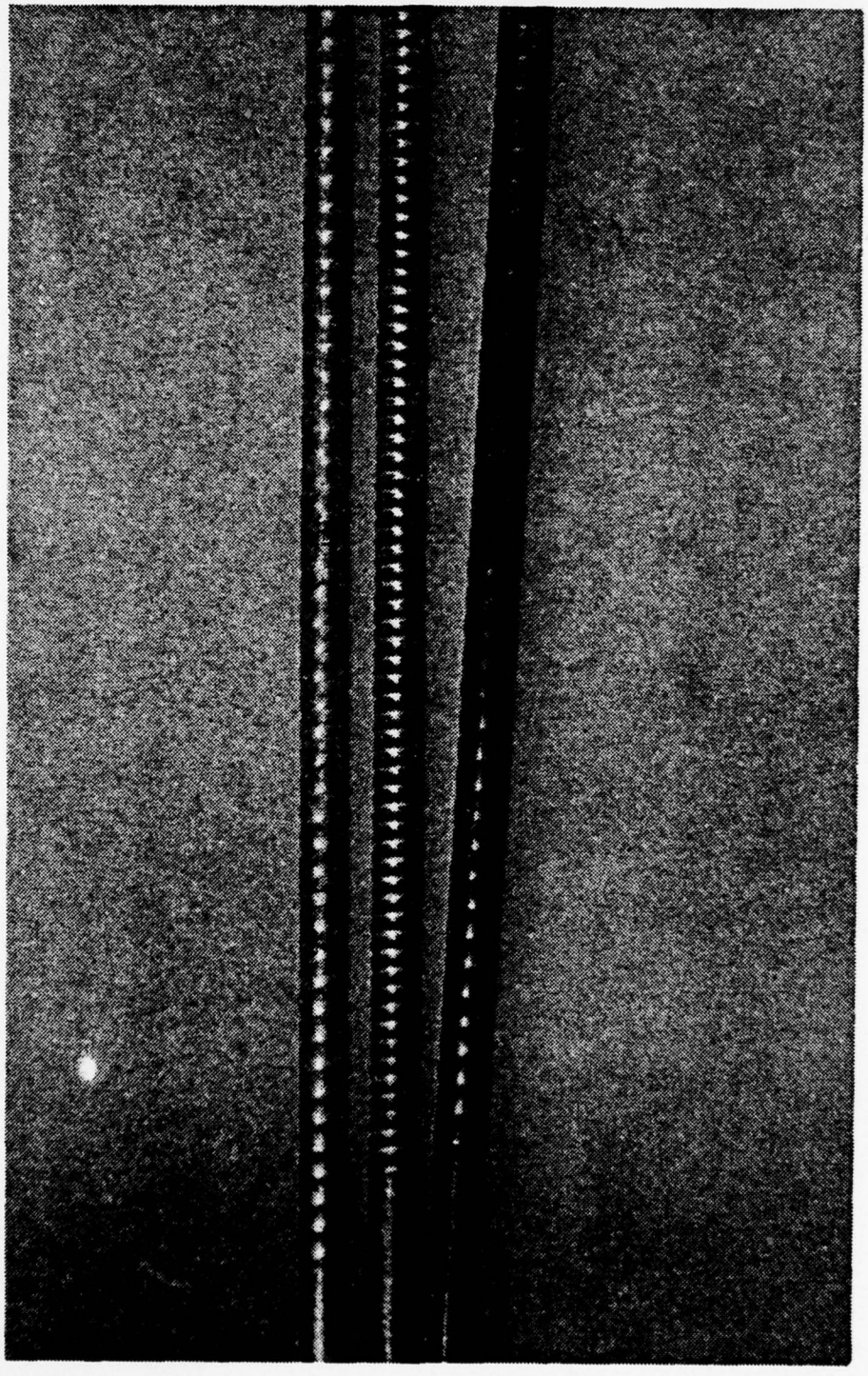

Figure 37. Photograph of Korodense Tubes.

VIII. TABLES

Channel Number	Location	Channel Number	Location
40	Tc_i	47	T_v
41	Tc_o	48	T_v
42	Tc_o	49	T_v
43	Tc_o	50	T_v
44	Tc_o	51	T_w
45	T_v	52	Hotwell
46	T_v		

Table 1. Location of Stainless Steel Sheathed Copper Constantan Thermocouples.

Channel Number	Location	Channel Number	Location
1	Hot Well	6	Condensate Header
2	Feedwater Tank	7	T_c into Cooling Tower
3	Condenser Window	8	T_c out of Cooling Tower
4	Tc_i	9	Cooling Tower Ambient
5	Tc_o		

Table 2. Location of Teflon Coated Copper Constantan Thermocouples

Tube	HA (Degrees)	Run Number	Date	Ac (in^2)	An (in^2)	Pw_i (in)	Pw_o (in)	D_H (in)	D_i (in)	D_o (in)	t_w (in)	R_w ($\frac{hr \cdot ft^2 {}^oF}{BTU}$) ($10^{-5}$)	Kc+Ke	Material	TYPE RUN	A_{met} in^2
1	45	1	7 OCT 77	0.135	70.686	1.87	2.20	0.289	0.524	0.630	0.144	4.376	0.330	Al	Practice	0.125
		2	11 OCT 77												Data	
		3	11 OCT 77												Data	
		7	7 NOV 77												Movie	
		11	9 JAN 78												Data	
		17	23 JAN 78												Isothermal	
2	30	8	28 NOV 77	0.127	70.686	1.96	2.31	0.259	0.530	0.630	0.124	3.784	0.400	Al	Data	0.110
		10	5 JAN 78												Data	
		15	24 JAN 78												Data	
		16	24 JAN 78												Isothermal	
3	60	9	29 NOV 77	0.145	70.686	1.65	2.01	0.350	0.530	0.629	0.131	3.978	0.26	Al	Data	0.115
		12	10 JAN 78												Data	
		18	23 JAN 78												Isothermal	
4	Smooth	4	18 OCT 77	0.212	70.460	1.630	1.957	0.519	0.519	0.623	0.050	18.370	0.0	CuNi	Data	
		5	20 OCT 77												Data	
		6	20 OCT 77												Data	
5	Smooth	13	11 JAN 78	0.221	71.025	1.665	1.973	0.530	0.530	0.628	0.049	2.981	0.1	Al	Data	
		14	14 JAN 78												Data	
6	30	PT-1	21 DEC 77	0.127	70.686	1.96	2.31	0.259	0.530	0.630	0.124	7.569		Al	Isothermal	
7	45	PT-2	21 DEC 77	0.135	70.686	1.87	2.20	0.289	0.524	0.630	0.144	8.752		Al	Isothermal	
8	60	PT-3	20 DEC 77	0.145	70.686	1.65	2.01	0.350	0.530	0.629	0.131	7.956		Al	Isothermal	

Table 3. TEST TUBE SUMMARY

% FLOW	T_v(°F)	T_w(°R)	Tc_i(°F)	Tc_o(°F)	ΔP(psi)
11	151.4	574.4	69.7	101.8	.77
21	151.2	565.4	69.8	91.1	2.68
31	151.3	561.0	69.9	86.2	5.50
41	151.2	557.8	70.3	83.4	9.32
51	151.3	555.8	70.8	81.8	13.92
61	151.0	554.2	71.2	80.7	19.56
71	150.8	552.8	71.6	79.9	26.44
74	150.8	552.6	71.7	79.8	29.21

Table 4. Raw Data for 45° Tube, Run 2, 11 OCT 77

% FLOW	T_v(°F)	T_w(°R)	Tc_i(°F)	Tc_o(°F)	ΔP(psi)
10	154.7	573.3	69.0	101.30	1.00
20	153.1	564.3	68.5	90.37	3.14
30	151.9	559.2	68.3	84.74	6.42
40	149.7	556.2	68.3	81.50	11.10
50	149.7	554.2	68.7	79.88	16.61
60	150.0	552.4	69.2	78.89	23.53
70	150.3	551.0	69.4	78.04	31.45
73	150.7	551.1	69.9	78.35	33.68

Table 5. Raw Data for 45° Tube, Run 3, 11 OCT 77

% FLOW	T_v(°F)	T_w(°R)	Tc_i(°F)	Tc_o(°F)	ΔP(psi)
10	152.3	574.7	66.3	84.5	.18
20	150.7	559.4	66.0	79.2	.54
30	151.1	554.4	65.6	76.5	1.11
40	151.1	552.2	65.8	74.8	1.88
50	150.7	551.0	66.0	73.8	2.75
60	150.6	549.0	66.3	73.2	3.82
70	149.3	547.0	66.5	72.5	5.07
80	149.1	546.3	66.7	72.2	6.39
90	149.5	546.1	66.7	71.7	7.91
100	149.4	545.2	66.9	71.6	9.58

Table 6. Raw Data for Smooth Tube, Run 4, 18 OCT 77

% FLOW	T_v(°F)	T_w(°R)	Tc_i(°F)	Tc_o(°F)	ΔP(psi)
10	149.9	581.6	64.2	99.4	.81
15	150.4	576.3	64.0	92.1	1.63
20	150.1	574.2	64.2	87.7	2.43
25	150.5	571.8	65.1	85.0	3.48
30	150.9	570.8	66.3	83.7	4.77
40	149.7	568.8	67.4	81.3	7.98
50	148.6	567.3	67.6	79.2	12.03
60	148.7	566.6	67.2	77.4	16.70
70	148.3	564.6	67.2	76.1	22.23
80	148.6	563.7	67.2	75.4	27.96

Table 7. Raw Data for 30° Tube, Run 8, 28 NOV 77

% FLOW	T_v(°F)	T_w(°R)	Tc_i(°F)	Tc_o(°F)	ΔP(psi)
10	154.1	579.6	70.5	106.4	.91
15	151.1	590.7	69.6	96.4	2.13
20	149.3	584.8	68.9	90.8	3.73
25	149.0	580.2	68.7	87.8	5.59
30	148.7	579.8	68.5	85.7	7.75
40	148.2	577.3	68.5	81.9	13.74
50	147.9	576.0	68.4	80.3	21.75
60	147.5	578.2	68.7	79.0	31.97
65	147.4	576.4	69.1	78.7	38.27

Table 8. Raw Data for 60° Tube, Run 9, 29 NOV 77

% FLOW	T_v(°F)	T_w(°R)	Tc_i(°F)	Tc_o(°F)	ΔP(psi)
15	152.2	567.02	69.9	95.9	1.75
20	151.3	563.0	67.2	90.0	2.57
25	151.4	560.1	67.6	86.9	3.86
30	151.3	557.8	68.0	84.7	5.32
40	151.5	554.9	68.1	81.7	9.03
50	151.5	552.8	68.7	80.1	13.35
60	151.2	551.5	69.0	79.0	18.95
70	151.1	549.5	69.4	78.6	25.71
76	151.2	549.0	69.8	77.9	30.03

Table 9. Raw Data for 45° Tube, Run 11, 9 JAN 78

% FLOW	T_v(°F)	T_w(°R)	Tc_i(°F)	Tc_o(°F)	ΔP(psi)
10.5	149.7	592.7	64.7	101.4	1.11
15	149.8	592.0	64.5	94.6	2.18
20	150.1	588.9	64.4	89.8	3.82
25	149.9	589.5	64.7	86.3	5.46
30	149.9	588.0	64.9	84.0	7.80
40	150.0	585.5	64.9	80.5	13.56
50	149.8	585.3	65.3	78.4	21.00
60	149.8	584.8	65.6	77.0	30.97
66	149.7	583.2	66.3	76.7	38.13

Table 10. Raw Data for 60° Tube, Run 12, 10 JAN 78

% FLOW	T_v(°F)	T_w(°R)	Tc_i(°F)	Tc_o(°F)	ΔP(psi)
10	151.6	585.7	64.5	84.3	.15
15	151.0	580.7	64.4	81.4	.29
20	150.5	575.4	64.4	79.3	.52
25	150.2	572.0	64.5	77.3	.77
30	149.9	566.4	68.7	76.8	1.10
40	149.9	561.8	64.9	75.1	1.84
50	149.7	559.6	65.3	74.0	2.82
61	149.7	558.9	65.6	73.4	3.98
70	149.5	557.1	66.2	73.1	5.12
81	149.5	555.6	66.3	72.5	6.69
89	149.6	555.1	66.7	72.5	7.88

Table 11. Raw Data for Smooth Al Tube, Run 14, 14 JAN 78

% FLOW	T_v(°F)	T_w(°R)	Tc_i(°F)	Tc_o(°F)	ΔP(psi)
10.5	151.3	585.0	61.8	97.2	.72
15	152.0	582.3	65.1	92.5	1.36
20	151.2	579.0	62.1	86.2	2.27
25	151.5	576.9	64.9	84.8	3.36
30	150.8	575.4	62.1	80.4	4.71
40.25	151.2	573.1	62.4	77.1	7.82
51	151.4	571.7	63.3	75.5	11.90
61	151.3	570.4	64.2	74.6	16.49
70	151.1	570.4	64.4	73.9	21.45
80	151.1	568.3	64.9	73.4	27.55

Table 12. Raw Data for 30° Tube, Run 15, 24 JAN 78

VELOCITY	UN	UC	HI	HO
FT/SEC	BTU/(F*HR*FT**2)	BTU/(F*HR*FT**2)	BTU/(F*HR*FT**2)	BTU/(F*HR*FT**2)
2.80	897.789	974.350	2091.847	2214.474
5.59	1137.684	1263.454	3531.258	2217.367
8.39	1247.034	1399.815	4802.957	2154.906
11.19	1343.093	1522.006	5986.328	2192.078
13.98	1413.917	1613.599	7120.023	2217.924
16.78	1453.151	1664.858	8209.422	2201.746
19.58	1500.384	1727.195	9255.820	2226.785
20.42	1523.266	1757.587	9588.148	2254.443
REYNOLDS NO	PLAIN END REYN NO	FLOW RATE PER AREA	FRICTION FACTOR	SIEDER TATE CONSTANT
14179.06	14179.06	624261.69	0.06349003	0.06498593
26560.74	26560.71	1249908.00	0.04885374	0.06548274
38514.71	38514.71	1875876.00	0.04408755	0.06574225
50379.06	50379.04	2501911.00	0.04267668	0.06588978
62504.00	62503.98	3127747.00	0.04091374	0.06594765
74838.44	74808.38	3753444.00	0.04023363	0.06596792
86923.06	86923.00	4379289.00	0.03947223	0.06599935
91114.44	91114.44	4566620.00	0.03881308	0.06595963

Table 13. 45^{o} Tube Results Based on Plain End Diameter, Run 3

NUSSELT NO	NU/PR1/3(U/UW)0.14	STANTON NO	J FACTOR	PERFORM FACTOR
245.56676	136.18736	0.00335546	0.0100215	0.3156869
417.71167	226.73499	0.00282780	0.0088765	0.3633893
570.39258	306.43945	0.00256209	0.0082521	0.3743486
712.52295	380.72998	0.00239394	0.0078235	0.3649318
848.20532	452.81885	0.00227745	0.0074853	0.3659083
978.28613	522.98853	0.00218813	0.0072061	0.3582133
1103.50635	589.99243	0.00211440	0.0069848	0.3539104
1142.43994	612.27612	0.00210056	0.0069121	0.3561726

XIN	PRESSURE DROP (PSI)	PRANDTL NO	U/UW
0.2660877D-03	0.91319	5.16143	1.04338
0.1576645D-03	2.81381	5.56146	1.03983
0.1159338D-03	5.71651	5.78034	1.03716
0.9302291D-04	9.88650	5.90793	1.03523
0.7821340D-04	14.74214	5.95860	1.03323
0.6783502D-04	20.87660	5.97643	1.03076
0.6016706D-04	27.87935	6.00415	1.02907
0.5608055D-04	29.81160	5.96914	1.02861

Table 13. Page 2

VELOCITY	UN	UC	HI	HO
FT/SEC	BTU/(F*HR*FT**2)	BTU/(F*HR*FT**2)	BTU/(F*HR*FT**2)	BTU/(F*HR*FT**2)
2.90	984.806	1077.696	2656.266	2104.015
5.71	1182.866	1319.468	4432.789	2054.844
8.59	1307.885	1476.950	6065.680	2038.297
11.30	1364.769	1549.901	7485.777	2063.589
14.12	1411.652	1610.650	8906.477	2088.135
16.87	1456.724	1669.590	10146.109	2081.374
19.75	1503.045	1730.722	11572.148	2110.157
20.86	1529.363	1765.710	12086.078	2141.937
REYNOLDS NO	PLAIN END REYN NO	FLOW RATE PER AREA	FRICTION FACTOR	SIEDER TATE CONSTANT
14793.03	14793.02	647289.88	0.04395237	0.07984662
27419.40	27419.38	1274654.00	0.03917475	0.08040088
40175.97	40175.97	1920332.00	0.03513127	0.08065790
52086.36	52086.30	2526011.00	0.03441302	0.08079267
64695.88	64695.85	3157827.00	0.03272974	0.08085269
75074.31	75074.25	3770897.00	0.03224261	0.08089513
89867.50	89867.50	4417056.00	0.03174709	0.08091748
94931.13	94931.06	4664812.00	0.03142755	0.08091527

Table 14. 45^{o} HA Tube Results Based on Plain End Diameter, Run 2.

NUSSELT NO	NU/PR1/3(U/UW)0.14	STANTON NO	J FACTOR	PERFORM FACTOR
311.60620	173.10159	0.00410939	0.0122168	0.5559120
523.61963	285.56543	0.00348112	0.0108279	0.5528002
719.79419	388.88306	0.00316120	0.0100394	0.5715379
888.56055	479.45728	0.00296554	0.0095209	0.5533292
1057.98267	570.68262	0.00282227	0.0091047	0.5563586
1205.86841	643.15283	0.00269229	0.0088562	0.5493457
1375.73438	742.88867	0.00262144	0.0085010	0.5355423
1436.79175	776.16968	0.00259245	0.0084054	0.5349083

XIN	PRESSURE DROP (PSI)	PRANDTL NO	U/UW
0.2576411D-03	0.67975	5.12591	1.04403
0.1544216D-03	2.34702	5.48580	1.03967
0.1128629D-03	4.77508	5.65961	1.03719
0.9145700D-04	8.09149	5.75253	1.03431
0.7687026D-04	12.02573	5.79432	1.03217
0.6748496D-04	16.89201	5.96605	1.03377
0.5916464D-04	22.81998	5.83971	1.02836
0.5664876D-04	25.19568	5.83813	1.02805

Table 14. Page 2.

VELOCITY	UN	UC	HI	HO
FT/SEC	BTU/(F*HR*FT**2)	BTU/(F*HR*FT**2)	BTU/(F*HR*FT**2)	BTU/(F*HR*FT**2)
4.20	1081.837	1194.985	3372.856	2081.727
5.59	1203.217	1344.840	4163.977	2198.542
6.99	1244.557	1396.695	4934.418	2117.199
8.39	1282.442	1444.586	5672.754	2082.068
11.19	1353.114	1534.888	7076.813	2076.317
13.98	1421.806	1623.882	8416.293	2114.211
16.78	1475.915	1694.849	9708.289	2145.087
19.58	1493.031	1717.458	10938.137	2117.126
21.26	1518.044	1750.640	11675.598	2135.634
REYNOLDS NO	PLAIN END REYN NO	FLOW RATE PER AREA	FRICTION FACTOR	SIEDER TATE CONSTANT
20739.99	20739.98	936801.25	0.04828855	0.07718998
26319.81	26319.80	1250093.00	0.03896766	0.07763565
32368.15	32368.15	1563023.00	0.03748142	0.07778352
38433.25	38433.23	1875939.00	0.03566075	0.07787979
50392.67	50392.64	2501900.00	0.03399715	0.07803279
62621.34	62621.31	3127659.00	0.03188531	0.07808661
74783.75	74783.69	3753462.00	0.03141809	0.07813078
86943.75	86943.75	4379274.00	0.03135428	0.07816279
94497.63	94497.63	4754561.00	0.03105935	0.07815289

Table 15. 45° HA Tube Results Based on Plain End Diameter, Run 11

NUSSELT NO	NU/PR1/3(U/UW)0.14	STANTON NO	J FACTOR	PERFORM FACTOR
397.10620	219.28432	0.00360469	0.0109737	0.4545068
493.08038	266.86182	0.00333376	0.0105374	0.5408268
585.42529	315.48657	0.00315927	0.0101103	0.5394839
673.85547	362.40112	0.00302592	0.0097617	0.5474755
842.29199	450.99341	0.00283005	0.0092469	0.5439785
1002.64746	536.97437	0.00269284	0.0088380	0.5543617
1156.94482	619.25122	0.00258762	0.0085239	0.5426066
1304.04053	698.85913	0.00249873	0.0082529	0.5264301
1391.78467	746.93188	0.00245669	0.0081074	0.5220610

XIA	PRESSURE DROP (PSI)	PRANDTL NO	U/UW
0.19546620-03	1.56341	5.31166	1.03790
0.15835880-03	2.24474	5.61954	1.03928
0.13364150-03	3.37451	5.72488	1.03729
0.11625210-03	4.62402	5.79432	1.03524
0.93193420-04	7.83902	5.90611	1.03322
0.78344500-04	11.48867	5.94587	1.03058
0.67935600-04	16.30243	5.97868	1.02938
0.60257570-04	22.14555	6.00252	1.02673
0.56469200-04	25.85863	5.99516	1.02571

Table 15. Page 2.

VELOCITY	UN	UC	HI	HO
FT/SEC	BTU/(F*HR*FT**2)	BTU/(F*HR*FT**2)	BTU/(F*HR*FT**2)	BTU/(F*HR*FT**2)
2.73	1005.911	1088.80	2558.655	2199.733
4.10	1124.049	1228.574	3472.457	2117.841
5.47	1220.007	1344.124	4359.434	2119.796
6.83	1264.016	1397.740	5142.164	2063.369
8.20	1315.519	1460.989	5940.676	2063.158
10.94	1412.180	1581.186	7441.180	2114.403
13.67	1479.344	1665.870	8849.250	2145.119
16.40	1526.603	1726.041	10191.156	2160.258
19.14	1555.338	1762.865	11471.727	2156.079
21.87	1621.171	1847.918	12733.016	2232.424
REYNOLDS NO	PLAIN END REYN NO	FLOW RATE PER AREA	FRICTION FACTOR	SIEDER TATE CONSTANT
13492.37	13492.37	610609.00	0.05272907	0.08144724
19383.80	19383.80	916562.25	0.04626318	0.08185810
25872.20	25872.18	1222062.00	0.03767957	0.08184803
31180.39	31180.37	1528453.00	0.03403658	0.08219850
37416.46	37416.43	1834142.00	0.03220741	0.08219850
49503.44	49503.41	2445814.00	0.02999793	0.08227324
61177.03	61177.97	3057795.00	0.02878457	0.08238320
72457.38	72457.38	3670071.00	0.02756030	0.08251011
83894.31	83894.25	4282229.00	0.02689816	0.08258379
95462.69	95462.63	4894288.00	0.02568418	0.08262604

Table 16. 30^{o} HA Tube Results Based on Plain End Diameter, Run 8.

NUSSELT NO	NU/PR1/3(U/UW)0.14	STANTON NO	J FACTOR	PERFORM FACTOR
305.15894	164.03896	0.00419496	0.0128984	0.4892316
416.23267	220.29890	0.00379159	0.0120468	0.5207937
522.48779	277.50684	0.00357015	0.0113342	0.6016088
618.53848	323.56982	0.00336608	0.0109871	0.6456063
715.05103	374.37988	0.00324065	0.0105777	0.6569518
896.47485	468.77637	0.00304384	0.0099941	0.6663171
1067.53735	556.05005	0.00289510	0.0095884	0.6662173
1231.31299	637.63550	0.00277759	0.0092914	0.6742581
1387.27075	717.59546	0.00267949	0.0090151	0.6703116
1540.58545	796.12842	0.00260207	0.0087836	0.6839718

XIN	PRESSURE DROP (PSI)	PRANDTL NO	U/UW
0.26840410-03	0.71692	5.39150	1.06090
0.19780420-03	1.41627	5.66338	1.05998
0.15755770-03	2.05062	5.65661	1.05670
0.13359320-03	2.89598	5.89714	1.05876
0.11563650-03	3.94608	5.89714	1.05717
0.92321180-04	6.53477	5.94950	1.05539
0.77634580-04	9.79928	6.02732	1.05494
0.67415590-04	13.51343	6.11811	1.05582
0.59891770-04	17.95308	6.17131	1.05396
0.53960030-04	22.39240	6.20202	1.05323

Table 16. Page 2.

VELOCITY	UN	UC	HI	HO
FT/SEC	BTU/(F*HR*FT**2)	BTU/(F*HR*FT**2)	BTU/(F*HR*FT**2)	BTU/(F*HR*FT**2)
2.87	1007.981	1091.235	2561.110	2207.490
4.10	1084.283	1181.224	3386.765	2015.483
5.47	1206.201	1327.386	4180.098	2130.173
6.83	1244.560	1373.989	4994.750	2039.984
8.20	1326.141	1474.102	5698.152	2127.195
11.00	1397.549	1562.866	7150.559	2110.247
13.94	1456.368	1636.793	8613.594	2113.407
16.68	1486.316	1674.718	9922.637	2094.192
19.14	1557.654	1765.840	11067.336	2178.322
21.87	1577.571	1791.481	12277.590	2166.688
REYNOLDS NO	PLAIN END REYN NO	FLOW RATE PER AREA	FRICTION FACTOR	SIEDER TATE CONSTANT
13808.52	13808.52	641411.81	0.04105258	0.07884783
19557.25	19557.25	916431.13	0.03809961	0.07892710
24672.25	24672.23	1222967.00	0.03469056	0.07943982
31113.88	31113.85	1528504.00	0.03269708	0.07935762
35740.06	35740.04	1835401.00	0.03160219	0.07976574
47119.37	47119.34	2463118.00	0.02877059	0.07993013
59441.99	59441.94	3121164.00	0.02698995	0.07997155
71097.31	71097.25	3733159.00	0.02602392	0.07997155
81317.94	81317.94	4284154.00	0.02567799	0.08000267
92934.81	92934.75	4896174.00	0.02519172	0.08000267

Table 17. 30^{o} HA Tube Results Based on Plain End Diameter, Run 15.

NUSSELT NO	NU/PR1/3(U/UW)0.14	STANTON NO	J FACTOR	PERFORM FACTOR
306.36499	161.77313	0.00399662	0.0125302	0.6104463
405.53906	213.93018	0.00369880	0.0116727	0.6127439
503.78638	259.30103	0.00341952	0.0112550	0.6488812
601.34546	311.85376	0.00326942	0.0106890	0.6538190
689.56006	350.21875	0.00310509	0.0104947	0.6641739
867.10547	437.79272	0.00290310	0.0099434	0.6912204
1045.06006	527.48340	0.00275969	0.0094839	0.7027691
1203.88257	608.71924	0.00265752	0.0091341	0.7019805
1343.28687	678.03589	0.00256320	0.0088997	0.6931750
1490.16042	754.47729	0.00250747	0.0086388	0.6858421

XIN	PRESSURE DROP (PSI)	PRANDTL NO	U/UW
0.25883990-03	0.61563	5.55136	1.06955
0.19574410-03	1.16619	5.60615	1.06710
0.15862740-03	1.88935	5.97136	1.07090
0.13275050-03	2.78209	5.91152	1.06645
0.11638260-03	3.87458	6.21359	1.07099
0.92749380-04	6.35120	6.33884	1.07020
0.76997010-04	9.56631	6.37072	1.06873
0.66836170-04	13.19578	6.37072	1.06685
0.59926810-04	17.14667	6.39476	1.06735
0.54019500-04	21.97151	6.39476	1.06411

Table 17. Page 2.

VELOCITY	UN	UC	HI	HO
FT/SEC	BTU/(F*HR*FT**2)	BTU/(F*HR*FT**2)	BTU/(F*HR*FT**2)	BTU/(F*HR*FT**2)
2.73	1066.492	1165.378	2660.438	2427.174
4.10	1136.249	1249.178	3587.184	2129.090
5.47	1210.606	1339.638	4436.484	2087.843
6.83	1289.270	1436.635	5243.469	2128.867
8.20	1376.239	1545.461	6041.813	2219.135
10.94	1411.511	1590.082	7533.922	2121.467
13.67	1548.044	1765.493	8962.973	2304.129
16.40	1612.906	1850.356	10386.133	2346.484
17.77	1635.113	1879.641	11046.805	2355.250
REYNOLDS NO	PLAIN END REYN NO	FLOW RATE PER AREA	FRICTION FACTOR	SIEDER TATE CONSTANT
14540.79	14540.78	609806.50	0.06179618	0.08057064
20515.66	20515.65	915702.56	0.06494856	0.08114439
26384.16	26384.13	1221674.00	0.06377429	0.08148623
32365.73	32365.73	1527559.00	0.06119281	0.08166528
38331.20	38331.17	1833453.00	0.05879678	0.08179092
50008.57	50008.54	2445434.00	0.05866732	0.08199942
61812.95	61812.90	3057318.00	0.05956741	0.08210731
73798.50	73798.44	3669066.00	0.06095305	0.08215642
79969.75	79969.69	3974805.00	0.06229433	0.08215380

Table 18. 60^{o} HA Tube Results Based on Plain End Diameter, Run 9:

NUSSELT NO	NU/PR1/3(U/UW)0.14	STANTON NO	J FACTOR	PERFORM FACTOR
314.55664	172.28468	0.00436965	0.0126927	0.4107940
427.15063	228.52122	0.00392210	0.0119354	0.3675329
530.50806	280.64502	0.00363452	0.0113692	0.3565456
628.38379	331.21143	0.00343537	0.0108998	0.3562430
725.17212	379.79199	0.00329767	0.0105680	0.3594583
906.56812	471.02563	0.00308250	0.0100432	0.3423774
1079.94775	558.78467	0.00293300	0.0096380	0.3235987
1252.17236	644.28516	0.00283152	0.0093420	0.3065296
1331.78223	687.01636	0.00278038	0.0091701	0.2944112

XIN	PRESSURE DROP (PSI)	PRANDTL NO	U/UW
0.25750910-03	0.83909	4.95068	1.07127
0.19102650-03	1.98642	5.30856	1.07151
0.15447840-03	3.46965	5.53164	1.06885
0.13071310-03	5.20348	5.65153	1.06512
0.11344670-03	7.20149	5.73695	1.06660
0.90986820-04	12.77814	5.88102	1.06628
0.76482450-04	20.27567	5.95678	1.06616
0.65003660-04	29.87845	5.99150	1.07006
0.62056220-04	35.83716	5.98967	1.06741

Table 18. Page 2.

VELOCITY	UN	UC	HI	HO
FT/SEC	BTU/(F*HR*FT**2)	BTU/(F*HR*FT**2)	BTU/(F*HR*FT**2)	BTU/(F*HR*FT**2)
2.87	1128.120	1239.359	3089.017	2365.905
4.10	1244.368	1381.104	4060.312	2316.060
5.47	1341.016	1501.184	5049.941	2319.488
6.83	1406.798	1584.104	6012.227	2304.811
8.20	1455.475	1646.094	6916.840	2294.006
10.94	1542.432	1758.196	8628.113	2319.027
13.67	1618.913	1858.262	10283.320	2365.588
16.40	1656.909	1908.502	11867.301	2358.680
18.04	1678.534	1937.250	12791.074	2361.761
REYNOLDS NO	PLAIN END REYN NO	FLOW RATE PER AREA	FRICTION FACTOR	SIEDER TATE CONSTANT
14375.63	14375.62	640980.44	0.06915611	0.09268099
19736.71	19736.71	916295.00	0.06636345	0.09311066
25554.14	25554.14	1222303.00	0.06539017	0.09343052
31397.22	31397.20	1528290.00	0.05954171	0.09361935
37157.32	37157.30	1834338.00	0.05912596	0.09377134
48514.59	48514.59	2446558.00	0.05778939	0.09400243
60038.51	60038.48	3058649.00	0.05732203	0.09411311
71558.13	71558.06	3670744.00	0.05886894	0.09418833
78950.00	78949.94	4037643.00	0.06003133	0.09415519

Table 19. 60^{0} HA Tube Results Based on Plain End Diameter, Run 12.

NUSSELT NO	NU/PR1/3(U/UW)0.14	STANTON NO	J FACTOR	PERFORM FACTOR
367.78687	196.37743	0.00482501	0.0146716	0.4243050
485.67310	254.22517	0.00443535	0.0139002	0.4189116
606.12231	313.65845	0.00413445	0.0132497	0.4052492
723.07666	370.57446	0.00393625	0.0127807	0.4293035
833.22632	424.72241	0.00377255	0.0123791	0.4187377
1041.93359	527.03076	0.00352773	0.0117619	0.4070600
1243.27954	625.73950	0.00336282	0.0112978	0.3941861
1435.93311	720.64746	0.00323350	0.0109196	0.3709807
1547.16455	779.33643	0.00316858	0.0106761	0.3556827

XIN	PRESSURE DROP (PSI)	PRANDTL NO	U/UW
0.2534010D-03	1.03638	5.30239	1.07402
0.1928127D-03	2.03101	5.54807	1.07914
0.1550447D-03	3.55940	5.73695	1.07947
0.1302374D-03	5.06551	5.85073	1.08286
0.1132106D-03	7.24494	5.94406	1.08300
0.9076385D-04	12.59272	6.08797	1.08271
0.7615745D-04	19.51987	6.15754	1.08400
0.6599403D-04	28.87004	6.20586	1.08429
0.6122723D-04	35.62096	6.18471	1.08153

Table 19. Page 2.

VELOCITY	UN	UC	HI	HO
FT/SEC	BTU/(F*HR*FT**2)	BTU/(F*HR*FT**2)	BTU/(F*HR*FT**2)	BTU/(F*HR*FT**2)
2.85	453.301	494.477	772.397	2135.684
5.70	648.151	735.806	1303.470	2282.383
8.55	780.095	910.586	1780.145	2359.185
11.40	854.622	1013.780	2227.799	2234.205
14.26	924.271	1113.296	2653.147	2243.180
17.11	973.114	1184.934	3060.342	2213.906
19.96	1014.229	1246.463	3448.593	2201.721
22.81	1057.175	1311.963	3831.846	2227.413
25.66	1074.677	1339.025	4205.781	2167.322
28.51	1119.477	1409.297	4569.375	2237.779
REYNOLDS NO	PLAIN END REYN NO	FLOW RATE PER AREA	FRICTION FACTOR	SIEDER TATE CONSTANT
12795.03	12795.03	637526.75	0.00892195	0.02460366
24739.24	24739.24	1275707.00	0.00638100	0.02470141
36429.55	36429.55	1914079.00	0.00582424	0.02475505
48134.88	48134.85	2552441.00	0.00556491	0.02478147
59785.38	59785.32	3190786.00	0.00513666	0.02479650
71728.75	71728.75	3829022.00	0.00495247	0.02480067
83453.75	83453.75	4467367.00	0.00483989	0.02480870
95271.13	95271.06	5105640.00	0.00465098	0.02481190
106861.81	106861.81	5744089.00	0.00455315	0.02482059
118761.50	118761.44	6382301.00	0.00446326	0.02481995

Table 20. Smooth Tube Results, Run 4.

NUSSELT NO	NU/PR1/3(U/UW)0.14	STANTON NO	J FACTOR	PERFORM FACTOR
90.99136	47.49323	0.00121224	0.0039431	0.8839028
154.16395	80.80347	0.00102207	0.0034111	1.0691328
210.99855	110.36467	0.00093017	0.0031482	1.0810795
264.34009	138.06836	0.00087287	0.0029748	1.0691147
315.00098	164.31064	0.00083153	0.0028473	1.1086264
363.40723	190.11552	0.00079926	0.0027376	1.1055317
409.64355	214.66443	0.00077195	0.0026495	1.0948715
455.22729	238.68694	0.00075050	0.0025781	1.1086121
499.82617	261.73950	0.00073217	0.0025208	1.1072636
543.02246	284.80005	0.00071592	0.0024644	1.1043139

XIN	PRESSURE DROP (PSI)	PRANDTL NO	U/UW
0.27199420-03	0.13488	5.86639	1.06229
0.16119640-03	0.38606	6.09700	1.04435
0.11604070-03	0.79305	6.22673	1.03919
0.94324820-04	1.34727	6.29146	1.03710
0.79204650-04	1.94326	6.33636	1.03602
0.68866180-04	2.69801	6.33884	1.03286
0.60936220-04	3.58895	6.35875	1.03004
0.54841740-04	4.50470	6.36671	1.02903
0.49966300-04	5.58158	6.38833	1.02917
0.45990320-04	6.75478	6.38673	1.02766

Table 20. Page 2.

% Flow	10	30	50	70
Taps	("Hg)	("Hg)	("Hg)	("Hg)
1-7	2.0	13.2	34.2	64.5
2-6	1.9	13.1	34.0	64.4
2-4	.7	4.6	11.6	21.4
2-3	0	.3	.8	1.4
3-5	1.4	9.2	23.6	44.5
3-4	.7	4.6	11.0	20.2
4-5	.7	4.9	12.7	24.5
5-6	.5	3.7	10.0	19.0
6-4	1.2	8.4	22.6	43.2

Table 21. Summary of Pressure Drops PT - 1, 30^{o}

% Flow	10	20	30	40	50	60
TAPS	("Hg)	(" Hg)	(" Hg)	("Hg)	("Hg)	("Hg)
1-7	2.3	7.7	17	28.8	43.6	61.5
2-6	2.2	7.5	16.8	28.3	43.03	60.5
2-4	.9	3.1	6.4	11.5	17.6	24.8
2-3	0	.2	.4	.8	1.2	1.7
3-5	1.7	5.6	12.5	21.3	32.2	45.3
3-4	.9	2.9	6.4	10.9	16.6	23.3
4-5	.9	2.8	6.2	10.5	15.7	22.2
5-6	.5	1.7	3.8	6.5	9.9	13.9
6-4	1.4	4.5	9.9	16.9	25.3	35.6

Table 22. Summary of Pressure Drops PT-2, 45^{o}

% Flow	10	15	20	25	30	40	50	60
Taps	("Hg)	("Hg)	("Hg)	("Hg)	("Hg)	("Hg)	("Hg)	("Hg)
1-7	2.4	5.4	8.9	13.9	19.7	34.5	53.5	78.2
2-6	2.3	5.1	8.6	13.6	19.4	34.0	53.0	77.0
2-4	.9	2.0	3.5	5.5	7.6	13.9	21.9	32.0
2-3	0	0	0	.1	0	.2	.4	.6
3-5	1.9	4.0	6.7	10.5	14.9	26.2	41.0	60.1
3-4	.9	2.1	3.5	5.5	7.7	13.8	21.7	31.7
4-5	.8	2.0	3.4	5.2	7.2	12.5	19.5	28.7
5-6	.5	1.4	2.2	3.2	4.5	7.8	11.8	16.8
6-4	1.4	3.1	5.3	5.5	11.6	20.1	31.1	45.2

Table 23. Summary of Pressure Drops PT - 3, 60^{o}

% Flow	$1-\sigma^2$	$\frac{\rho v^2}{2gc}$(psi)	ΔP_{Ac} (in Hg)	ΔP_T (in Hg)	ΔP_{smooth} (in Hg)	ΔP_{comp} (in Hg)	K_{cn}	ΔP_{exp} (in Hg)	K_e
20	0.608	0.555	0.741	0.375	0.0633	0.534	0.45	0.4135	0.35
30	0.608	1.26	1.68	0.837	0.1345	1.208	0.46	1.108	0.42
40	0.608	2.18	2.91	1.43	0.2211	1.899	0.40	1.718	0.37
50	0.608	3.41	4.55	2.15	0.3270	2.849	0.39	2.949	0.40
60	0.608	4.86	6.49	3.03	0.4570	3.895	0.37	4.155	0.39

$$\frac{\Sigma Kc_i}{i} = 0.41 \qquad \frac{\Sigma Ke_i}{i} = 0.39$$

Table 24. Summary of $K_{cn} + K_e$ determination PT-2, 45^o.

% Flow	$1-\sigma^2$	$\frac{\rho v^2}{2gc}$(psi)	ΔP_{Ac} (in Hg)	ΔP_T (in Hg)	ΔP_{smooth} (in Hg)	ΔP_{comp} (in Hg)	K_{cn}	ΔP_{exp} (in Hg)	K_e
10	0.661	0.151	0.219	0.1	0.018	0.122	0.37	0.11	0.33
30	0.661	1.36	1.97	0.657	0.133	0.940	0.31	1.447	0.48
50	0.661	3.77	5.47	1.68	0.334	2.633	0.32	4.123	0.50
70	0.661	7.40	10.75	3.18	0.617	4.862	0.30	8.062	0.50

$\Sigma Kc_i/i = 0.32$ $\Sigma Ke_i/i = 0.45$

Table 25. Summary of $K_{cn} + K_e$ determination PT-1, 30^o.

% Flow	$1-\sigma^2$	$\frac{\rho v^2}{2gc}$(psi)	ΔP_{Ac} (in Hg)	ΔP_T (in Hg)	ΔP_{smooth} (in Hg)	ΔP_{comp} (in Hg)	K_{cn}	ΔP_{exp} (in Hg)	K_e
15	0.568	0.261	0.326	0.248	0.033	0.7595	1.32	-0.2385	-.42
20	0.568	0.463	0.578	0.415	0.055	1.1285	1.11	-0.1145	-0.11
25	0.568	0.724	0.904	0.650	0.085	1.6035	1.01	0.1115	0.07
30	0.568	1.04	1.30	0.920	0.119	2.1705	0.95	0.4205	0.18
40	0.568	1.85	2.31	1.62	0.200	3.770	0.93	0.5900	0.15
50	0.568	2.89	3.61	2.54	0.302	5.493	0.87	1.119	0.18
60	0.568	4.17	5.20	3.72	0.419	7.6705	0.84	1.371	0.15

$\Sigma Kc_i/i = 1.00$, $\Sigma Ke_i/i = 0.03$

Table 26. Summary of $K_{cn} + K_e$ determination PT-3, 60°.

$\dot{m}$ $(\frac{lbm}{sec})$	0.260	0.781	1.30	1.82
Re_s	13,492	37,416	61,178	83,894
f_s	0.0073	0.0060	0.0054	0.0051
G_s $(\frac{lbm}{hr \cdot ft^2})$	610,609	1,834,142	3,057,795	4,282,229
ΔP_s (psi)	0.0082	0.0607	0.152	0.281
V_{TS} $(\frac{ft}{hr})$	17,100	51,300	85,500	119,700
$\rho \frac{V_{TS}^2}{2gc}$ (psi)	0.151	1.36	3.77	7.40
$(K_c + K_e)_1$	0.40	0.40	0.40	0.40
$(K_c + K_e)_2$	0.77	0.77	0.77	0.77
$\Delta P_{exp/con_1}$ (psi)	0.0604	0.544	1.51	2.96
$\Delta P_{exp/con_2}$ (psi)	0.116	1.0472	2.903	5.70
ΔP_{2-6} (psi)	0.84	5.96	15.47	29.31
ΔP_{TS_1} (psi)	0.7714	5.355	13.808	26.069
ΔP_{TS_2} (psi)	0.7758	4.852	12.415	23.329
G_{TS} $(\frac{lbm}{hr \cdot ft^2})$	1,060,726	3,186,201	5,311,884	7,438,923
f_{TS_1}	0.0092	0.00707	0.00656	0.00631
f_{TS_2}	0.00852	0.00641	0.00589	0.00565
ΔP_{3-5} (psi)	0.637	4.18	10.72	20.25
f_{3-5}	0.00867	0.00632	0.00582	0.00561

Table 27. Friction Factor Summary, PT-1, 30°

$\dot{m}$ $(\frac{lbm}{sec})$	.530	.800	1.050	1.310	1.570
Re_s	27,419	40,176	52,086	64,696	75,074
f_s	.0063	.0059	.0056	.0053	.0052
G_s $(\frac{lbm}{hr \cdot ft^2})$	1,274,654	1,920,332	2,526,011	3,157,827	3,770,897
ΔP_s (psi)	.0288	.0612	.1006	.1488	.2081
V_{TS} $(\frac{ft}{hr})$	32,796	49,428	64,980	81,216	96,984
$\rho \frac{V_{TS}^2}{2gc}$ (psi)	.555	1.26	2.18	3.41	4.86
$(K_c + K_e)_1$	.33	.33	.33	.33	.33
$(K_c + K_e)_2$	.80	.80	.80	.80	.80
$\Delta P_{exp/con_1}$ (psi)	.183	.416	.719	1.13	1.60
$\Delta P_{exp/con_2}$ (psi)	.444	1.01	1.74	2.73	3.89
ΔP_{2-6} (psi)	3.39	7.65	12.88	19.58	27.53
ΔP_{TS_1} (psi)	3.19	7.17	12.06	18.30	25.72
ΔP_{TS_2} (psi)	2.92	6.58	11.04	16.70	23.43
G_{TS} $(\frac{lbm}{hr \cdot ft^2})$	2,036,156	3,067,574	4,035,097	5,044,372	6,023,701
f_{TS_1}	0.0115	0.0114	0.111	0.0108	0.0106
f_{TS_2}	0.0106	0.0105	0.0101	0.0098	0.0097
ΔP_{3-5} (psi)	2.55	5.69	9.69	14.63	20.62
f_{3-5}	0.0108	0.0107	0.0103	0.0099	0.0097

Table 28. Friction Factor Summary, PT-2, 45°

$\dot{m}$ ($\frac{lbm}{sec}$)	.260	.390	.520	.650	.780	1.04	1.30	1.56
Re_s	14,590	20,516	26,384	32,366	38,331	50,009	61,813	73,799
f_s	.00719	.0066	.0062	.0061	.0059	.0056	.0054	.0052
G_s ($\frac{lbm}{hr \cdot ft^2}$)	609,807	915,703	1,221,674	1,527,559	1,833,453	2,445,434	3,057,318	3,669,066
ΔP_s (psi)	.0073	.0151	.0252	.0388	.0540	.0912	.1375	.1907
V_{TS} ($\frac{ft}{hr}$)	14,976	22,464	29,952	37,440	44,928	59,904	74,880	89,856
$\rho \frac{V_{TS}^2}{2gc}$ (psi)	.116	.261	.463	.724	1.04	1.85	2.89	4.17
$(K_c + K_e)_1$	0.26	0.26	0.26	0.26	0.26	0.26	0.26	0.26
$(K_c + K_e)_2$	1.03	1.03	1.03	1.03	1.03	1.03	1.03	1.03
$\Delta P_{exp/con_1}$ (psi)	.030	.068	.120	.188	.270	.481	.751	1.084
$\Delta P_{exp/con_2}$ (psi)	.119	.269	.477	.746	1.071	1.906	2.977	4.295
ΔP_{2-6} (psi)		2.3	3.91	6.19	8.83	15.47	24.12	35.04
ΔP_{TS_1} (psi)		2.217	3.765	5.963	8.506	14.90	23.23	33.77
ΔP_{TS_2} (psi)		2.016	3.408	5.405	7.705	13.47	21.01	30.55
G_{TS} ($\frac{lbm}{hr \cdot ft^2}$)	927,828	1,393,253	1,858,792	2,324,200	2,789,622	3,720,759	4,651,749	5,582,531
f_{TS_1}		.0207	.0197	.0200	.0198	.0195	.0194	.0196
f_{TS_2}		.0188	.0179	.0181	.0179	.0176	.0176	.0177
ΔP_{3-5} (psi)		1.82		4.78	6.76	11.92	18.66	27.35
f_{3-5}		.0191	.0179	.0180	.0177	.0175	.0175	.0178

Table 29. Friction Factor Summary, PT-3,60°

VELOCITY	UN	UC	HI	HO
FT/SEC	BTU/(F*HR*FT**2)	BTU/(F*HR*FT**2)	BTU/(F*HR*FT**2)	BTU/(F*HR*FT**2)
2.73	488.400	495.615	795.671	1892.122
4.10	624.533	636.379	1088.436	2071.428
5.47	723.819	739.779	1355.690	2093.225
6.83	767.002	784.947	1606.147	1861.651
8.20	869.770	892.918	1844.962	2093.431
10.94	973.898	1003.013	2300.931	2074.568
13.67	1042.662	1076.104	2738.538	2013.695
16.68	1119.605	1158.257	3205.604	2025.395
19.14	1155.698	1196.928	3570.714	1985.576
22.15	1195.047	1239.186	4001.812	1957.371
24.33	1218.468	1264.387	4313.445	1937.246

REYNOLDS NO	PLAIN END REYN NO	FLOW RATE PER AREA	FRICTION FACTOR	SIEDER TATE CONSTANT
12380.23	12380.22	611337.56	0.00818781	0.02603895
18237.22	18237.22	917426.25	0.00643062	0.02613116
24008.91	24008.91	1223465.00	0.00657208	0.02617024
29686.12	29686.12	1529574.00	0.00619052	0.02620375
35545.68	35545.65	1835547.00	0.00625662	0.02621048
46968.25	46968.20	2447714.00	0.00583917	0.02623834
58452.98	58452.95	3059835.00	0.00576367	0.02625190
71175.63	71175.56	3733100.00	0.00541742	0.02625785
81811.75	81811.69	4283784.00	0.00528872	0.02625275
94460.00	94459.94	4957106.00	0.00516044	0.02625955
103960.63	103960.63	5446567.00	0.00501575	0.02625445

Table 30. Smooth Tube Results, Run 14.

NUSSELT NO	NU/PR1/3(U/UW)0.14	STANTON NO	J FACTOR	PERFORM FACTOR
95.71916	48.95593	0.00130226	0.0042698	1.0429764
131.40237	66.97650	0.00116679	0.0039496	1.2283754
163.91167	83.58055	0.00110833	0.0037243	1.1333761
194.68430	99.17580	0.00105151	0.0035628	1.1510429
223.41072	114.57864	0.00100525	0.0034117	1.0905838
278.92114	143.34367	0.00094007	0.0032125	1.1003141
332.13989	170.84618	0.00089500	0.0030687	1.0648327
388.87549	200.04294	0.00085869	0.0029485	1.0885162
433.08325	223.57669	0.00083355	0.0028586	1.0809984
485.49585	250.89069	0.00080728	0.0027731	1.0747519
523.20117	270.83032	0.00079156	0.0027171	1.0825481

XIN	PRESSURE DROP (PSI)	PRANDTL NO	U/UW
0.27365400D-03	0.11146	5.93706	1.07978
0.20006260-03	0.19705	6.07113	1.07545
0.16053090-03	0.35808	6.15985	1.06983
0.13541970-03	0.52710	6.23681	1.06644
0.11803860-03	0.76715	6.25235	1.05841
0.94650310-04	1.27300	6.31706	1.05260
0.79527020-04	1.96346	6.34878	1.04991
0.67940160-04	2.74693	6.36272	1.04908
0.60592770-04	3.53128	6.35077	1.04601
0.54422770-04	4.61377	6.36671	1.04407
0.50490590-04	5.41815	6.35475	1.04297

Table 30. Page 2.

30/2

VELOCITY	UN	UC	HI	HO
FT/SEC	BTU/(F*HR*FT**2)	BTU/(F*HR*FT**2)	BTU/(F*HR*FT**2)	BTU/(F*HR*FT**2)
4.63	984.806	1077.656	2319.808	1865.755
9.11	1182.866	1319.468	3871.312	1822.426
13.73	1307.885	1476.950	5297.375	1851.937
18.05	1364.769	1549.901	6537.594	1830.135
22.56	1411.652	1610.650	7778.332	1825.329
26.94	1456.724	1669.560	8860.945	1845.808
31.56	1503.045	1730.722	10106.363	1871.168
33.33	1529.363	1765.710	10555.172	1899.166
REYNOLDS NO	PLAIN END REYN NO	FLOW RATE PER AREA	FRICTION FACTOR	SIEDER TATE CONSTANT
13032.94	14793.02	1033993.CO	0.00949973	0.04256132
24157.02	27419.38	2036156.CO	0.00846710	0.04285675
35395.82	40175.57	3067574.CO	0.00759317	0.04295378
45889.07	52086.30	4035097.CO	0.00743793	0.04306561
56958.31	64695.85	5044372.CO	0.00707411	0.04309760
66141.88	75074.25	6023701.CO	0.00696882	0.04312021
79175.06	89867.50	7055888.00	0.00686171	0.04313213
83636.13	94931.06	7451658.00	0.00679265	0.04313094

Table 31. 45^{o} HA Tube Results Based on Hydraulic Diameter, Run 2.

NUSSELT NO	NU/PR1/3(U/UW)0.14	STANTON NO	J FACTOR	PERFORM FACTOR
150.09053	83.37738	0.00224667	0.0066791	1.4061737
252.21068	137.54779	0.00190318	0.0059198	1.3983040
346.22021	187.31267	0.00172828	0.0054887	1.4456987
427.99097	230.93922	0.00162131	0.0052052	1.3996410
509.59546	274.87891	0.00154258	0.0049777	1.4073019
580.82715	309.78540	0.00147192	0.0048418	1.3895636
662.64648	357.82520	0.00143318	0.0046476	1.3546486
692.05444	373.85474	0.00141733	0.0045954	1.3530436

XIN	PRESSURE DROP (PSI)	PRANDTL NO	U/UW
0.28511950-03	0.67975	5.12591	1.04403
0.17089120-03	2.34702	5.48580	1.03967
0.12489990-03	4.77508	5.65961	1.03719
0.10121120-03	8.09149	5.75253	1.03431
0.85068810-04	12.02573	5.79432	1.03217
0.74682540-04	16.89201	5.96605	1.03377
0.65474670-04	22.81998	5.83971	1.02836
0.62690580-04	25.19568	5.83813	1.02805

Table 31. Page 2.

31/2

VELOCITY	UN	UC	HI	HO
FT/SEC	BTU/(F*HR*FT**2)	BTU/(F*HR*FT**2)	BTU/(F*HR*FT**2)	BTU/(F*HR*FT**2)
6.70	1081.837	1194.985	2945.631	1846.116
8.94	1203.217	1344.840	3636.542	1949.018
11.17	1244.557	1396.695	4309.398	1877.371
13.40	1282.442	1444.586	4954.215	1846.392
17.87	1353.114	1534.868	6180.422	1841.352
22.34	1421.806	1623.882	7351.977	1874.741
26.81	1475.915	1694.849	8478.594	1901.939
31.28	1493.031	1717.458	9552.652	1877.308
33.96	1518.044	1750.640	10196.703	1893.612
REYNOLDS NO	PLAIN END REYN NO	FLOW RATE PER AREA	FRICTION FACTOR	SIEDER TATE CONSTANT
18272.33	20739.98	1496463.00	0.01043695	0.04114523
23188.25	26319.80	1996922.00	0.00842233	0.04138280
28516.98	32368.15	2496802.00	0.00810111	0.04146164
33860.43	38433.23	2996680.00	0.00770760	0.04151294
44396.91	50392.64	3996582.00	0.00734804	0.04159449
55170.59	62621.31	4996181.00	0.00689159	0.04162318
65885.94	74783.69	5995850.00	0.00679061	0.04164673
76599.13	86943.75	6995534.00	0.00677681	0.04166378
83254.25	94497.63	7595025.00	0.00671307	0.04165852

Table 32. 45^{o} HA Tube Results Based on Hydraulic Diameter, Run 11.

3211

NUSSELT NO	NU/PR1/3(U/UW)0.14	STANTON NO	J FACTOR	PERFORM FACTOR
191.27292	135.62199	0.00197074	0.0059995	1.1496668
237.50034	168.53860	0.00182262	0.0057610	1.3680210
281.58022	151.95970	0.00172722	0.0055275	1.3646193
324.57422	174.55685	0.00165432	0.0053369	1.3848343
405.70410	217.22867	0.00154723	0.0050554	1.3759861
482.94189	258.64258	0.00147222	0.0048319	1.4022493
557.26318	298.27344	0.00141469	0.0046601	1.3725233
628.11377	336.61743	0.00136609	0.0045120	1.3315992
670.37720	359.77246	0.00134311	0.0044325	1.3205471

XIN	PRESSURE DROP (PSI)	PRANDTL NO	U/UW
0.21631330-03	1.56341	5.31166	1.03790
0.17524650-03	2.24474	5.61954	1.03928
0.14769480-03	3.37451	5.72488	1.03729
0.12865080-03	4.62402	5.79432	1.03524
0.10313280-03	7.83902	5.90611	1.03322
0.86700280-04	11.46867	5.94587	1.03068
0.75181130-04	16.30243	5.97868	1.02938
0.66723930-04	22.14555	6.00252	1.02673
0.62513940-04	25.85863	5.99516	1.02571

Table 32. Page 2.

VELOCITY	UN	UC	HI	HO
FT/SEC	BTU/(F*HR*FT**2)	BTU/(F*HR*FT**2)	BTU/(F*HR*FT**2)	BTU/(F*HR*FT**2)
4.75	1005.911	1088.809	2159.786	1845.092
7.12	1124.049	1228.574	2931.138	1777.275
9.50	1220.007	1344.124	3679.848	1778.893
11.87	1264.016	1397.740	4340.555	1732.128
14.25	1315.519	1460.585	5014.586	1731.954
16.00	1412.180	1581.186	6281.188	1774.426
23.75	1479.344	1665.870	7469.750	1799.872
28.50	1526.603	1726.041	8602.469	1812.410
33.25	1555.338	1762.865	9683.414	1808.948
37.99	1621.171	1847.918	10748.070	1872.145
REYNOLDS NO	PLAIN END REYN NO	FLOW RATE PER AREA	FRICTION FACTOR	SIEDER TATE CONSTANT
11453.87	13492.37	1060726.00	0.00853875	0.03830084
16455.20	19383.80	1592216.00	0.00749168	0.03849404
21963.29	25872.18	2122919.00	0.00610168	0.03848931
26465.51	31180.37	2655169.00	0.00551176	0.03865411
31763.39	37416.43	3186201.00	0.00521554	0.03865411
42024.21	49503.41	4248774.00	0.00485775	0.03868925
51934.93	61177.97	5311884.00	0.00466126	0.03874099
61510.20	72457.38	6375506.00	0.00446301	0.03880066
71219.13	83894.25	7438923.00	0.00435578	0.03883529
81039.69	95462.63	8502169.00	0.00415919	0.03885515

Table 33. 30^{o} HA Tube Results Based on Hydraulic Diameter, Run 8.

NUSSELT NO	NU/PR1/3(U/UW)0.14	STANTON NO	J FACTOR	PERFORM FACTOR
125.87767	67.66585	0.00203839	0.0062675	1.4680090
171.69571	90.87314	0.00184239	0.0058537	1.5627193
215.52605	114.47156	0.00173479	0.0055074	1.8052206
255.31165	133.47241	0.00163562	0.0053388	1.9372387
294.95825	154.43169	0.00157468	0.0051399	1.9709864
369.79565	193.37029	0.00147905	0.0048563	1.9993877
440.35864	229.37048	0.00140677	0.0046591	1.9990864
507.61602	263.02417	0.00134967	0.0045148	2.0232105
572.24878	295.00781	0.00130200	0.0043806	2.0113745
635.49023	328.40210	0.00126438	0.0042681	2.0523643

XIN	PRESSURE DROP (PSI)	PRANDTL NO	U/UW
0.3059835D-03	0.71692	5.39150	1.06090
0.2254986D-03	1.41627	5.66338	1.05998
0.1796175D-03	2.05062	5.65661	1.05670
0.1522975D-03	2.69598	5.89714	1.05876
0.1318267D-03	3.94608	5.89714	1.05717
0.1052470D-03	6.53477	5.94950	1.05539
0.8850422D-04	9.79928	6.02732	1.05494
0.7685441D-04	13.51343	6.11811	1.05582
0.6827721D-04	17.95338	6.17131	1.05396
0.6151458D-04	22.39240	6.20202	1.05323

Table 33. Page 2.

33/2

VELOCITY	UN	UC	HI	HO
FT/SEC	BTU/(F*HR*FT**2)	BTU/(F*HR*FT**2)	BTU/(F*HR*FT**2)	BTU/(F*HR*FT**2)
4.99	1007.981	1091.235	2161.859	1851.512
7.12	1084.283	1181.224	2858.799	1692.418
9.50	1206.201	1327.386	3528.467	1787.491
11.87	1244.560	1373.989	4216.125	1712.737
14.25	1326.141	1474.102	4809.871	1785.024
19.12	1397.549	1562.866	6035.863	1770.983
24.22	1456.368	1636.793	7270.824	1773.602
28.97	1486.316	1674.718	8375.797	1757.679
33.25	1557.654	1765.840	9342.043	1827.368
37.99	1577.571	1791.481	10363.637	1817.734
REYNOLDS NO	PLAIN END REYN NO	FLOW RATE PER AREA	FRICTION FACTOR	SIEDER TATE CONSTANT
11722.25	13808.52	1114235.CC	0.00664790	0.03707841
16602.44	19557.25	1591988.CO	0.00616971	0.03711569
20944.64	24672.23	2124491.CO	0.00581764	0.03735683
26413.04	31113.85	2655258.00	0.00529483	0.03731817
30340.27	35740.04	3188386.CO	0.00511753	0.03751008
40000.34	47119.34	4278834.CO	0.00465900	0.03758739
50461.18	59441.94	5421966.CO	0.00437064	0.03760686
60355.56	71097.25	6485100.00	0.00421421	0.03760688
69032.00	81317.94	7442267.CO	0.00415819	0.03762148
78693.75	92934.75	8505445.CO	0.00407944	0.03762148

Table 34. 30^{o} HA Tube Results Based on Hydraulic Diameter, Run 15.

NUSSELT NO	NU/PR1/3(U/UW)0.14	STANTON NO	J FACTOR	PERFORM FACTOR
126.37529	66.73128	0.00194201	0.0060886	1.8317347
167.28424	88.24586	0.00179729	0.0056719	1.8386250
207.81166	106.96164	0.00166159	0.0054690	1.9470692
248.05482	128.63960	0.00158866	0.0051939	1.9618845
284.44287	144.46503	0.00150881	0.0050995	1.9929533
357.68042	180.58934	0.00141066	0.0048316	2.0741100
431.08643	217.58662	0.00134097	0.0046083	2.1067637
498.60034	251.09613	0.00129152	0.0044384	2.1063976
554.10425	279.68872	0.00125521	0.0043245	2.0799761
614.69800	311.22095	0.00121841	0.0041977	2.0579739

XIN	PRESSURE DROP (PSI)	PRANDTL NO	U/UW
0.2950800D-03	0.61563	5.55136	1.06955
0.2231500D-03	1.16619	5.60615	1.06710
0.1808367D-03	1.88935	5.97136	1.07090
0.1513368D-03	2.78209	5.91152	1.06645
0.1326772D-03	3.87458	6.21359	1.07099
0.1057352D-03	6.35120	6.33884	1.07020
0.8777741D-04	9.56631	6.37072	1.06873
0.7619739D-04	13.19578	6.37072	1.06685
0.6831715D-04	17.14667	6.39476	1.06735
0.6158282D-04	21.97151	6.39476	1.06411

Table 34. Page 2.

34/2

VELOCITY	UN	UC	HI	HO
FT/SEC	BTU/(F*HR*FT**2)	BTU/(F*HR*FT**2)	BTU/(F*HR*FT**2)	BTU/(F*HR*FT**2)
4.16	1366.492	1165.378	2667.624	2404.894
6.24	1136.249	1249.178	3596.873	2105.852
8.32	1210.606	1339.638	4448.473	2064.592
10.40	1289.270	1436.635	5257.629	2105.629
12.48	1376.239	1545.461	6058.141	2196.075
16.64	1411.511	1590.082	7554.281	2098.219
20.80	1548.044	1765.493	8987.191	2281.327
24.96	1612.906	1850.356	10414.195	2328.842
27.04	1635.113	1879.641	11076.656	2332.644
REYNOLDS NO	PLAIN END REYN NO	FLOW RATE PER AREA	FRICTION FACTOR	SIEDER TATE CONSTANT
14610.18	14540.78	927828.50	0.01762798	0.05314794
20613.57	20515.65	1393253.00	0.01852725	0.05352641
26510.09	26384.13	1858792.00	0.01819225	0.05375187
32520.23	32365.73	2324200.00	0.01745586	0.05386998
38514.15	38331.17	2789622.00	0.01677322	0.05395288
50247.28	50008.54	3720759.00	0.01673544	0.05409040
62107.98	61812.90	4651749.00	0.01699220	0.05416159
74150.69	73798.44	5582531.00	0.01738748	0.05419397
80351.44	79969.69	6047717.00	0.01777009	0.05419226

Table 35. 60^{o} HA Tube Results Based on Hydraulic Diameter, Run 9.

NUSSELT NO	NU/PR1/3(U/UW)0.14	STANTON NO	J FACTOR	PERFORM FACTOR
208.28722	114.08023	0.00287967	0.0083647	0.9490276
282.84253	151.31786	0.00258473	0.0078656	0.8490843
351.28198	185.83249	0.00239547	0.0074925	0.8237019
416.09106	219.31526	0.00226396	0.0071831	0.8230014
480.18164	251.48387	0.00217322	0.0069845	0.8304325
600.29517	311.89551	0.00203142	0.0066186	0.7509709
715.09961	370.00562	0.00193289	0.0063516	0.7475873
829.14063	426.62109	0.00186628	0.0061565	0.7081543
881.85547	454.91602	0.00183232	0.0060432	0.6801574

XIN	PRESSURE DROP (PSI)	PRANDTL NO	U/UW
0.2565302D-03	0.83909	4.95068	1.07127
0.1903004D-03	1.98642	5.30856	1.07151
0.1538910D-03	3.46965	5.53164	1.06885
0.1302162D-03	5.20348	5.65153	1.06512
0.1130154D-03	7.20149	5.73695	1.06660
0.9063952D-04	12.77814	5.88102	1.06628
0.7619167D-04	20.27567	5.95678	1.06616
0.6575279D-04	29.87845	5.99150	1.07006
0.6182023D-04	35.83716	5.98967	1.06741

Table 35. Page 2.

35/2

VELOCITY	UN	UC	HI	HO
FT/SEC	BTU/(F*HR*FT**2)	BTU/(F*HR*FT**2)	BTU/(F*HR*FT**2)	BTU/(F*HR*FT**2)
4.37	1128.120	1239.359	3097.358	2343.345
6.24	1244.368	1381.104	4071.278	2293.301
8.32	1341.016	1501.184	5063.578	2296.742
10.40	1436.798	1584.104	6028.473	2282.010
12.48	1455.475	1646.054	6935.523	2271.170
16.64	1542.432	1758.156	8651.414	2296.281
20.80	1618.910	1858.262	10311.086	2343.027
24.96	1656.909	1908.502	11859.359	2336.089
27.45	1678.534	1937.250	12825.637	2339.183
REYNOLDS NO	PLAIN END REYN NO	FLOW RATE PER AREA	FRICTION FACTOR	SIEDER TATE CONSTANT
14444.23	14375.62	975260.00	0.01972748	0.06113640
19830.91	19736.71	1394154.00	0.01893088	0.06141986
25676.11	25554.14	1859749.00	0.01865321	0.06163083
31547.09	31397.20	2325313.00	0.01698486	0.06175517
37334.68	37157.30	2790965.00	0.01686627	0.06185565
48746.17	48514.59	3722469.00	0.01648501	0.06200807
60325.09	60038.48	4653774.00	0.01635169	0.06208111
71899.63	71558.06	5585084.00	0.01679297	0.06213072
79326.88	78949.94	6143326.00	0.01712454	0.06210886

Table 36. 60^{o} HA Tube Results Based on Hydraulic Diameter, Run 12.

NUSSELT NO	NU/PR1/3(U/UW)0.14	STANTON NO	J FACTOR	PERFORM FACTOR
243.53391	130.03336	0.00317975	0.0096688	0.9802404
321.59375	168.33809	0.00292296	0.0091605	0.9677798
401.35034	207.69231	0.00272467	0.0087317	0.9362164
478.79395	245.38040	0.00259406	0.0084227	0.9917915
551.73022	281.23438	0.00248617	0.0081580	0.9673802
689.52749	348.97900	0.00232483	0.0077513	0.9404003
823.25049	414.33984	0.00221615	0.0074454	0.9106585
950.81909	477.16481	0.00213093	0.0071962	0.8570498
1024.47339	516.04663	0.00208815	0.0070357	0.8217081

XIA	PRESSURE DROP (PSI)	PRANDTL NO	U/UW
0.2524378D-03	1.03638	5.30239	1.07402
0.1920795D-03	2.03101	5.54807	1.07914
0.1544552D-03	3.55940	5.73695	1.07947
0.1297422D-03	5.06551	5.85073	1.08286
0.1127801D-03	7.24494	5.94406	1.08300
0.9041886D-04	12.59272	6.08757	1.08271
0.7586795D-04	19.51987	6.15794	1.08400
0.6574312D-04	28.87004	6.20586	1.08429
0.6099441D-04	35.62096	6.18471	1.08153

Table 36. Page 2.

FLOW RATE PER AREA	VELOCITY	PRESSURE DROP	REYNOLDS NUMBER	FRICTION FACTOR
378467.50	6077.60	0.19006	3508.75	0.01991610
473084.44	7597.00	0.22739	4385.93	0.01524970
551932.06	8863.17	0.30989	5116.92	0.01526828
630778.94	10129.32	0.39138	5847.91	0.01476437
709626.56	11395.50	0.42990	6578.89	0.01281342
788474.44	12661.67	0.53344	7309.89	0.01287876
1001618.88	16084.44	0.77342	9285.93	0.01157134
2003238.00	32168.89	2.60380	18571.88	0.00973874
3004856.00	48253.30	5.17533	27857.81	0.00860303
4006475.00	64337.77	8.32052	37143.76	0.00778048
5108256.00	82030.63	12.31664	47358.28	0.00708447
6109877.00	98115.06	17.05826	56644.23	0.00685852
7011335.00	112591.06	22.27742	65001.59	0.00680181

Table 37. 45° HA Tube Isothermal Pressure Drop Results, Run 17.

FLOW RATE PER AREA	VELOCITY	PRESSURE DROP	REYNOLDS NUMBER	FRICTION FACTOR
318469.69	5114.54	0.08016	2663.24	0.01063054
410658.38	6595.06	0.13053	3434.18	0.01041080
494466.31	7941.00	0.18023	4135.03	0.00991476
586655.00	9421.52	0.24982	4905.97	0.00976321
670462.63	10767.45	0.30904	5606.82	0.00924670
754270.56	12113.38	0.35509	6307.67	0.00839482
838078.94	13459.32	0.43399	7008.53	0.00831079
1064632.00	17097.71	0.66863	8903.11	0.00793441
2129265.00	34195.45	2.10699	17806.23	0.00625074
3193898.00	51293.16	4.02533	26709.34	0.00530746
4258531.00	68390.88	6.07808	35612.46	0.00450790
5323323.00	87198.31	9.65592	45405.85	0.00440536
6494260.00	104296.06	13.03133	54308.99	0.00415532
7452428.00	119684.00	16.61499	62321.78	0.00402376
8517063.00	136781.75	21.18219	71224.88	0.00392752

Table 38. 30^{o} HA Tube Isothermal Pressure Drop Results, Run 16.

FLOW RATE PER AREA	VELOCITY	PRESSURE DROP	REYNOLDS NUMBER	FRICTION FACTOR
367049.68	5894.25	0.23686	4121.15	0.03195684
440459.81	7073.10	0.29976	4945.38	0.02809657
513869.94	8251.95	0.38461	5769.61	0.02647585
587279.44	9430.79	0.46867	6593.84	0.02470345
660689.63	10609.64	0.57469	7418.07	0.02393144
734100.00	11788.50	0.65718	8242.30	0.02216704
932545.75	14975.23	0.85790	10470.41	0.01793201
1865091.00	29950.47	3.57351	20940.83	0.01867560
2797636.00	44925.69	7.43823	31411.22	0.01727499
3730183.00	59900.94	12.78048	41881.65	0.01669620
4662728.00	74876.13	19.47328	52352.05	0.01628134
5595275.00	89851.38	28.92947	62822.48	0.01679688

Table 39. 60^{o} HA Tube Isothermal Pressure Drop Results, Run 18.

APPENDIX A

CALIBRATION PROCEDURES

1. Rotameters

The three rotameters installed in the test condenser and by-pass line were calibrated by the use of a scale and a stop watch. The procedure that was used is as follows:

a. Establish flow through the rotameter at a specified percent level.

b. Record weight of container at time zero.

c. Record weight of container at time zero.

d. Determine flow rate for specified level by dividing the weight gain by the elapsed time.

2. Thermocouples

All thermocouples used in the test apparatus were calibrated in a silicone oil bath against a platinum resistance thermometer. The output of the platinum resistance thermometer was determined by the use of a Wheatstone bridge and is accurate to the nearest $0.02^{o}F$ ($0.01^{o}C$). The Autodata Nine Recorder, the output device for all sheathed thermocouples, is accurate to the nearest $0.2^{o}F$ ($0.1^{o}C$) and all sheathed thermocouples were found to record the same temperature that was indicated by the platinum standard.

3. Pressure Transducer

Calibration of the absolute pressure transducer was done by using a mercury manometer. The amplifier for the transducer had an excitation voltage of 16.2 volts. A second voltage setting was used to set the scale of the output so that the output corresponded to centimeters of mercury. The calibration showed a linear relationship between the transducer and the actual pressure. The output of the transducer when multiplied by ten is equal to the pressure in centimeters of mercury.

APPENDIX B

PROCEDURES FOR PREPARING AND INSTALLING THE ALUMINUM TUBES

The enhanced section of the tubes manufactured by General Atomic Company had a larger outside diameter than the corresponding smooth end. This fact necessitated that a special procedure be developed to allow installation of these tubes with the wall thermocouple installed. The smooth aluminum tube was prepared in a manner similar to the aluminum augmented tubes, except for the special installation procedures mentioned above. Therefore, these procedures also apply to the smooth aluminum tube, except step A. 1 is ignored and all of step C is disregarded.

A. PREPARATION PROCEDURES

1. File the plastic thermocouple connector to a size that will allow the connector to pass through the swagelock fitting.

2. Cut a 4-inch long groove approximately 0.025 inch deep in the wall of the tube. The groove is cut from the edge of the enhanced section back into the plain end section at one end.

3. Install the thermocouple bead at approximately the middle of the enhanced section. Insure that the bead location is orientated 90^{o} to the 0.025 inch deep groove and that the bead is in contact with the tube. This insures that the thermocouple bead will be at the same location on all tubes.

Use an appropriate high temperature cement, such as DEVCON, to install the bead.

4. Cement the thermocouple bead into the 0.025 inch deep groove.

5. After the cement dries, insure that the excess cement is removed by scraping with a pocket knife and filing smooth so as to allow a smooth fit in the swagelock fitting.

B. TUBE CLEANING PROCEDURE

Prior to each run, the aluminum test tube must be cleaned thoroughly. The procedure used is as follows:

1. Lightly brush the exterior of the tubes with a wire brush.

2. Fill the flood tube 2/3 full (The flood tube is a 1-inch ID, 48 inch long plexiglass tube with a 1-inch thick piece of flat plexiglass glued to one end.) with a 10 percent solution of sodium hydroxide (NaOH).

3. Insert the test tube into the flood tube.

4. Using a 3/4 inch test tube brush, brush the inside surface of the test tube. The brush must be inserted with a twisting motion to insure that the flutes are being cleaned.

5. Leave the test tube in the flood tube until a foaming action is observed over the entire outside surface and the solution has bubbled up through the inside of the test tube. This should take about two minutes.

6. After removing the test tube from the flood tube, thoroughly rinse the inside and the outside with tap water. The tube should have a dull silvery appearance and should be well wet by the water.

C. INSTALLATION

The fluted aluminum test tubes were installed by following the procedure listed below:

1. Insert the tube into the test condenser through the tube sheet which the thermocouple lead will pass through.

2. Install the test tube swagelock fitting and seals over the thermocouple case and the thermocouple lead. Do not allow the lead to be seized by the swagelock fitting as this will destroy the thermocouple.

3. Install the upper dummy tube's swagelock fitting.

4. Connect the cooling water lines to the test tube.

5. Reinsulate the test condenser and the cooling water lines.

APPENDIX C

OPERATING PROCEDURES

1. Light-off Procedure

a. Boiler Operation

(1) Energize main circuit breaker located in power panel P-2.

(2) Turn key switch on--located on right side of main control board.

(3) Energize circuit breaker on left side of main control panel by depressing start.

(4) Energize individual circuit breakers on left side of main control panel. The following list identifies each circuit breaker:

(a) Feed pump

(b) Outlets

(c) Hot water heater (feedwater tank)

(d) Condensate pump

(e) Boiler

(f) Cooling tower

(g) Cooling water pump (only when using closed cooling water system)

(5) Insure water level is up in the feedwater tank. Turn switch on to energize heater.

(6) Energize instrumentation.

(a) Autodata 9 machine and amplifier.

(b) Multichannel pyrometer.

(7) Turn on the switch to the feed pump to recirculate water in feedwater tank.

(8) Insure nitrogen level in cold trap is at full mark (if installed) and start vacuum pump.

(9) After feedwater tank has reached a temperature of 140°F, insure water level in boiler is above low level mark and energize boiler.

(10) Open valve DS-1.

b. House Steam Operation

Follow steps (1) through (4), (6) and (8) as outlined above for the boiler.

2. Operation

a. Cooling Water System

(1) Open valve CW-1; then open valve CW-2 one turn to prime the cooling water pump, keeping valves CW-3 and CW-4 closed.

(2) Energize pump, and close valve CW-2. Open valve CW-3 one turn until flow is established, then open valve CW-4 to purge air.

(3) Open valves CW-3 and CW-4 to obtain desired flow rates.

(4) Vent both sides of the 12-ft manometer.

(5) When using the house water supply remove plug from sump and open valve CW-2 with valve CW-1 closed. Follow step 3.

b. Steam System

(1) Boiler Operation

(a) When boiler has reached the desired pressure (approximately 3 psig) open valve MS-1.

(b) Insure valves MS-6 and MS-5 are open.

(c) Open valve MS-3 to obtain desired steam flow rate to test condenser. Open valve MS-4 as necessary to maintain boiler pressure at desired level.

(2) House Steam

(a) Insure valve MS-1 is closed. Open valve MS-2.

(b) Follow steps (b) and (c) for boiler use.

c. Condensate and Feedwater System

(1) Using Boiler

(a) To collect drains in test condenser hotwell operate with valve C-1 closed. After test run has been completed, open valve and condensate will drain into secondary condenser.

(b) The condensate pump is operated intermittently, when level in secondary condenser dictates. When pump is secured, keep valve C-2 closed. When pump is required, start pump and then open valve C-2. In this mode keep valve C-3 closed.

(c) While feed pump is running (continuous operation) valve FW-1 must be fully open and valve FW-2 must be throttled so that a positive flow is insured. Valve FW-3 is a solenoid valve which is actuated by the boiler controls.

(d) When boiler is energized, valve FW-4 must be fully open.

(e) Make-up is added to the system through the top of the feedwater tank by removing anode.

(2) Using House Steam

(a) Follow step (a) for using boiler.

(b) To pump condensate from secondary condenser hotwell, start pump, and open valve C-3. In this mode keep valve C-2 closed.

(c) Delete steps (c) through (e) for using boiler.

3. Securing System

a. Using Boiler

(1) Close valves MS-3 and MS-4. Secure power to boiler and then close MS-1.

(2) Pump condensate from secondary condenser hotwell to feedwater tank. Secure valve C-2.

(3) Secure power to heater.

(4) Secure vacuum pump.

(5) Secure cooling water pump or close valve CW-2 when using house water supply. Close valves CW-3 and CW-4.

(6) Secure instrumentation.

(7) Bottom blow boiler to remove deposits. Repeat twice, blowing from high water mark to low water mark.

(8) Secure power to feed pump.

(9) De-energize individual circuit breakers.

(10) De-energize circuit breaker on control panel; depress stop. Turn key switch off.

b. Using House Steam

(1) Close valve MS-2.

(2) Pump condensate into return line; close valve C-3.

(3) Follow steps (4) through (6), (9) and (10) as outlined for procedure using boiler.

4. Secondary Systems

a. Vacuum System

Vacuum is established by mechanical vacuum pump and is controlled by a vacuum regulator mounted on instrument board mounted by test condenser.

b. Desuperheater

Valve DS-1 controls flow of feedwater ($140^{o}F$) to spray nozzles. Optimum flow level is between 15 and 20 percent flow on rotameter. Condensate is collected in a small tank below desuperheater so the mass flow rate can be determined.

5. Safety Devices

a. Emergency Power Shut-Off

To secure all power to the system in an emergency, depress the red button on the right side of the main control panel.

b. Boiler

(1) The mercury switches mounted on the main control panel secure power to the heating elements of the boiler when the steam pressure exceeds 25 psig. Power is restored to the heating elements when the pressure drops to approximately 15 psig.

(2) A low water level limit switch is contained within the boiler, and when the water level inside the boiler drops below a preset level, power is secured to the boiler and will not be restored until the water level is above this preset height.

(3) The relief valve mounted on the boiler is set to lift at 30 psig.

APPENDIX D

SAMPLE CALCULATIONS

A sample calculation is performed here to illustrate how the data reduction program, Appendix H progresses to the results. Tube number 1, run number 2 at 60 percent flow on the large rotameter was selected at random to perform this analysis. This tube and run number are the same as that used for the error analysis in Appendix E.

Section 2 of this appendix corresponds to the calculations performed for N = 1 in the data reduction program. The calculations for N = 2 will be demonstrated in section 3 of this appendix. The water property calculations are shown in section 1.

INPUT PARAMETERS

Tube Number	1
Run Number	2
Tube Inside Diameter, Plain End (D_i)	0.0436667 ft
Tube Inside Diameter, Test Section (D_h)	0.02408333 ft
Tube Outside Diameter, (D_o)	0.0525 ft
Inside Wetted Perimeter (Pw_i)	0.155833 ft
Outside Wetted Perimeter (Pw_o)	0.183333 ft
Test Section Cross Sectional Area(Ac)	0.0009375 ft^2
Outside Nominal Surface Area (A_n)	0.490874 ft^2
Wall Resistance (R_w)	4.3761×10^{-5} $\frac{hr \cdot ft^2 \, ^oF}{BTU}$

Cooling Water In (Tc_i)	$71.24^{o}F$
Cooling Water Out (Tc_o)	$80.74^{o}F$
Average Cooling Water Temperature (T_b, T_{br})	$75.99^{o}F$, $533.59^{o}R$
Steam Vapor Temperature (T_v)	$151.07^{o}F$
Tube Wall Temperature (T_w)	$554^{o}R$
Tube Pressure Drop (ΔP_m)	19.56929 psi
% Flow	60
Tube Inlet Contraction Factor (Kc)	0.33*
Tube Outlet Expansion Factor (Ke)	0.33*

*See Appendix I.

Section 1, Water Properties

$$\mu_{H_2O} = \exp[(0.004606532)(533.59)+(4759.5941)/(533.59) - 10.59252566]$$

$$\mu_{H_2O} = 2.19333 \frac{lbm}{ft \cdot hr}$$

$$k = 0.32159931 + (0.000697989)(75.99)-(0.12506 \times 10^{-5})(75.99)^2 -(0.2072 \times 10^{-10})(75.99)^3$$

$$k = 0.36741 \frac{BTU}{hr \cdot ft \cdot {}^{o}F}$$

$$\rho = 62.707172 - (0.0043955304)(75.99) - (0.000046076921)(75.99)^2$$

$$\rho = 62.10706 \frac{lbm}{ft^3}$$

$$c_p = 1.0121559 - (0.00024618473)(75.99) + (0.10282155 \times 10^{-5})(75.99)^2$$

$$c_p = 0.99939 \frac{BTU}{lbm\,^oF}$$

$$\dot{m} = GPM \times \rho = (11.28)(60)(\frac{231}{1728})(62.10700)$$

$$\dot{m} = 5647.22266 \frac{lbm}{hr} = 1.57 \frac{lbm}{sec}$$

$$Pr = \frac{\mu c_p}{k}$$

$$= \frac{(2.1933)(0.99939)}{.36741} = 5.966$$

Section 2, Plain-End-Tube Reduction

1. Determination of cooling water velocity

$$v = \frac{4\dot{m}}{\rho \pi D_i^2} \qquad v_{TS} = \frac{\dot{m}}{\rho A_c}$$

$$v = \frac{(4)(5647.22266)}{(62.10706)(\pi)(.043667)^2} \qquad = \frac{5647.22266}{(0.0009375)(62.10706)}$$

$$v = 60716.023 \frac{ft}{hr} \qquad v_{TS} = 96989.04 \frac{ft}{hr}$$

$$= 16.87 \frac{ft}{sec} \qquad = 26.94 \frac{ft}{sec}$$

2. Determination of Mass Flow Rate per Unit Area

$$G = \frac{4\dot{m}}{\pi D_i^2} = \rho v$$

$$= (62.10706)(60716.023)$$

$$= 3{,}770{,}893.659 \ \frac{lbm}{ft^2 \cdot hr}$$

$$= 1047.47 \ \frac{lbm}{ft^2 \cdot sec}$$

3. Determination of Reynolds Number

$$Re = \frac{D_i G}{\mu_{H_2O}}$$

$$= \frac{(0.0436667)(3770893.659)}{2.1933}$$

$$Re = 75{,}075.22$$

4. Determination of Overall Heat Transfer Coefficient

$$U_n = \frac{\dot{m} c_p}{An} \ln \left(\frac{T_v - Tc_i}{T_v - Tc_o} \right)$$

$$= \frac{(5647.22266)(0.99939)}{0.490874} \ln \left[\frac{151.07 - 71.24}{151.07 - 80.74} \right]$$

$$= 1456.83 \ \frac{BTU}{hr \cdot ft^2 \ ^oF}$$

5. Determination of Corrected Overall Heat Transfer Coefficient

$$U_c = \frac{1}{\frac{1}{U_n} - R_w}$$

$$= \frac{1}{\frac{1}{1456.83} - 4.3761 \times 10^{-5}}$$

$$U_c = 1556.03 \frac{BTU}{hr \cdot ft^2 \, ^oF}$$

6. Determination of Friction Factor

$$f_s = \frac{0.046}{Re^{0.2}}$$

$$= \frac{0.046}{75075.22^{0.2}}$$

$$f_s = 0.00487$$

$$\Delta P_s = \frac{4 f_s G^2 (\frac{L_s}{D_i})}{\rho \, 2g_c}$$

$$\Delta P_s = \frac{(4)(0.00487)(3770893.659)^2(\frac{1.2604}{.0436667})}{(62.10706)(2)(4.17 \times 10^8)(144)}$$

$$\Delta P_s = 1.072 \text{ psi}$$

$$\Delta P_{exp/con} = \frac{\rho \, v_{TS}^2}{2g_c} \, [Kc + Ke]$$

$$= \frac{(62.107172)(96989.04)^2}{(2)(4.17 \times 10^8)\,(144)} \, [0.33]$$

$$\Delta P_{exp/con} = 1.6054 \text{ psi}$$

$$\Delta P_{TS} = \Delta P - \Delta P_s - \Delta P_{exp/con}$$

$$= 19.56929 - 1.072 - 1.6054$$

$$= 16.89 \text{ psi}$$

$$f_{TS} = \frac{\rho \Delta P_{TS} 2 g_c}{4G^2 \left(\frac{L_{TS}}{D_i}\right)}$$

$$= \frac{(62.107172)(16.89)(2)(4.17 \times 10^8)(144)}{(4)(3770893.657)^2 \left(\frac{3}{.0436667}\right)}$$

$$f_{TS} = 0.032246$$

7. Determination of Wilson Plot Parameters

(a) Ordinate

$$Y = \frac{1}{U_n}$$

$$Y = \frac{1}{1456.83}$$

(b) Abscissa

$$X = \frac{1}{Re^{0.8} Pr^{1/3}} \left(\frac{\mu_{H_2O}}{\mu_w}\right) 0.14$$

$$\mu_w = \exp[(0.004606532)(554)+(4759.5941/(554) - 10.59252566]$$

$$\mu_w = 1.7347 \frac{\text{lbm}}{\text{ft} \cdot \text{hr}}$$

$$X = \frac{1}{(75075.22)^{0.8}(5.966)^{1/3}(\frac{2.19333}{1.7347})^{0.14}}$$

$$X = 6.71086 \times 10^{-5}$$

8. Determination of Sieder Tate Constant

$$c_i = \frac{D_o}{Mk}$$

$M = 1.76639$, from linear regression subroutine

$$c_i = \frac{0.0525}{(1.76639)(0.36741)}$$

$$c_i = 0.080895$$

9. Determination of Inside Heat Transfer Coefficient

$$h_i = \frac{c_i}{D_i} k \, Re^{0.8} \, Pr^{1/3} \, (\frac{\mu_{H_2O}}{\mu_w})^{0.14}$$

$$= (\frac{0.080895}{0.043667}) \, (0.36741)(75075.22)^{0.8}(5.966)^{1/3} \, (\frac{2.19333}{1.7347})^{0.14}$$

$$h_i = 10142.384 \frac{BTU}{hr \cdot ft^2 \, ^oF}$$

10. Determination of Outside Heat Transfer Coefficient

$$h_o = \frac{1}{\frac{1}{U_n} - R_w - D_i \frac{D_o}{h_i}}$$

$$= \frac{1}{6.86422 \times 10^{-4} - 8.75223 \times 10^{-5} - \frac{(0.0525)}{(0.0436667)(10142.384)}}$$

$$h_o = 2081.777 \frac{BTU}{hr \cdot ft^2 \, ^oF}$$

11. Determination of Nusselt Number

$$Nu = \frac{h_i D_i}{k}$$

$$= 1205.43$$

12. Determination of Stanton Number

$$St = \frac{Nu}{RePr}$$

$$= \frac{1205.43}{(75075.22)(5.966)}$$

$$= 2.691 \times 10^{-3}$$

13. Determination of Performance Factor

$$TPF = \frac{2xJ}{f_{TS}}$$

$$J = St\ Pr^{2/3}$$

$$J = 8.8529 \times 10^{-3}$$

$$TPF = \frac{(2)(8.8529 \times 10^{-3})}{.032246}$$

$$TPF = 0.5491$$

Section 3. Tube Reduction Based Upon Hydraulic Diameter

1. Determination of Velocity*

$$v_{TS} = 26.94 \text{ ft/sec, } 96989.04 \text{ ft/hr}$$

* See Section 2 of this Appendix.

2. Determination of Mass Rate Flow per Unit Area

$$G = \frac{\dot{m}}{Ac} = \frac{5647.22266}{.0009375}$$

$$G = 6023704.171 \frac{lbm}{ft^2 \cdot hr}$$

$$= 1673.25 \frac{lbm}{ft^2 \cdot hr}$$

3. Determination of Reynolds Number

$$Re = \frac{D_h G}{\mu_{H_2O}}$$

$$= \frac{(0.02408333)(6023704.171)}{2.1933}$$

$$= 66,142.74$$

4. Determination of Overall Heat Transfer Coefficient*

$$U_n = 1456.83 \frac{BTU}{hr \cdot ft^2 \ ^oF}$$

5. Determination of Corrected Overall Heat Transfer Coefficient*

$$U_c = 1669.73 \frac{BTU}{hr \cdot ft^2 \ ^oF}$$

6. Determination of Friction Factor*

$$\Delta P_{TS} = 16.89 \text{ psi}$$

*See Section 2 of this Appendix.

$$f_{TS} = \frac{\rho \Delta P_{TS} 2 g_c}{4\ G^2 (\frac{L_{TS}}{D_h})}$$

$$= \frac{(62.107172)(16.89)(2)(4.17 \times 10^8)(144)}{(4)(6023704.171)^2\ (\frac{3}{0.02408333})}$$

$$f_{TS} = 0.006968$$

7. Determination of Wilson Plot Parameters

(a) Ordinate

$$Y = \frac{1}{U_n}$$

$$Y = 6.86422 \times 10^{-4}$$

(b) Abscissa

$$X = \frac{1}{Re^{0.8}\ Pr^{1/3} (\frac{\mu_{H_2O}}{\mu_w})^{0.14}}$$

$$X = \frac{1}{66142.74^{0.8} \times 5.966^{1/3} \times (\frac{2.1933}{1.7347})^{0.14}}$$

$$X = 7.4266 \times 10^{-5}$$

8. Determination of Sieder Tate Constant

$$c_i = \frac{AnD_h}{Pw_i L_{TS} Mk_b}$$

$$= \frac{(0.490874)(0.0240833)}{(0.155833)(3)(1.59616)(0.36741)}$$

$$c_i = 0.04312$$

9. Determination of Inside Heat Transfer Coefficient

$$h_i = \frac{c_i k}{D_h} Re^{0.8} Pr^{1/3} \left(\frac{\mu_{H_2O}}{\mu_w}\right)^{0.14}$$

$$= \frac{(0.04312)(0.36741)}{(0.0240833)} (66142.74)^{0.8} (5.966)^{1/3} \left(\frac{2.1933}{1.7347}\right)^{0.14}$$

$$= 8857.72 \frac{BTU}{hr \cdot ft^2 {}^oF}$$

10. Determination of Outside Heat Transfer Coefficient

$$h_o = \frac{1}{\frac{Pw_o L}{A_n U_n} - \frac{Pw_o}{P_{bar}} R_w - \frac{Pw_o}{Pw_i h_i}}$$

$$h_o = \frac{1}{\frac{(0.18333)(3)}{(0.490874} 6.86422 \times 10^{-4} - \frac{0.1833}{0.1695815} 8.75223 \times 10^{-5} - \frac{}{\frac{.18333}{.155833} 1.12896 \times 10^{-4}}}$$

$$h_o = 1846.2 \frac{BTU}{hr \cdot ft^2 {}^oF}$$

11. Determination of Nusselt Number

$$Nu = \frac{h_i D_h}{k}$$

$$= \frac{(8857.72)(0.0240833)}{0.36741}$$

$$Nu = 580.61$$

12. Determination of Stanton Number

$$St = \frac{Nu}{RePr}$$

$$St = \frac{580.61}{(66142.74)(5.966)}$$

$$St = 1.4714 \times 10^{-3}$$

13. Determination of Tube Performance Factor

$$TPF = \frac{2 \times J}{f_{TS}}$$

$$J = St\ Pr^{2/3}$$

$$J = 1.4714 \times 10^{-3}\ 5.966^{2/3}$$

$$J = 4.84 \times 10^{-3}$$

$$TPF = \frac{(2)(4.84 \times 10^{-3})}{0.006968}$$

$$TPF = 1.39$$

APPENDIX E

ERROR ANALYSIS

The basic equations used in this section are reproduced from Pence [13]. The general form of the Kline and McClintock [26] "second order" equation is used to compute the probable error in the results. For some resultant, R, which is a function of primary variables X_1, X_2, ... X_n, the probable error in R, δR is given by:

$$\delta R = \left[\left(\frac{\delta R}{\delta X_1}\ \delta X_1\right)^2 + \left(\frac{\delta R}{\delta X_2}\ \delta X_2\right)^2 + \ldots + \left(\frac{\delta R}{\delta X_n}\ \delta X_n\right)^2\right]^{1/2} \quad \text{(E-1)}$$

where δX_1, δX_2, ..., δX_n is the possible error in each of the measured variables.

The overall heat transfer coefficient is given by equation (4), in Chapter III as:

$$U_n = \frac{\dot{m}\ cp}{An}\ \ln\ \left[\frac{T_v - Tc_i}{T_v - Tc_o}\right] . \quad (4)$$

By applying equation (E-1) to equation (4), the following equation results:

$$\frac{\delta U_n}{U_n} = \left[\left(\frac{\delta An}{An}\right)^2 + \left(\frac{\delta cp}{cp}\right)^2 + \left(\frac{\delta \dot{m}}{\dot{m}}\right)^2 + \left(\frac{\delta T_v\ (Tc_i - Tc_o)}{(T_v - Tc_i)(T_v - Tc_o)\ln\frac{T_v - Tc_i}{T_v - Tc_o}}\right)^2 + \left(\frac{\delta Tc_o}{(T_v - Tc_o)\ln\frac{T_v - Tc_i}{T_v - Tc_o}}\right)^2\right]^{1/2} \quad \text{(E-2)}$$

The following are the values assigned to the variables.

$$\delta cp = 0.001 \text{ BTU/lbm } ^{o}F$$

$$\delta mc = 0.01 \dot{m} \text{ lbm/hr}$$

$$\delta TS = 0.2 \ ^{o}F$$

$$\delta Tc_o = 0.2 \ ^{o}F$$

$$\delta Tc_i = 0.2 \ ^{o}F$$

$$\delta An = 0.008 \text{ ft}^2$$

The probable error in the Reynolds' number is given by:

$$\frac{\delta Re}{Re} = \left[\left(\frac{\delta G}{G}\right)^2 + \left(\frac{\delta \mu}{\mu}\right)^2 + \left(\frac{\delta D_i}{D_i}\right)^2\right]^{1/2} , \qquad \text{(E-3)}$$

where,

$$\frac{\delta G}{G} = \left[\left(\frac{0.01\dot{m}}{\dot{m}}\right)^2 + \left(\frac{\delta D_i}{D_i}\right)^2\right]^{1/2} , \qquad \text{(E-4)}$$

$$\delta \mu = 0.01 \text{ lbm/ft}\cdot\text{hr}, \text{ and}$$

$$\delta D_i = 0.00042 \text{ ft} .$$

The probable error in the coefficient c_i is given by:

$$\frac{\delta c_i}{c_i} = \left[\left(\frac{\delta D_o}{D_o}\right)^2 + \left(\frac{\delta slope}{slope}\right)^2 + \left(\frac{\delta k}{k}\right)^2\right]^{1/2} , \qquad \text{(E-5)}$$

where:

$$\delta D_o = 0.00092 \text{ ft} ,$$

$$\delta k = 0.001 \frac{\text{BTU}}{\text{hr}\cdot\text{ft}\cdot{}^{o}F} , \text{ and}$$

$$\delta \text{ slope} = 0.065 \text{ slope}.$$

The probable error in the inside heat transfer coefficient is given by:

$$\frac{\delta h_i}{h_i} = \left[\left(\frac{\delta k}{k}\right)^2 + \left(\frac{\delta D_i}{D_i}\right)^2 + \left(\frac{\delta c_i}{c_i}\right)^2 + \left(\frac{0.08\delta Re}{Re}\right)^2 + \left(\frac{0.333\delta Pr}{Pr}\right)^2 + \left(\frac{0.14\left(\mu/\mu_w\right)}{\mu/\mu_w}\right)^2\right]^{1/2}, \quad \text{(E-6)}$$

where:

$$\delta k = 0.001 \frac{BTU}{hr \cdot ft \cdot {}^{o}F} ,$$

$$\delta D_i = 0.00042 \text{ ft} ,$$

$$\delta c_i = \text{from equation (E-5)} ,$$

$$\delta Re = \text{from equation (E-3)} ,$$

$$\delta Pr = 0.01 , \text{ and}$$

$$\delta\left(\frac{\mu}{\mu_w}\right) = 0.01 .$$

The probable error in the outside heat transfer coefficient is given by:

$$\frac{\delta h_o}{h_o} = \left[\left(\frac{\delta U_o}{U_o^2\left(\frac{1}{U_o} - R_w - \frac{D_o}{D_i h_i}\right)}\right)^2 + \left(\frac{\delta R_w}{\left(\frac{1}{U_o} - R_w - \frac{D_o}{D_i h_i}\right)}\right)^2 + \left(\frac{\left(\frac{D_o}{D_i h_i}\right)\left(\frac{\delta h_i}{h_i}\right)}{\frac{1}{U_o} - R_w - \frac{D_o}{D_i h_i}}\right)^2\right]^{1/2} , \quad \text{(E-7)}$$

where:

δU = from equation (E-2) ,

δR_w = 8.75×10^{-6} hr·ft^2·^{o}F/BTU, and

δh_i = from equation (E-6).

The probable error in the Nusselt number is given by:

$$\frac{\delta Nu}{Nu} = \left[\left(\frac{\delta h_i}{h_i}\right)^2 + \left(\frac{\delta D_i}{D_i}\right)^2 + \left(\frac{\delta k}{k}\right)^2 \right]^{1/2} , \qquad \text{(E-8)}$$

where:

δh_i = as found in equation (E-6) ,

δD_i = 0.00042 ft, and

δk = 0.001 $\frac{BTU}{hr \cdot ft \cdot {}^oF}$

The probable error in the Stanton number is given by:

$$\frac{\delta St}{St} = \left[\left(\frac{\delta Nu}{Nu}\right)^2 + \left(\frac{\delta Re}{Re}\right)^2 + \left(\frac{\delta Pr}{Pr}\right)^2 \right]^{1/2} , \qquad \text{(E-9)}$$

where:

δNu = as found in equation (E-8),

δRe = as found in equation (E-3), and

δPr = 0.01 .

The probable error in the friction factor is given by:

$$\frac{\delta f}{f} = \left[\left(\frac{\delta \Delta P_{TS}}{\Delta P_{TS}}\right)^2 + \left(2\,\frac{\delta G}{G}\right)^2 + \left(\frac{\delta L}{L}\right)^2 + \left(\frac{\delta \rho}{\rho}\right)^2 + \left(\frac{D_h}{D_h}\right)^2 \right]^{1/2} , \qquad \text{(E-10)}$$

where:

$\delta\Delta P_{TS}$ = 0.009 ΔP

δG = as found in equation (E-4),

δL = .0042 ft ,

δf_{ρ} = 0.05 lbm/ft^3, and

δD_h = 0.00042 ft .

The probable error in the Tube Performance Factor is given by:

$$\frac{\delta TPF}{TPF} = \left[\left(\frac{\delta St}{St}\right)^2 + \left(\frac{4}{3}\frac{\delta Pr}{Pr}\right)^2 + \left(\frac{\delta f}{f}\right)^2 \right]^{1/2}, \qquad \text{(E-11)}$$

where:

St = as found in equation (E-9),

Pr = 0.01, and

f = as found in equation (E-10).

For Run #2 at 60 Percent Flow

$$\frac{\delta U_n}{U_n} = \left(\frac{.008}{.490874}\right)^2 + (.001)^2 + \left(\frac{.01\dot{m}}{\dot{m}}\right)^2 + \left(\frac{(2)(-9.45)}{(79.83)(70.335)\ln(1.135)}\right)^2 + \left(\frac{0.2}{(70.335)\ln(1.135)}\right)^2 \Big]^{1/2}$$

$$\frac{\delta U_n}{U_n} = 0.030$$

$$\therefore \quad U_{n,\,60\%} = 1456 \pm 50 \ \frac{BTU}{hr \cdot ft^2\ ^oF}$$

$$\frac{\delta G}{G} = \left[.01^2 + \left(\frac{.00042}{.024083}\right)^2 \right]^{1/2} = 0.02$$

$$\frac{\delta Re}{Re} = \left[(.02)^2 + \left(\frac{.01}{2.19}\right)^2 + \left(\frac{.00042}{.024083}\right)^2 \right]^{1/2}$$

$$\frac{\delta Re}{Re} = .027 \qquad \therefore \ Re = 66142 \pm 1786$$

$$\frac{\delta c_i}{c_i} = \left[\left(\frac{.00042}{.0525}\right)^2 + (.065)^2 + \left(\frac{.001}{.36741}\right) \right]^{1/2}$$

$$\frac{\delta c_i}{c_i} = .066$$

$$\therefore \quad c_{i,\,60\%} = .0431 \pm .0028$$

$$\frac{\delta h_i}{h_i} = \left[\left(\frac{.001}{.36741}\right)^2 + \left(\frac{.00042}{.024083}\right)^2 + (.066)^2 + (.08 \times .027)^2 + \left(\frac{.01}{5.966}\right)^2 + \left(\frac{0.14 \times .01}{1.034}\right)^2 \right]^{1/2}$$

$$\frac{\delta h_i}{h_i} = .068$$

$$\therefore \underline{h_{i,\ 60\ \%} = 8861 \pm 603 \frac{BTU}{hr \cdot ft^2\ ^oF}}$$

$$\frac{\delta h_o}{h_o} = \left[\left(\frac{50}{1670^2 \left(\frac{1}{1670} - 8.75 \times 10^{-5} - \frac{.0525}{8861 \times .0437} \right)} \right)^2 + \left(\frac{8.75 \times 10^{-6}}{\left(\frac{1}{1670} - 8.75 \times 10^{-5} - \frac{}{8861 \times .0437} \right)} \right)^2 + \left(\frac{\frac{.0525}{8861 \times .0437} \times .068}{\frac{1}{1670} - 8.73 \times 10^{-5} - \frac{0.525}{8861 \times .0437}} \right)^2 \right]^{1/2}$$

$$\frac{\delta h_o}{h_o} = 0.058$$

$$\therefore \underline{h_{o,\ 60\%} = 1846 \pm 107 \frac{BTU}{hr \cdot ft^2\ ^oF}}$$

$$\frac{\delta Nu}{Nu} = \left[(.068)^2 + \left(\frac{.00042}{.024083} \right)^2 + \left(\frac{.001}{.36741} \right)^2 \right]^{1/2}$$

$$\frac{\delta Nu}{Nu} = 0.070$$

$$\therefore \underline{Nu = 581 \pm 41}$$

$$\frac{\delta St}{St} = \left[(.07)^2 + (.027)^2 + \left(\frac{.01}{5.966}\right)^2 \right]^{1/2}$$

$$\frac{\delta St}{St} = .075$$

$$\therefore St = .001472 \pm .000110$$

$$\frac{\delta f}{f} = \left[(.009)^2 + (2 \times .02)^2 + \left(\frac{.0042}{3}\right)^2 + \left(\frac{.05}{62.1}\right)^2 + \left(\frac{.00042}{.024083}\right)^2 \right]^{1/2}$$

$$\frac{\delta f}{f} = .045$$

$$\therefore f = .00697 \pm .00031$$

$$\frac{\delta TPF}{TPF} = \left[(.075)^2 + \left(\frac{4}{3} \times \frac{.01}{5.966}\right)^2 + (.045)^2 \right]^{1/2}$$

$$\frac{\delta TPF}{TPF} = 0.087$$

$$\therefore TPF = 1.39 \pm .12$$

APPENDIX F

AREA RATIOS, SAMPLE CALCULATIONS AND RESULTS

To determine the relative performance of the General Atomic tubes as compared to smooth tubes, it is necessary to define a method for comparing the augmented tubes to the smooth tube. Such a comparison is found in Bergles [3] and is described in Chapter III of this report for the case where $R_{ext} = 0$. By solving the equations as shown in Chapter III, it is found that

$$Re_s = \sqrt{\frac{Re_a^3 \, f_a}{2 \, Nu_a / Pr^{0.4}}} \quad . \tag{F-1}$$

In this case, for a given cooling water flow rate, Re_a, f_a, Nu_a and Pr are all found in Tables 14 through 19 depending on which tube is being investigated. Also, knowing Re_s permits the solving of the area ratio:

$$\frac{A_a}{A_s} = \frac{.046 \, Re_s^{2.8}}{Re_a^3 \, f_a} \quad . \tag{F-2}$$

For run 2, 45°, the summary of area ratios are listed below:

Re_a	f_a	Nu_a	Pr	Re_s	A_a/A_s
40176	.035	719	5.66	56191	.40
64696	.033	1058	5.79	92332	.41
89868	.032	1376	5.84	130750	.42
94931	.031	1437	5.84	136720	.42

For run 2, 45^{o}, the summary of area ratios are listed below.

Re_a	f_a	Nu_a	Pr	Re_s	A_a/A_s
25872	.038	522	5.66	35510	.39
37416	.032	715	5.90	48827	.37
61178	.029	1067	6.03	79902	.37
83894	.027	1387	6.17	109089	.37
95463	.026	1541	6.20	123396	.37

For run 9, 60^{o}, the summary of area ratios are listed below.

Re_a	f_a	Nu_a	Pr	Re_s	A_a/A_s
26384	.064	531	5.53	46836	.47
38331	.059	725	5.74	67897	.47
61813	.059	1080	5.96	114781	.48
79970	.062	1332	5.99	156065	.50

By expanding on Bergles' [3] procedure to include the case where $R_{ext} \neq 0$, as shown in Chapter III of this report, the following equation can be found.

$$v_s = \left[\frac{f_a \, v_a^3 \, c}{U_a \; .046} \left(\frac{\rho D_i}{\mu}\right)^{1/5}\right] \frac{1}{2.3} \qquad \text{(F-3)}$$

again, for a selected v_a. values of v_s, f_a, and U_a can be found. Knowing v_s,

$$U_s = c \sqrt{v_s} \qquad \text{(F-4)}$$

where $c = 251$ is a constant and was found as shown in Chapter III.

An area ratio is now found from

$$\frac{A_a}{A_s} = \frac{U_s}{U_a} \; . \qquad \text{(F-5)}$$

AD-A055 430 NAVAL POSTGRADUATE SCHOOL MONTEREY CALIF F/G 13/1
AN EXPERIMENTAL INVESTIGATION OF ENHANCED HEAT TRANSFER ON HORI--ETC(U)
MAR 78 D J REILLY

UNCLASSIFIED NPS69-78-011 NL

3 OF 3
ADA
055430

END
DATE
FILMED
8-78
DDC

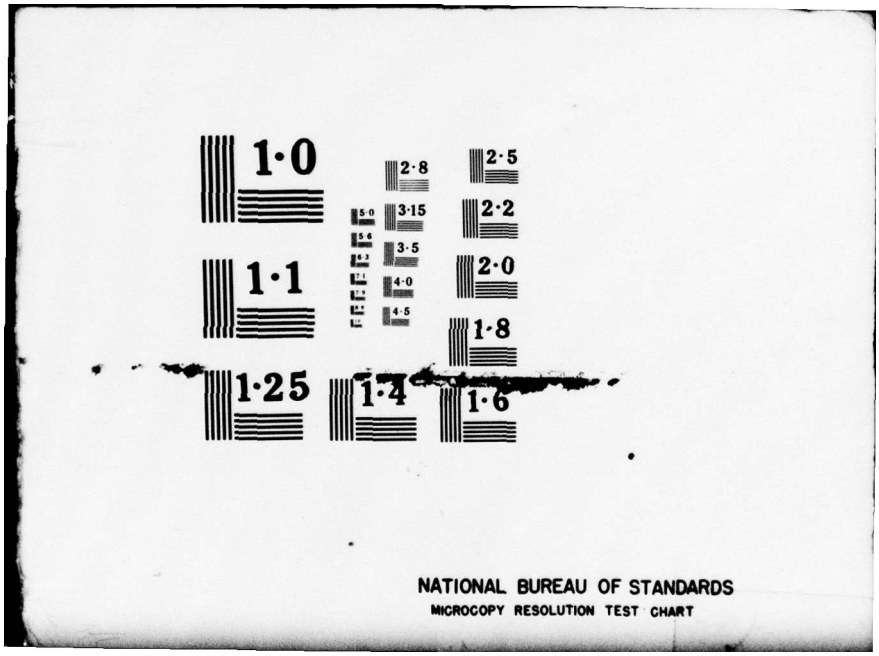
1·0
1·1
1·25
1·4
1·6
1·8
2·0
2·2
2·5
2·8
3·15
3·5
4·0
4·5
NATIONAL BUREAU OF STANDARDS
MICROCOPY RESOLUTION TEST CHART

For run 8, 30^{o}, and using the procedure outlined in Chapter III:

$$D_i = 0.53 \text{ in}$$

$$\mu_{avg} = 2.17 \text{ lbm/ft·hr}$$

$$\rho = 62.1 \text{ lbm/ft}^3$$

$$Tc_i = 65^{o}F$$

By applying the temperature correction factor to U_n as found in reference [21], U_a is found from:

$$U_a = \frac{U_n}{.96} \quad . \qquad \text{(F-6)}$$

For $v_a = 2.73$ fps, substituting the required values above into equation (F-3), it is shown that

$$v_s = \left[\left(\frac{(.053)(2.73)^3\ 251}{(1050)(.046)}\right)\ \left(\frac{(62.1)(.53)(3600)^{1/5}}{(2.17)(12)}\right)\right]^{\frac{1}{2.3}}$$

$$v_s = 4.39 \text{ fps} \quad .$$

By substituting this value into equation (F-4),

$$U_s = 251\ \sqrt{4.39}$$

$$= 526\ \frac{BTU}{hr\cdot ft^2\ ^{o}F} \quad .$$

Using the results of equations (F-4) and (F-6), the area ratio is found,

$$\frac{A_a}{A_s} = \frac{526}{1050} = 0.50$$

A Reynolds number corresponding to v_s is found from

$$Re_s = \frac{\rho D_i v_s}{\mu} = \frac{(62.1)(\frac{.53}{12})(4.39)(3600)}{2.17}$$

$$Re_s = 19975$$

For run 8, 30^o, the remaining area ratios for $R_{ext} \neq 0$ are:

v_a fps	v_s fps	$\frac{A_a}{A_s}$	Re_s
5.47	8.63	.58	39268
8.20	13.22	.67	60153
13.67	23.31	.79	106065
19.14	34.36	.91	156344
21.87	39.35	.93	179050

Similarly for run 2, 45^o, the summary of area ratios for $R_{ext} \neq 0$ are found to be:

$$Tc_i = 70^o, \; U_a = U_n$$

v_a fps	v_s fps	$\frac{A_a}{A_s}$	Re_s
2.90	4.52	.54	21012
8.59	14.95	.74	69497
14.12	26.81	.92	124630
19.75	39.88	1.05	185387
20.86	42.32	1.07	196730

and for run 9, 60^{o}, the summary of the area ratios for $R_{ext} \neq 0$ are found to be:

v_a fps	v_s fps	$\frac{A_a}{A_s}$	Re_s
2.73	4.69	.51	22157
5.47	11.14	.69	52629
8.20	17.24	.76	81448
13.67	32.08	.92	151557
17.77	44.97	1.03	212454

APPENDIX G

CALCULATION OF WALL THICKNESS AND WALL RESISTANCE

There were three methods considered for determining the wall thickness which are:

1. Anular Area Method

A nominal outside area is found using an outside diameter of 5/8 inch and substituting into equation (G-1) written as:

$$D_i = \sqrt{D_o^2 - \frac{4\ Amet}{\pi}} \quad , \qquad (G\text{-}1)$$

where Amet is found in Table 3. The wall thickness is found by substituting D_i and D_o into equation (G-2), written as:

$$t_w = \frac{D_o - D_i}{2} \quad . \qquad (G\text{-}2)$$

2. Displaced Volume Method

The volume desplacement, V_D, of the tube is measured. An average perimeter, $\overline{P}$, is determined from equation (G-3) below. After substitution of V_D and $\overline{P}$, the wall thickness is found from equation (G-4) below:

$$\overline{P} = \frac{P_o + P_i}{2} \quad , \qquad (G\text{-}3)$$

$$t = \frac{V_D}{\overline{P}\ L_t} \quad . \qquad (G\text{-}4)$$

3. Indirect Measurement Method

A photograph of the cross section of the experimental tube is enlarged. The wall thickness could generally be

measured from the enlarged photograph. However, as seen in Figure 13, the wall thickness varies around the periphery of the tube.

Method 1 was selected. Method 2 was rejected because it was felt that the displaced volume would be extremely difficult to measure. Method 3 was rejected because of the non-continuous variations of the wall thickness.

The wall thickness for each tube is:

tube 1

$D_i = 0.4811$ in

$t_w = 0.07195$ in,

tube 2

$D_i = 0.5006$ in

$t_w = 0.062215$ in, and

tube 3

$D_i = 0.4942$ in

$t_w = 0.0654$ in.

The wall resistance is calculated by solving equation (G-5), written as:

$$R_w = \frac{t_w}{k_w} , \qquad \text{(G-5)}$$

where K_w is found to be 137 BTU/ hr·^oF·ft in the Handbook of Tables for Applied Engineering Science [27].

For tube number 1:

$$R_w = 4.3761 \times 10^{-5} \frac{hr \cdot ft^2 \cdot {}^oF}{BTU} .$$

For tube number 2:

$$R_w = 3.7844 \times 10^{-5} \ \frac{\text{hr ft}^2\ ^\circ\text{F}}{\text{BTU}}.$$

For tube number 3:

$$R_w = 3.9781 \times 10^{-5} \ \frac{\text{hr ft}^2\ ^\circ\text{F}}{\text{BTU}}.$$

APPENDIX H

DATA REDUCTION PROGRAM

```
1 IV G LEVEL  21                MAIN              DATE = 78075        08/48/09
C
C     DEFINITION OF SYMBOLS USED IN THE PROGRAM
C     AC=TEST TUBE CROSS SECTIONAL AREA IN SQUARE FEET
C     ACT1=A CHANGING VARIABLE
C     ACT2=A CHANGING VARIABLE
C     ACT3=A CHANGING VARIABLE
C     ACT4=A CHANGING VARIABLE
C     AN=AREA OF STEAM SIDE OF TEST TUBE IN SQUARE FEET BASED ON 5/8 IN OD
C     B=Y INTERCEPT AND SLOPE OF EQUATION OBTAINED BY LINEAR REGRESSION
C     CI=SIEDER TATE CONSTANT
C     CP=COOLING WATER SPECIFIC HEAT
C     CORR=THE NON RECOVERABLE LOSS COEFFICIENTS DUE TO EXPANSION AND CONTRACTION IN
C     THE TEST SECTION OF THE TEST TUBE
C     DELY=THE OUTPUT ARRAY OF THE DIFFERENCES BETWEEN Y AND YC
C     DELP=TEST TUBE PRESSURE DROP
C     DELPC=PLAIN END PRESSURE DROP CORRECTION
C     DELPEC=NON RECOVERABLE PRESSURE DROP CORRECTION
C     DI=INSIDE DIAMETER OF TUBE IN FEET
C     DH=HYDRAULIC DIAMETER OF TUBE IN FEET
C     DLTP=PRESSURE DROP ACROSS TEST SECTION OF TEST TUBE
C     DO=OUTSIDE DIAMETER OF TUBE IN FEET
C     DOTM=COOLING WATER MASS FLOW RATE
C     F=PERCENT OF FULL SCALE ON THE ROTAMETER OF WATER FLOWING THROUGH THE TUBE
C     FC=CALIBRATION CORRECTION FOR COOLING WATER FLOW THROUGH ROTAMETER
C     FRIFAC=TEST SECTION FRICTION FACTOR
C     FSMTH=PLAIN END FRICTION FACTORC
C     G=MASS FLOW RATE PER UNIT AREA
C     HI=INSIDE HEAT TRANSFER COEFFICIENT
C     HO=OUTSIDE HEAT TRANSFER COEFFICIENT
C     H2O=COOLING WATER CONDUCTIVITY
C     LSQPL2=LINEAR REGRESSION SUBROUTINE(SEE REFERENCE   )
C     PBAR=AVERAGE OF PO AND PW
C     PNU=NUSSELT NUMBER
C     PO=OUTSIDE WETTED PERIMETER
C     PR=COOLING WATER PRANDTL NUMBER
C     PW=WETTED PERIMETER OF COOLING WATER SIDE OF TEST TUBE IN FEET
C     RATMHL=RATIO OF WATER VISCOSITY TO TUBE WALL VISCOSITY
C     RE=COOLING WATER REYNOLDS NUMBER
```

```
C REAN=TUBE PERFORMANCE FACTOR
C RE2=PLAIN END REYNOLDS NUMBER
C RE3=TEST SECTION REYNOLDS NUMBER
C RHO=COOLING WATER DENSITY
C RHOP=COOLING WATER DENSITY
C RW=WALL RESISTANCE
C SB=ESTIMATED ERROR OF B
C ST=STANTON NUMBER
C TB=AVERAGE OF INLET AND OUTLET COOLING WATER TEMPERATURES
C TBR=TB IN DEGREES RCENGTEN
C TCI=COOLING WATER INLET TEMPERATURE IN DEGREES F
C TCO=COOLING WATER OUTLET TEMPERATURE IN DEGREES F
C TS=VAPOR TEMPERATURE MEASURED AT INLET TO THE CONDENSER
C TW=TEST TUBE WALL TEMPERATURE IN DEGREES RCENGTEN
C UC=CORRECTED OVERALL HEAT TRANSFER COEFFICIENT
C UN=OVERALL HEAT TRANSFER COEFFICIENT
C V=COOLING WATER VELOCITY
C VTS=VELOCITY OF COOLING WATER IN TEST SECTION OF TEST TUBE
C WALMHU=VISCOSITY AT TEST TUBE WALL
C WMHU=COOLING WATER VISCOSITY
C WI=VARIABLE WEIGHTS USED IN LINEAR REGRESSION SUBROUTINE
C X=MATRIX OF COORDINATE POINTS PASSED TO LINEAR REGRESSION SUBROUTINE
C Y=MATRIX OF ORDINATE POINTS PASSED TO LINEAR REGRESSION SUBROUTINE
C YCOORD=PNU/PR**(1/3)/(U/UW)**.14
C YO=THE OUTPUT ARRAY OF DEPENDENT VARIABLES
      REAL * 8 X,Y,WI,YO,DELY,B,SB
      DIMENSION TS(20),TB(20),TBR(20),TW(20),UC(20),UN(20),RE(20),F(20),
     1FC(20),V(20),PR(20),X(20),Y(20),RATMHU(20),WI(20),YO(20),DELY(20),
     2B(2),SB(2),TCI(20),TCO(20),HI(20),HO(20),H2OK(20),G(20),PNU(20),FR
     3IFC(20),CK(20),YCOORD(20),ST(20),FCHECK(20),DELP(20),RE2(20),CBJ(
     420),REAN(20),RHOP(20),VTS(20),RE3(20),DLTP(20)
      READ(5,102)JK
      DO 101 L=1,JK
      READ(5,102)M
  102 FORMAT(I10)
C ZERO ALL MATRICES
      DO 1 I=1,20
      TS(I)=0.0
      TB(I)=0.0
      TBR(I)=0.0
      TW(I)=0.0
      UN(I)=0.0
      UC(I)=0.0
      RE(I)=0.0
      F(I)=0.0
```

```
      FC(I)=0.0
      V(I)=0.0
      PR(I)=0.0
      X(I)=0.0
      Y(I)=0.0
      RATMHU(I)=0.0
      WI(I)=0.0
      YO(I)=0.0
      DELY(I)=0.0
      TCI(I)=0.0
      TCO(I)=0.0
      HI(I)=0.0
      HO(I)=0.0
      H2CK(I)=0.0
      G(I)=0.0
      PNU(I)=0.0
      PRIPAC(I)=0.0
      CK(I)=0.0
      YCORRD(I)=0.0
      ST(I)=0.0
      PCHECK(I)=0.0
      DELP(I)=0.0
      RHOP(I)=0.0
      VTS(I)=0.0
      RES(I)=0.0
      DLTP(I)=0.0
    1 CONTINUE
      B(1)=0.0
      B(2)=0.0
      SB(1)=0.0
      SB(2)=0.0
C
C READ IN THE RAW DATA AND ALL CONSTANTS
C
      READ(5,103)AC,PW,DO,PC,DH,AN,RW
  103 FORMAT(6F10.7,E12.5)
      READ(5,104) (TS(K),TB(K),TBR(K),TW(K),TC_.K),TCO(K),F(K),FC(K),K=1
     1,M)
      READ(5,104) (DELP(K),K=1,M)
  104 FORMAT(8F10.5)
      READ(5,105)DI,CORR
  105 FORMAT(2F10.7)
      WRITE(6,298)
  298 FORMAT('1',1X,'UNCORRECTED PRESSURES AND WATER PROPERTIES'//)
      DO 10 I=1,M
      WRITE(6,299)DELP(I)
   10 CONTINUE
  299 FORMAT(1X,F10.5)
      N=0
      PBAR=(PO+PW)/2
C
C  CALCULATE WATER PROPERTIES
C
      WRITE(6,200)RW
  200 FORMAT(1X,E12.5)
   99 N=N+1
      DO 2 I=1,M
      IF(N.GT.1)GO TO 99
      ACT1=0.0046065327*TBR(I)
      ACT2=4755.5541/TBR(I)
      WMHU=EXP(ACT1+ACT2-10.59252566)
      WRITE(6,201)WMHU
  201 FORMAT(1X,F10.5)
      ACT1=0.0006979899*TB(I)
      ACT2=0.12506E-05*TB(I)**2
      ACT3=0.2072E-10*TB(I)**3
      H2CK(I)=0.32159931+ACT1-ACT2-ACT3
      WRITE(6,201)H2CK(I)
      ACT1=0.4269533046E-02*TB(I)
      ACT2=0.4637692IE-04*TB(I)**2
      RHO=62.707172-ACT1-ACT2
      WRITE(6,201)RHO
      RHOP(I)=RHO
```

```
      ACT1=0.24618473E-03*TB(I)
      ACT2=0.10282155E-05*TB(I)**2
      CP=1.0121559-ACT1+ACT2
      WRITE(6,201)CP
      ACT1=0.004606532*TW(I)
      ACT2=4759.5941/TW(I)
      WALMHU=EXP(ACT1+ACT2-10.59252566)
      WRITE(6,201)WALMHU
      RATMHU(I)=(WMHU/WALMHU)**0.14
      DOTM=F(I)*FC(I)*RHO*150.7916667
      WRITE(6,201)DOTM
      V(I)=4.*DOTM/(RHO*3.141593*DI**2)
      VTS(I)=DOTM/(RHO*AC)
      RE(I)=RHO*DI*V(I)/WMHU
      ACT1=1.27324/DI**2
      G(I)=ACT1*DOTM
      RE2(I)=DI*G(I)/WMHU
      RE3(I)=DOTM*DH/(AC*WMHU)
      PR(I)=CP*WMHU/H2OK(I)
C
C CALCULATE THE OVERALL HEAT TRANSFER COEFFICIENTS
C
      ACT1=TS(I)-TCI(I)
      ACT2=TS(I)-TCO(I)
      ACT3=ACT1/ACT2
      ACT4=ALOG(ACT3)
      UN(I)=DOTM*CP*ACT4/AN
      ACT1=1./UN(I)
      ACT2=ACT1-RW
      UC(I)=1./ACT2
      Y(I)=ACT1
      GO TO 34
C
C CALCULATE THE PRESSURE DROP AND FRICTION FACTOR
C
   99 RE(I)=RE3(I)
      V(I)=VTS(I)
   34 CONTINUE
      IF(RE2(I).LT.3.E04)GO TO 36
      FSMTH=0.046/RE2(I)**0.2
      GO TO 35
   36 FSMTH=0.079/RE2(I)**0.25
   35 ACT1=4.0*FSMTH*G(I)**2/DI
      ACT2=RHOP(I)*1.20096E+11
      DELPC=1.260*ACT1/ACT2
      IF(N.GT.1)GO TO 31
      GO TO 30
   31 G(I)=G(I)*(DI**2/(1.27324*AC))
   30 ACT1=VTS(I)**2/1.20096E+11
      DELPEC=RHOP(I)*ACT1*CCRR
      DLTP(I)=DELP(I)-DELPC-DELPEC
      IF(N.GT.1)GO TO 33
      ACT1=DLTP(I)*RHO*1.20096E+11
      ACT2=12.*G(I)**2/DI
      GO TO 32
   33 ACT1=DLTP(I)*RHOP(I)*1.20096E+11
      ACT2=12.*G(I)**2/DH
   32 PRIFAC(I)=ACT1/ACT2
C
C CALCULATE THE WILSON PLOT PARAMETERS
C
      ACT1=1./RE(I)**0.8
      ACT2=1./PR(I)**0.33
      ACT3=1./RATMHU(I)
      X(I)=ACT1*ACT2*ACT3
    2 CONTINUE
      REAL*8 TITLE(10)/10*' '/
      CALL LSQPL2(M,1,X,Y,WI,YO,DELY,B,SB,TITLE)
C
C DETERMINE THE SIEDER TATE CONSTANT
C
      IF(N.EQ.1)GO TO 96
      CI=(AN/(PW*3.))*(DH/B(2))
```

```
      GO TO 95
   96 CI=DO/B(2)
   95 CONTINUE
      DO 3 I=1,M
      CK(I)=CI/H2OK(I)
    3 CONTINUE
C
C  CALCULATE THE INSIDE AND OUTSIDE HEAT TRANSFER COEFFICIENTS
C
      DO 4 I=1,M
      IF(N.EQ.1)GO TO 94
      ACT1=CI/DH
      ACT2=RE(I)**0.8
      GO TO 93
   94 ACT1=CI/DI
      ACT2=RE2(I)**0.8
   93 ACT3=PR(I)**(1./3.)
      HI(I)=ACT1*ACT2*ACT3*RATMHU(I)
      IF(N.EQ.1)GO TO 92
      ACT1=PO*3./(AN*UN(I))
      ACT2=(PO/PBAR)*RW
      ACT3=PC/(PW*HI(I))
      ACT4=ACT1-ACT2-ACT3
        HO(I)=1./ACT4
      GO TO 91
   92 ACT1=DO/(DI*HI(I))
      ACT2=Y(I)-RW-ACT1
      HO(I)=1./ACT2
   91 CONTINUE
C
C  CALCULATE THE NUSSELT NUMBER, THE STANTON NUMBER, AND THE TUBE PERFORMANCE
C  FACTOR
C
      IF(N.EQ.1)GO TO 38
      PNU(I)=HI(I)*DH/H2OK(I)
      GO TO 37
   38 PNU(I)=HI(I)*DI/H2OK(I)
   37 ACT1=PNU(I)/PR(I)**(1./3.)
      YCCORD(I)=ACT1/RATMHU(I)
      ST(I)=PNU(I)/(RE(I)*PR(I))
      CBJ(I)=ST(I)*PR(I)**(2./3.)
      REAN(I)=2.*CBJ(I)/FRIFAC(I)
      V(I)=V(I)/3600.
    4 CONTINUE
C
C  OUTPUT SECTION OF PROGRAM STARTS HERE
C
      WRITE(6,204)
  204 FORMAT('1',12X,'VELOCITY',21X,'UN',24X,'UC',24X,'HI',24X,'HO'//)
      WRITE(6,205)
  205 FORMAT(14X,'FT/SEC',14X,'BTU/( F*HR*FT**2)', 9X,'BTU/( F*HR*FT**2)
     1',10X,'BTU/( F*HR*FT**2)',10X,'BTU/( F*HR*FT**2)'///)
      DO 5 I=1,M
      WRITE(6,206)V(I),UN(I),UC(I),HI(I),HO(I)
  206 FORMAT(9X,F10.2,8X,4(8X,F10.3,8X)/)
    5 CONTINUE
      WRITE(6,207)
  207 FORMAT('0',8X,'REYNOLDS NO',11X,' PLAIN END REYN NO',9X,'FLOW RATE
     1 PER AREA',7X,'  FRICTION FACTOR',10X,'SIEDER TATE CONSTANT'//)
      DO 6 I=1,M
      WRITE(6,208)RE(I),RE2(I),G(I),FRIFAC(I),CK(I)
    6 CONTINUE
  208 FORMAT(1X,3(8X,F10.2,8X),2(8X,F10.8,8X)/)
      WRITE(6,209)
  209 FORMAT('1',9X,'NUSSELT NO',12X,'NU/PR1/3(U/UW)0.14',11X,'STANTON N
     1O',17X,'J FACTOR',14X,' PERFORM FACTOR '//)
      DO 7 I=1,M
      WRITE(6,210)PNU(I),YCCORD(I),ST(I),CBJ(I),REAN(I)
    7 CONTINUE
  210 FORMAT(1X,2(8X,F10.5,8X),8X,F10.8,8X,2(8X,F10.7,8X)/)
      WRITE(6,211)
  211 FORMAT('0',12X,'XIN',13X,'PRESSURE DROP (PSI)',15X,'PRANDTL NO',19
     1X,'U/UW'//)
```

```
RAN IV G LEVEL  21                    MAIN                    DATE = 78075          08/48/09

2                     DO 8 I=1,M
3                     WRITE(6,212)X(I),OLTP(I),PR(I),RATMHU(I)
4                   8 CONTINUE
5                 212 FORMAT(5X,E15.7,13X,F10.5,16X,F10.5,16X,F10.5/)
6                     DO 20 I=1,M
7                     V(I)=V(I)*3600.
8                  20 CONTINUE
9                     IF(N.LT.2)GO TO 90
0                1001 CONTINUE
1                     STOP
2                     END
```

APPENDIX I

PRESSURE TAP TUBE REDUCTION, SAMPLE CALCULATION FOR PT-2, 45° AT 60 PERCENT FLOW

In an attempt to more accurately describe the actual pressure drop in the three foot test section of the General Atomic tubes, an alternate method to that presented in [19] for predicting the pressure drop was sought. Using a specially constructed tube, (see Figure 14), several pressure drops were measured across different sections of the tube. These pressure drops are summarized in Tables 21, 22, and 13 and were used as follows to arrive at a satisfactory method for predicting the actual pressure drop in the three foot section of tube.

To determine a contraction loss factor, the pressure drop at the entrance must first be determined using

$$\Delta P_{cn} = \Delta P_{6-5} - \Delta P_{Ac} - \Delta P_T - \frac{\Delta P_s}{2} \text{ (in Hg)}$$

where:

ΔP_{6-5} = pressure drop measured between taps 6 and 5 as seen on Figure 15

ΔP_{Ac} = pressure drop due to the area change at the inlet

ΔP_T = pressure drop between tap 5 and the beginning of the test section

ΔP_s = pressure drop in smooth section between tap 6 and the beginning of the tube.

Now

$$\Delta P_{6-5} = 13.9 \text{ in Hg}$$

and

$$\Delta P_{Ac} = \frac{\rho V_{TS}^2}{2g} \left(1 - \sigma^2 \right) ,$$

where

$$\frac{\rho V_{TS}^2}{2g_c} = 10.57 \text{ in Hg,}$$

and

$$\sigma = \frac{A_{TS}}{A_s} .$$

Therefore,

$$\rightarrow \Delta P_{Ac} = 6.43 \text{ in Hg.}$$

$$\Delta P_T = \frac{\frac{\Delta P_{3-5}}{L_{3-5}} \quad 36 - L_{3-5}}{2} ,$$

where

$$\Delta P_{3-5} = 45.3 \text{ in Hg ,}$$

and

$$L_{3-5} = 31.75 \text{ in .}$$

Therefore,

$$\rightarrow \Delta P_T = 3.03 \text{ in Hg}$$

$$\Delta P_s = \frac{4 f_s G^2 (\frac{L}{D})}{\rho 2 g_c (144)(.4551)} ,$$

where

$$f_s = \frac{.046}{Re^{0.2}} ,$$

and

$$\frac{L}{D} = (\frac{.229}{.04367}) = 5.24$$

Therefore,

$$\rightarrow \Delta P_s = .048 \text{ in Hg , and}$$

$$\Delta P_{cn} = 4.42 \text{ in Hg .}$$

Knowing the inlet pressure loss due to contraction we can determine the contraction loss factor from the relationship:

$$\Delta P_{cn} = K_{cn} \frac{\rho V_{TS}^2}{2g_c} ,$$

$$\rightarrow \quad K_{cn} = 0.42 \ .$$

Similarly at the exit, we know

$$\Delta P_e = \Delta P_{2-6} - \Delta P_{5-6} - \Delta P_{5-3} - \Delta P_T + \Delta P_{Ac} - \frac{\Delta P_s}{2} (\text{in Hg})$$

where :

$\Delta P_{2-6} = 60.5$ in Hg ,

$\Delta P_{5-6} = 13.9$ in Hg ,

$\Delta P_{5-3} = 45.3$ in Hg ,

$\Delta P_T = 3.03$ in Hg ,

$\Delta P_{Ac} = 6.43$ in Hg ,

$\Delta P_s/2 = .024$ in Hg , and

$\therefore \quad \Delta P_e = 4.68$ in Hg

From

$$\Delta P_e = K_e \frac{\rho V_{TS}^2}{2g_c} ,$$

it is found that

$$K_e = 0.44 \ .$$

The assumption that K_c and K_e varied only slightly over the range of flows used in this experiment was invoked as before. Thus the contraction loss factors and the expansion loss factors were calculated at each of the measured flow points, and an average of these individual values was used in determining the non-recoverable losses due to expansion and

contraction. The subscript 2 will be used to define the friction factor and the variables used to determine the friction factor found by using the expansion and contraction loss factors as found above. Similarly, for the case where K_{cn} and K_e are found using [19], the subscript 1 will be used.

The following constants are defined.

$$D_{TS} = D_h = 0.0241 \text{ ft}$$

$$\left(\frac{L}{D}\right)_{TS} = 124.5$$

$$L_{TS} = 3 \text{ ft}$$

$$D_{3-5} = D_h = 0.0241 \text{ ft}$$

$$\left(\frac{L}{D}\right)_{3-5} = 109.8$$

$$L_{3-5} = 2.65 \text{ ft}$$

$$(K_{cn} + K_e)_1 = 0.33$$

$$(K_{cn} + K_e)_2 = 0.80$$

To determine the friction factor using each of the above loss factors, the pressure drop in the test section must be found from:

$$(\Delta P_{TS})_{1,2} = \Delta P_{2-6} - \Delta P_s - (\Delta P_{exp/con})_{1,2} \text{ (psi)}$$

where:

$$\Delta P_{2-6} = 27.53 \text{ psi},$$

$$\Delta P_s = .022 \text{ psi},$$

$$(\Delta P_{exp/con})_1 = \frac{\rho V_{TS}^2}{2g_c} (K_c + K_e)_1 = 1.59 \text{ psi , and}$$

$$(\Delta P_{exp/con})_L = \frac{\rho V_{TS}}{2g_c} (K_c + K_e)_2 = 3.85 \text{ psi .}$$

Now from

$$f_{TS} = \frac{\Delta P_{TS} \rho 2g_c}{4 G^2 (\frac{L}{D})_{TS}} ,$$

and

$$f_{3-5} = \frac{\Delta P_{3-5} \rho 2g_c}{4 G^2 (\frac{L}{D})_{3-5}} ,$$

it can be found that:

$$(f_{TS})_1 = 0.0108 ,$$

$$(f_{TS})_2 = 0.0096 , \text{ and}$$

$$(f_{TS})_{3-5} = 0.0097 .$$

It is easily seen that the experimental results indicate that the actual friction factor in the test section is less than that computed using the traditional methods presented in [19]. It is also noted that $(f_{TS})_{3-5}$ is very nearly equal to $(f_{TS})_2$. The only real significance that can be attached to that fact, however, is that the pressure drop was reduced to the outer limits of the three foot section satisfactorily. Since, however, the pressure drop between taps 3 and 5 was used in determining the reduction procedure - the subsequent friction factor is coupled to f_{3-5}. There is

obviously much more experimental work required in this area before a universally accepted method can be determined.

BIBLIOGRAPHY

1. Search, H. T., A Feasibility Study of Heat Transfer Improvement in Marine Steam Condensers, MSME, Naval Postgraduate School, Monterey, CA, March 1978.

2. Bergles, A. E., Survey of Augmentation of Two Phase Heat Transfer, paper presented at ASHRAE Semi-Annual Meeting, Dallas, Texas, February, 1976.

3. Bergles, A. E. and Jensen, M. K., Enhanced Single-Phase Heat Transfer for Ocean Thermal Energy Conversion Systems, Report HTL-13 ISU-ERI-AMES-77314, ERI Project 1278, April 1977.

4. Palen, J., Cham, B., and Taborek, J., Comparison of Condensation of Steam on Plain and Turbotec Spirally Grooved Tubes in a Baffled Shell - and - Tube Condenser, Heat Transfer Research, Inc., Report 2439-300/6, January 1971.

5. Eiessenberg, D. M., An Investigation of the Variables Affecting Steam Condensation on the Outside of a Horizontal Tube Bundle, PhD dissertation, University of Tennessee, December 1972.

6. Newson, I. H. and Hodgson, T. K., "The Development of Enhanced Heat Transfer Condenser Tubing", 4th International Symposium on Fresh Water From the Sea, Vol. 1, pp. 69-94, 1973.

7. Watkinson, A. P., Miletti, D. L., and Tarasoof, P., "Heat Transfer and Pressure Drop of Internally Finned Tubes," AIChE Symposium Series, No. 131, Vol. 69, 1973.

8. Catchpole, J. P. and Drew, B. C. H., "Evaluation of Some Shaped Tubes for Steam Condensers," Steam Turbine Condensers, NEL Report No 619, pp 68-82, August, 1976.

9. Young, E. H., Withers, J. G., and Lampert, W. B., Heat Transfer Characteristics of Corrugated Tubes in Steam Condensing Applications, AIChE Paper No. 3, August 11, 1975.

10. Rothfus, Robert R., Concurrent Studies of Enhanced Heat Transfer and Materials for Ocean Thermal Exchangers; Progress Report: ERDA Contract No. EY 76-S-02-2641-1 for Period 1 July 1975 to 31 July 1976.

11. General Atomic Company, Tubing For Augmented Heat Transfer, Proposal AP 62-112, July 23, 1976.

12. Beck, A. C., A Test Facility to Measure Heat Transfer Performance of Advanced Condenser Tubes, MSME Thesis, Naval Postgraduate School, December 1976.

13. Pence, D., An Experimental Study of Steam Condensation On A Single Horizontal Tube, MSME, Naval Postgraduate School, Monterey, CA, March 1978.

14. Acurex Autodata, Autodata Nine Technical Manual.

15. Holman, J. P., Heat Transfer, 4th ed., McGraw-Hill, 1976.

16. Wilson, E. E., A Basis for Rational Design of Heat Transfer Apparatus, paper presented at the Spring meeting of the Society of Mechanical Engineers, Buffalo, NY, June 1965.

17. Briggs, D. E., and Young, E. H., "Modified Wilson Plot Techniques for Obtaining Heat Transfer Correlations for Shell and Tube Heat Exchangers," Heat Transfer-Philadelphia, Vol. 65, No. 92, pp 35-45, 1969.

18. Subroutine, NPS COMPUTER FACILITY, LEAST SQUARES POLYNOMINAL FITTING, Programmed by D. E. Harrison, Nov. 1969.

19. KAYS and LONDON, Compact Heat Exchangers, McGraw-Hill, 1964.

20. KNUDSEN and KATZ, Fluid Dynamics and Heat Transfer, McGraw-Hill, 1958.

21. Department of the Navy, Bureau of Ships, Design Data Sheet DDS 4601-1, 15 OCT 1953.

22. AEC - Department of the Interior, Report ORNL-TM-4248, ORCON1: A Fortran Code for the Calculation of a Steam Condenser of Circular Cross Section, by J. A. Hafford,

23. Reynolds, O., Trans.Roy.Soc. (LONDON), 174A:935(1883).

24. Colburn, A. P., Trans, AIChE, 29:174, (1933).

25. Webb, R. L., Eckert, E. R. G., Goldstein, R. J., "Heat Transfer and Friction in Tubes With Repeated-Rib Roughness," International Journal of Heat And Mass Transfer, Vol. 14, 1971, pp 601-618.

26. The Chemical Rubber Company, Handbook of Tables for Applied Engineering Science, CRC Press, 1976.

27. Kline, S. J., and McClintock, F. A., Describing Uncertainties In Single Sample Experiments, Mech. Engin. Vol. 74, p 3-8, January 1953.

INITIAL DISTRIBUTION LIST

		No. Copies
1.	Defense Documentation Center Cameron Station Alexandria, Virginia 22314	2
2.	Library, Code 0142 Naval Postgraduate School Monterey, California 93940	2
3.	Department Chairman, Code 69 Department of Mechanical Engineering Naval Postgraduate School Monterey, California 93940	2
4.	Office of Research Administration, Code 012A Naval Postgraduate School Monterey, California 93940	1
5.	Professor Paul J. Marto, Code 69Mx Department of Mechanical Engineering Naval Postgraduate School Monterey, California 93940	20
6.	LT David Reilly, USN 106 Leidig Circle Monterey, California 93940	4
7.	CDR N. P. Nielsen, USN Naval Sea Systems Command (033) 2221 Jefferson Davis Hwy, CP#6 Arlington, Virginia 20360	1
8.	Mr. Charles Miller Naval Sea Systems Command (0331) 2221 Jefferson Davis Hwy, CP#6 Arlington, Virginia 20360	2
9.	Mr. Frank Ventriglio Naval Sea Systems Command (0331) 2221 Jefferson Davis Hwy, CP#6 Arlington, Virginia 20360	1
10.	Mr. Arthur Chaikin Naval Sea Systems Command (0331) 2221 Jefferson Davis Hwy, CP#6 Arlington, Virginia 20360	1

11. CAPT J. K. Parker, USN — 1
Naval Sea Systems Command (PMS-301)
2221 Jefferson Davis Hwy, CP#6
Arlington, Virginia 20360

12. CDR D. W. Barns, USN
Naval Sea Systems Command (PMS-301.3) — 1
2221 Jefferson Davis Hwy, CP#6
Arlington, Virginia 20360

13. Mr. Walter Aerni — 1
Naval Ship Engineering Center (6145)
Washington, D. C. 20362

14. Mr. Wayne L. Adamson
Naval Ship Research & Development Center(2761) — 1
Annapolis, Maryland 21402

15. Mr. Gil Carlton — 1
Naval Ship Engineering Center (6723)
Philadelphia, Pennsylvania 19112

16. Dr.David Eissenberg — 1
Oak Ridge National Laboratory
Post Office Box Y
Oak Ridge, Tennessee 37830

17. Miss Eleanor J. Macnair — 1
Ship Department
Ministry of Defence
Director - General Ships, Block B
Foxhill, Bath, Somerset
ENGLAND

18. Mr. Kurt Bredehorst — 1
NAVSEC 6147D
Department of the Navy
Hyattsville, Maryland 02782

19. Professor Kenneth J. Bell — 1
School of Chemical Engineering
Oklahoma State University
Stillwater, OK 74074

20. Professor A. E. Bergles — 1
Department of Mechanical Engineering
Iowa State University
Ames, IA 50010

21. Mr. Sigmond Gronich — 1
Division of Solar Energy
Department of Energy
600 E. Street, NW
Washington, DC 20545

22. Professor James G. Knudsen — 1
Engineering Experimental Station
Oregon State University
Covell Hall-219
Corvallis, OR 97331

23. Dr. Abrahim Lavi — 1
OTEC Branch
Division of Solar Energy
Department of Energy
Washington, DC 20545

24. Dr. A. L. London — 1
4020 Amaranta Avenue
Palo Alto, CA 94306

25. Mr. Norman F. Sather — 1
Argonne National Laboratory
9700 S. Cass Avenue
Argonne, IL 60439

26. Mr. Jack S. Yampolsky — 2
Senior Technical Advisor
Advanced Projects Division
General Atomic Company
P.O. Box 81608
San Diego, California 92138

27. Mr. M. K. Ellingsworth — 1
Office of Naval Research
800 N. Quincy Street
Arlington, VA 22217

28. Mr. R. Muench — 1
David W. Taylor Naval Ship
Research and Development Center
Annapolis Laboratory
Annapolis, MD 21402

29. Mr. W. Thielbar — 1
Naval Weapons Center
China Lake, CA 93555

30. Code 03 — 1
Naval Sea Systems Command
Washington, DC 20362

31. Mr. John Michele — 1
OakRidge National Laboratory
OakRidge, TN 37830